THESIS APPROVAL

GRADUATE SCHOOL, KASETSART UNIVERSIT

Master of Engineering (Chemical Engineering)
DEGREE

Chemical Engineering
FIELD

Chemical Engineering
DEPARTMENT

TITLE: Development of an Approximate Input/Output Linearizing Controller Using Taylor Series Technique Applied in FPGA Device

NAME: Mr. Issarush Kajornrungsilp

THIS THESIS HAS BEEN ACCEPTED BY

THESIS ADVISOR
(Assistant Professor Chanin Panjapornpon, Ph.D.)

THESIS CO-ADVISOR
(Associate Professor Sunun Limtrakul, D.Sc.)

DEPARTMENT HEAD
(Associate Professor Phungphai Phanawadee, D.Sc.)

APPROVED BY THE GRADUATE SCHOOL ON _____

DEAN
(Associate Professor Gunjana Theeragool, D.Agr.)

THESIS

DEVELOPMENT OF AN APPROXIMATE INPUT/OUTPUT LINEARIZING CONTROLLER USING TAYLOR SERIES TECHNIQUE APPLIED IN FPGA DEVICE

ISSARUSH KAJORNRUNGSILP

A Thesis Submitted in Partial Fulfillment of
the Requirements for the Degree of
Master of Engineering (Chemical Engineering)
Graduate School, Kasetsart University
2011

Issarush Kajornrungsilp 2011: Development of an Approximate Input/Output Linearizing Controller Using Taylor Series Technique Applied in FPGA Device. Master of Engineering (Chemical Engineering), Major Field: Chemical Engineering, Department of Chemical Engineering. Thesis Advisor: Assistant Professor Chanin Panjapornpon, Ph.D. 114 pages.

Input/Output (I/O) linearization is a control technique that applies a process model in a controller synthesis. It is an attractive method for many applications in chemical industries. In spite of many advances in control theory, practical implementation of I/O linearization is still sluggishly compared to other model-based techniques. The formulation of I/O controller basically requires the differentiation and inversion of the process model, which becomes cumbersome as the complexity of the model increases.

This work presented a new approach to the formulation of an approximate input/output (I/O) linearizing controller for non-minimum phase processes. The time derivatives of outputs are truncated around the nominal equilibrium point by applying the Taylor series expansion. The open-loop state observer is used to estimate the unmeasured state variables of the process. The compensator is used to estimate a disturbance in the process. The developed controller system is in a sample form, and the control algorithm is more applicable to embed into the control hardware device such as the NI C-RIO. The performance of the embedded model-based controller is illustrated through real-time implementation of the pilot process exhibiting non-minimum phase behavior. The results show that the controller provides good performance for set-point tracking and output disturbance rejection.

_____ _____ __ / __ / __

Student's signature Thesis Advisor's signature

ACKNOWLEDGEMENTS

I would like to express my deepest gratitude to my advisor, Assistant Professor Dr. Chanin Panjapornpon, for his encouragement and support in the course of my dissertation. I greatly appreciate his strong commitment to excellence in both teaching and research.

I am grateful to Associate Professor Dr. Sunun Limtrakul for agreeing to participate in my dissertation as Co-Advisor and for her valuable suggestions. I would like to thank Associate Professor Dr. Apinya Duangchan and Assistant Professor Dr. Sumet Umchid for agreeing to serve on my thesis committee.

I deeply thank to Postgraduate Education and Research Development Office (PERDO) and Department of Chemical Engineering at Kasetsart University for the financial supports. I would like to express my special thank to all colleagues and my best friends for their warm friendships, suggestions and all supports.

I hereby thank the many talent individuals who have made me an inspiration. Especially, Archimedes of Syracuse the greatest scientist of Greek for his aphorism, "*Δο′ς μοι που′ στω′ χαι ταυ′ χινα′σω.*" - "Give me a place to stand and I will move the Earth", it makes me too interested in the science and engineering. I very appreciate to "Sun Tzu (孫武)" for his epigram "知己知彼，百战不殆。"- "if you know your enemy or opponent very well, then you can beat him many times". This expression is making me to check my problem carefully and observe everything that occurs around me.

Finally, I wish to thank my parents for their unconditional love and support in many aspects of life. They always find ways to lift me up when I am down.

Issarush Kajornrungsilp

February 2011

TABLE OF CONTENTS

Page

LIST OF TABLES

LIST OF FIGURES

LIST OF FIGURES (Continued)

LIST OF FIGURES (Continued)

LIST OF FIGURES (Continued)

LIST OF ABBREVIATIONS

A	=	reactant
c_p	=	heat capacity of feed and product [kJ kg^{-1} K^{-1}]
c_{p_j}	=	heat capacity of jacket fluid [kJ kg^{-1} K^{-1}]
C_A	=	concentration of A [kmol/m^3, mol/l]
$C_{A_{ss}}$	=	steady state concentration of reactant A [kmol/m^3, mol/L]
C_{Ai}	=	initial concentration of reactant A [kmol/m^3, mol/L]
C_B	=	concentration of B [mol/L]
$C_{B_{ss}}$	=	steady state concentration of B [mol/L]
D	=	differential operator
E_a, E_1, E_2	=	activation energy for rate constant [kJ/kmol]
F	=	reactor feed flow rate [m^3/hr]
F_j	=	jacket coolant flow rate [L/hr]
$f(x,u)$	=	nonlinear vector function
k_0	=	rate constant [hr^{-1}]
k_{A0}	=	rate constant of reaction $A \rightarrow B$ [L mol^{-1} hr^{-1}]
k_{B0}	=	rate constant of reaction $B \rightarrow C$ [hr^{-1}]
K_c	=	tuning parameter of the PI controller
m	=	number of manipulated inputs
N	=	series truncation order
n	=	number of state variables
p	=	prediction step
q	=	cooling rate of the reactor [K/hr]
r	=	relative order of the output y
R	=	universal gas constant [kJ $kmol^{-1}$ K]
S	=	heat transfer surface area [m^2]
t	=	time [hr]
T	=	reactor temperature [K]
T_i	=	temperature of a feed stream [K]

LIST OF ABBREVIATIONS (Continued)

T_{ss}	=	steady-state reactor temperature [K]
T_j	=	jacket temperature [K]
T_{ji}	=	jacket inlet temperature [K]
u	=	vector of manipulated inputs
V	=	reactor volume [m^3]
V_j	=	jacket volume [m^3]
x	=	vector of state variables
x_{ss}	=	nominal equilibrium point
$\tilde{x}$	=	vector of estimated states
y	=	vector of controlled outputs
y_{sp}	=	vector of set-points
$\tilde{y}$	=	vector of estimated outputs
$\hat{d}$	=	estimated disturbances
$-\Delta H_1, -\Delta H_2$	=	heat of reaction [kJ/mol]
β	=	tuning parameter
γ	=	parameter of reactor model [m^3 K $kmol^{-1}$]
ξ	=	vector of the zero dynamics
ψ	=	compact form of the feedback controller
ρ	=	density of liquid mixture in the reactor [kg L^{-1}]
ρ_j	=	density of the jacket fluid [kg L^{-1}]
τ_i	=	tuning parameter of the PI controller
v	=	new corrected set-point
ASIC	=	Application-specific integrated circuit
CSTR	=	Continuous stirred tank reactor
DCS	=	Distributed control system
DGC	=	Differential geometric control
FPGA	=	Field-programmable gate array
I/O	=	Input/output

LIST OF ABBREVIATIONS (Continued)

ISE	=	Integral square error
MBC	=	Model-based control
MPC	=	Model predictive control
NI C-RIO	=	National instruments compact reconfigurable I/O
NI C-DAQ	=	National instruments compact data acquisition
NMBC	=	Nonlinear model-based control
PI	=	Proportional-integral
PID	=	Proportional-integral-derivative
PLD	=	Programmable logic device
VI	=	Virtual instrument
VHDL	=	VHSIC hardware description language

DEVLOPMENT OF AN APPROXIMATE INPUT/OUTPUT LINEARIZING CONTROLLER USING TAYLOR SERIES TECHNIQUE APPLIED IN FPGA DEVICE

INTRODUCTION

Chemical processes generally associate with the exothermic reaction. Sometimes, the processes exhibit a phenomenon called non-minimum phase behavior or inverse response. Initially, the output response of the process goes in the opposite direction of its final desired set-point. The examples of the process with non-minimum behavior are the exothermic reaction of cyclopentadiene to cyclopentanol in a continuous stirred tank reactor (Van de Vusse, 1964), chemical reactors (Kravaris and Daoutidis, 1990; Ball and Gray, 1995; Kanter *et al*., 2002), fermentation reactors (Agrawal *et al*.,1982; Dochain, 1992; Henson,1992), and reboilers (Ogunnaike, 1994). The non-minimum phase process is quite difficult to design the controller because it has unstable zero dynamics that the eigenvalues of zeros lie in the right-half complex plane. It creates the instability of a linear controller. The traditional controller such as a proportional-integral-derivative (PID) controller cannot guarantee the closed-loop stability because it provides a wrong compensation leading to deterioration in controllability (Kwok *et al.*, 2000).

Input/output (I/O) linearization is a method in a class of differential-geometric control that has received considerable attention from many researchers in the past decade due to guaranteeing closed-loop stability and having fewer tuning parameters than typical model predictive control (Panjapornpon *et al.*, 2006). The I/O linearization was initially developed for unconstrained, minimum-phase process (Palanki and Kravaris, 1997; Guardabassi and Savaresi, 2001; Balasubramhanya and Doyle III, 2000). It has been extended for the control problems of non-minimum behavior, whether the process is stable (Niemiec and Kravaris, 2003; Shkolnikov and Shtessel, 2000; Wu., 1999, Kurtz and Henson., 1997; Jo *et al*., 1998), or unstable (Panjapornpon *et al.*, 2006; Kam and Tade, 1999). The formulation of the I/O

controller basically requires the differentiation and inversion of the process model. The more complex the process model is, the more complex the controller equations. Sometime, this full-length controller equation is difficult to implement into control hardware due to a limitation on memory and calculation capability of control hardware. Some attempts were made to develop the techniques for simplifying the formulation of the I/O controller. For examples, a nonlinear model is transformed into a linear state-space model or transfer function before applying into controller synthesis (Kendi and Doyle III, 1996). The special formulations of state transformation with pole-placement technique (Kazantzis and Kravaris, 2000; Dubljevic, 2003) were applied to develop the I/O controller in the series form. The other simplifying techniques that were mentioned in the related geometric approach are the approximation model into a polynomial form (Lukes, 1969; Lee *et al*., 2000). However, all these mentioned methods are applicable to minimum phase behavior only, and they cannot set the speed of the closed-loop process responses. The efficiencies of the proposed control systems were only tested with the numerical simulation.

To decrease the complexity of the controller synthesis, this work presents a new formulation of approximate I/O linearization in the form of simplified solution. The proposed method is applicable to the process, whether minimum or non-minimum phase. The time derivative of the output is truncated around the nominal equilibrium point by applying the Taylor series expansion. The static feedback controller is obtained by solving the equation of requesting closed-loop I/O response. The state observer is applied for estimating unmeasured state variables. The compensator is used to estimate a process disturbance. The proposed control system is embedded into the Field-programmable gate array (FPGA) control device. The efficiency of the embedded model-based controller is tested through the real-time implementation of the pilot process exhibiting non-minimum phase behavior.

OBJECTIVES

1. Develop the simplified technique of the I/O linearization that is suitable for FPGA control hardware device

2. The control system is configured into the FPGA based control device.

3. Evaluate the performance of the embedded control device with the non-minimum phase pilot process in real-time test.

Scopes of thesis

1. The control system is developed for non-minimum phase processes.

2. The combination of the approximated I/O linearization and the Taylor series technique is focused in the controller synthesis.

3. The control system is consisted of the feedback controller, compensator, and open-loop state observer.

4. The effectiveness of the proposed control scheme is tested through the numerical simulation.

5. The control system is then configured into the FPGA based control device.

6. The performance of the embedded control device is tested with the non-minimum phase pilot process.

Impact of results

The control device with embedded model-based controller is a prototype control hardware that successfully integrates the model-based technique into the microcontroller level. The developed feedback controller is in a simple form, and it is straightforward to embed the controller equation into the control hardware. This work presents a new trend to apply the advance control technique into the FPGA hardware as a stand-alone control device. With the outstanding performance, the embedded model-based controller has the potential to replace the traditional PID control device that has been used for many decades. It also has the potential to use as a local central control unit of the process sectors for decreasing the calculation load of the main distributed control system (DCS).

LITERATURE REVIEW

1. Control problem of non-minimum phase in chemical process

The non-minimum phase behavior, or called inverse response, is frequently occurred in the chemical processes with the exothermic reaction. The output subjected to a step change input will give the initial response in the opposite direction to where the output variable goes at a steady state (Garcia-Gabin and Camacho, 2003). The example of non-minimum phase behavior is the reaction of cyclopentadiene to cyclopentanol in a continuous stirred tank reactor (CSTR) (Van de Vusse, 1964). The chemical reaction of such a process can be described by:

$$\underset{\text{Cyclopentadiene (A)}}{C_5H_6} \xrightarrow{k_1/(+H_2O)} \underset{\text{Cyclopentanol (B)}}{C_5H_7OH} \xrightarrow{k_2/(+H_2O)} \underset{\text{Cyclopentanediol (C)}}{C_5H_8(OH)_2}$$

$$2C_5H_6 \xrightarrow{k_3} \underset{\text{Dicyclopentadiene(D)}}{C_{10}H_{12}}$$

Initially, the cyclopentadiene coverts to dicyclopentatiene more than cyclopentanol due to the effect of low reaction temperature. The reaction rate of cyclopentadiene to cyclopentanol subsequently increases with the increase in the reaction temperature. Other examples of non-minimum phase behaviors are the substrate concentration in the bioreactor (Dochain, 1992), the temperature in the ethylene glycol reactive distillation column (Kumar and Daoutidis, 1999), the product purity of the distillation column (Jacobsen, 1999), the crystallization process of potassium chloride (Rohani *et al*., 1999), the polymerization reaction of the methyl methacrylate (Fuente *et al*., 2006), and the boiler steam drum level (Shamsuzzoha and Lee, 2008). When the process desires to operate in the non-minimum phase region, the traditional linear controllers such as the proportional-integral (PI) or proportional-integral-derivative (PID) controllers generally give the control action in the wrong direction because of the RHP eigenvalues of zero dynamics leading to the degradation of control performance (Kwok *et al.*, 2000).

2. Model-based control technique for non-minimum phase process

The development of high-performance control strategies is required for chemical processes due to increased demands on the product quality, productivity, and environmental impact. However, most controller design techniques are based on linear models that do not account for process nonlinearities. Linear control theory applied under specific simplifying assumptions can successfully control many processes around fixed operating conditions. However, the linear controller does not yield satisfactory results for these processes with large disturbances and wide-range operation. This drawback of the linear controller aroused the interest in designing controllers based on nonlinear control theory (Biswas *et al.*, 2007). From the limitation mentioned above, the advanced process control such nonlinear model-based control (NMBC) receives more attention from both industries and researchers. Basically, NMBC can be grouped into three main categories, which are differential geometric control (DGC), model predictive control (MPC), and Lyapunov-based control technique.

2.1 Differential geometric control (DGC)

The DGC uses a method of a differential geometry to transform a nonlinear system into a linear one. The controller is obtained by analytical model inversion. The technique of DGC is an interested technique for applying in real-time implementation due to a few numbers of tuning parameter. The DGC feedback controller was initially designed for the stable open-loop system without consideration of input constraints (Dore *et al*., 1995). However, the DGC controller cannot be used directly for the process with non-minimum phase behavior. In order to control such process, a special technique such as the approximate input/output (I/O) linearization controller is introduced. The approximate I/O linearization is a powerful approach that has a capability of handling the process exhibiting complex behavior such non-minimum phase process (Kravaris *et al.*, 1998; Allgower and Doyle, 1998). The control action of approximate I/O Linearization controller can be described in a set of equations that requires less calculating time and computational load compared to

MPC. Other special DGC techniques for controlling the non-minimum phase processes are exact linearization technique with Lyapunov theory (Wu, 1999), I/O linearization with pole placement technique (Dublijevic and Kazantzis, 2002), equivalent output control (Niemiec and Kravaris, 2003), approximate input-state linearization (Panjapornpon *et al.*, 2006), and I/O linearization with stability constraint (Panjapornpon and Soroush, 2007).

2.2 Model predictive control (MPC)

The MPC is an optimization-based strategy in which a nonlinear process model is used to predict the effect of future manipulated input moves on future values of the controlled outputs. At each time step, a sequence of input moves is calculated by solving an open-loop optimal control problem. A feedback controller is obtained by implementing only the first calculated input and resolving the optimization problem at the next sampling instant using new process measurements. The constrained optimization can develop in continuous or discrete-time formulations depending on the scope of work. The performance of this controller depends on the number of time step of prediction and control horizons. The higher the number of time step, the better the control performance is. The large number of time step induces the increase in the computation time. Although the MPC has the ability to handle the multivariable control problem, it does not guarantee the closed-loop stability.

2.3 Lyapunov-based control

Lyapunov's method is based on construction of a function of the system state coordinates that serves as a generalized norm of the solution of the dynamical system. There are two dominant methods of Lyapunov stability are used to investigate the stability of nonlinear systems, called indirect and linearization methods. The linearization method or direct method is to determine the stability properties of a nonlinear process by constructing a Lyapunov function as real positive definite for a process and examining how this function develops in the time domain. The indirect method determines the stability of the nonlinear system through the eigenvalues of the

Jacobian matrix of the linearization system around equilibrium. If the derivatives of Lyapunov function respect with time is a negative value, then the system must eventually settle down to a normal equilibrium point, whether minimum or non-minimum phase systems. Although the Lyapunov-based control guarantees the closed-loop stability of nonlinear systems, it is difficult to find Lyapunov functions that guarantee stability.

3. Real-time implement of model-based control

Although some DGC and MPC methods can use for non-minimum phase processes, the control algorithms are quite complicated and unsuitable for implementing into existing control hardware. The DGC and MPC require adding the state observer and the compensator into the control system to estimate state information and ensure the closed-loop stability. By adding more algorithms, the computational loads in the distributed computer system increase as well.

DGC is an interesting approach for real-time implementation. The calculation of DGC control action can perform faster than that of MPC because the DGC does not require the optimization routine for calculating the control action. Most control algorithms of DGC are still complicated and unsuitable for implementing into existing control hardware. The development of the DGC method that is suitable for working in the real-time condition needs to be developed.

For the implementation of MPC, the software and hardware using for the MPC should have the capability to perform the optimization routine and handle the high computational loads. Although commercial control hardware for the MPC is available (Agachi *et al.*, 2007), the cost of implementation and maintenance of commercial systems are quite expensive.

4. The techniques for simplifying the formulation of the I/O linearizing controller

The formulation of I/O linearizing controller basically requires the differentiation and inversion of the process model, which becomes cumbersome as the complexity of the model increase. In addition, the obtained controller equation is frequently complex, and sometime it is difficult to implement due to the limitation of the control hardware. Some attempts were made to develop the techniques for simplifying the formulation of the I/O controller. For example, the nonlinear model is transformed into linear state-space model or transfer function before applying into the controller synthesis (Kendi and Doyle III, 1996). The special formulation of state transformation with pole replacement techniques in both continuous-time (Kazantzis and Kravaris, 2000) and discrete-time systems (Dubljevic, 2003) are applied to develop the I/O controller in the series form. All these mentioned methods are applicable only to minimum phase behavior. The other simplifying techniques that were mentioned in related geometric approach are the approximation model into the polynomial form (Lukes, 1969; Lee *et al*., 2000). In this technique, the stability of the closed-loop system is ensured in the small attraction region.

5. Input-output (I/O) linearization control

The I/O linearization method is used for developing the proposed control technique in this research. The brief review of the control method is explained as follows:

Consider a general class of multivariable processes described by the continuous-time, mathematical model of the form:

$$\begin{aligned} \dot{x} &= f(x,u) \\ y &= h(x) \end{aligned} \tag{1}$$

where $x \in R^n$, $u \in R^m$, and $y \in R^m$ denote the vector of the state variables, the manipulated inputs, and the controlled outputs, respectively. For the nonlinear process in the form of equation (1), the relative order of the output y_i with respect to the manipulated inputs is denoted by r_i, where r_i is the smallest integer for which a change in the manipulated input u can affect the output, $\partial[d^{r_i} y_i / dt^{r_i}] / \partial u \neq 0$. The following notation is used:

$$\begin{aligned} y_i &= h_i(x) \\ \frac{dy_i}{dt} &\triangleq \left[\frac{\partial h_i(x)}{\partial x}\right] f(x,u) = h_i^1(x) \\ &\vdots \\ \frac{d^{r_i-1} y_i}{dt} &\triangleq \left[\frac{\partial h_i^{r_i-2}(x)}{\partial x}\right] f(x,u) = h_i^{r_i-1}(x) \\ \frac{d^{r_i} y_i}{dt} &\triangleq \left[\frac{\partial h_i^{r_i-1}(x)}{\partial x}\right] f(x,u) = h_i^{r_i}(x,u) \qquad i = 1,...,m \end{aligned} \tag{2}$$

The following assumptions are made:

1) The relative orders $r_1, \ldots, r_m$ are finite.

2) The characteristic matrix of the process, $\frac{\partial}{\partial u} h_i^{r_i}(x,u) \neq [0 \cdots 0]$, is non-singular on $X \times U$.

3) The process is controllable and observable locally (around the nominal steady state).

4) The matrices $\partial f / \partial x$ and $[\partial h / \partial x][\partial f / \partial x]^{-1}[\partial f / \partial u]$ evaluated at nominal steady state pair, (x_{ss}, u_{ss}), are non-singular.

In case of the controlled output y does not have a finite relative order ($r = \infty$), it means that the manipulated input u does not affect the controlled output, y.

For implementing the I/O linearization method, the closed-loop output responses of the following form are requested:

$$\begin{aligned} (\beta_1 D+1)^{r_1} y_1 &= y_{sp_1} \\ &\vdots \\ (\beta_m D+1)^{r_m} y_m &= y_{sp_m} \end{aligned} \tag{3}$$

where $D=d/dt$, and $\beta_1,\ldots,\beta_m$ are the time constants of the process outputs, $y_1,\ldots,y_m$. The inversion of the state feedback controller based on the I/O linearization is represented by:

$$u = \psi(x, y_{sp}) \tag{4}$$

The controller in equation (4) is limited to the minimums phase stable process, in which the eigenvalues of poles and the zero dynamics of the process are in the left-half of the complex plane. The definition of the zero dynamics is mentioned as follows:

Zero dynamics

The zero dynamics is a dynamic of the uncontrolled states evolving in the system. To investigate this property, the stability of the following dynamic system (ζ) is used in the investigation:

$$\begin{aligned} \dot{\zeta}_1 &= F_1\left(y, \dot{y}, \ldots, \frac{d^{r-1}y}{dt^{r-1}}, \zeta_1, \ldots, \zeta_{n-r}\right) \\ &\vdots \\ \dot{\zeta}_{n-r} &= F_{n-r}\left(y, \dot{y}, \ldots, \frac{d^{r-1}y}{dt^{r-1}}, \zeta_1, \ldots, \zeta_{n-r}\right) \end{aligned} \tag{5}$$

In the case where the output is a constant value, the dynamics of the output can be assumed to be zero without loss of generality. The zero dynamics in equation (5) will be:

$$\begin{aligned} \dot{\zeta}_1 &= F_1\left(0,0,\ldots,0,\zeta_1,\ldots,\zeta_{n-r}\right) \\ &\vdots \\ \dot{\zeta}_{n-r} &= F_{n-r}\left(0,0,\ldots,0,\zeta_1,\ldots,\zeta_{n-r}\right) \end{aligned} \tag{6}$$

If the eigenvalues of the dynamics in equation (6) lies in the left-half of complex plane, the process has stable mode in zero dynamics.

6. Taylor's formula for multivariable system

Approximation of function by polynomial is an important technique in such fields as interpolation and curve fitting, computer graphics and computer aided design. Multi-component variables provide a concise way to describe the higher partial derivatives in Taylor polynomial in higher dimensions. Let f be a real-valued function defined on an open subset U of R^n. f is of class U if all iterated partial derivatives of f, of order at most k, exist and are continuous on U. More precisely, this means that, given any sequence $i_1, i_2, ..., i_q$, where $q \leq k$ and each i_j is one of the integers 1 through n, the iterated partial derivative

$$D_{i_1} D_{i_2} \ldots D_{i_q} f$$

exists and is continuous on U.

Then, the Taylor formula of degree k,

$$P_{f,a}^{k}(a+\bar{h}) = \sum_{m=0}^{k} \sum_{i \in i_n^m} \frac{1}{i!} D_i f(a) \bar{h}^i \tag{7}$$

is called the Taylor polynomial of degree *k* of *f* at *a*.

The example of Taylor polynomial of degree 2 of *f* around the point *a* can be formulated by:

$$P^2_{f,a}(a+\bar{h}) = \sum_{m=0}^{2}\sum_{i\in i_2^m}\frac{1}{i!}D_i f(a)\bar{h}^i$$

$$= \underbrace{\frac{1}{0!0!}D_{(0,0)}f(a)h_1^0h_2^0}_{f(a)} + \underbrace{\frac{1}{1!0!}D_{(1,0)}f(a)h_1^0h_2^0 + \frac{1}{0!1!}D_{(0,1)}f(a)h_1^0h_2^1}_{term\ of\ \deg ree1:\ first\ derivative}$$

$$+ \underbrace{\frac{1}{2!0!}D_{(2,0)}f(a)h_1^2h_2^0 + \frac{1}{1!1!}D_{(1,1)}f(a)h_1h_2 + \frac{1}{0!2!}D_{(0,1)}f(a)h_1^0h_2^2}_{term\ of\ \deg ree2:\ second\ derivative}$$

The Taylor polynomial of degree 2 equation can write more simplify as

$$P^2_{f,a}(a+\bar{h}) = f(a) + D_{1,0}f(a)h_1 + D_{0,1}f(a)h_2$$

$$+\frac{1}{2}D_{2,0}f(a)h_1^2 + D_{1,1}f(a)h_1h_2 + \frac{1}{2}D_{0,2}f(a)h_2^2$$

7. The control hardware device

To increase the applicability of the MBC, the embedded device is introduced to support high performance computing applications. The embedded device is generally called the application specific integrated circuit (ASIC), which is a chip designed for a particular application. Figure 1 shows the ASIC that can be categorized into two groups: Programmable logic device (PLD) and Field-programmable gate array (FPGA).

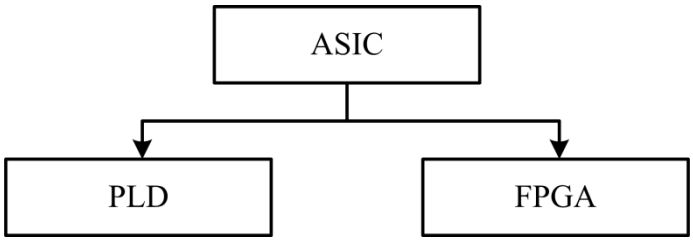

Figure 1 Diagram of the application specific integrated circuit (ASIC)

7.1 Programmable logic device (PLD)

The PLD is an electronic device used to build reconfigurable digital circuits. The PLD allows a user to implement the algorithm in the form of logic *AND* and *OR* gates. The PLD is based on a small number of logic blocks, and a global programmable interconnect. A generic architecture of PLD is shown in Figure 2.

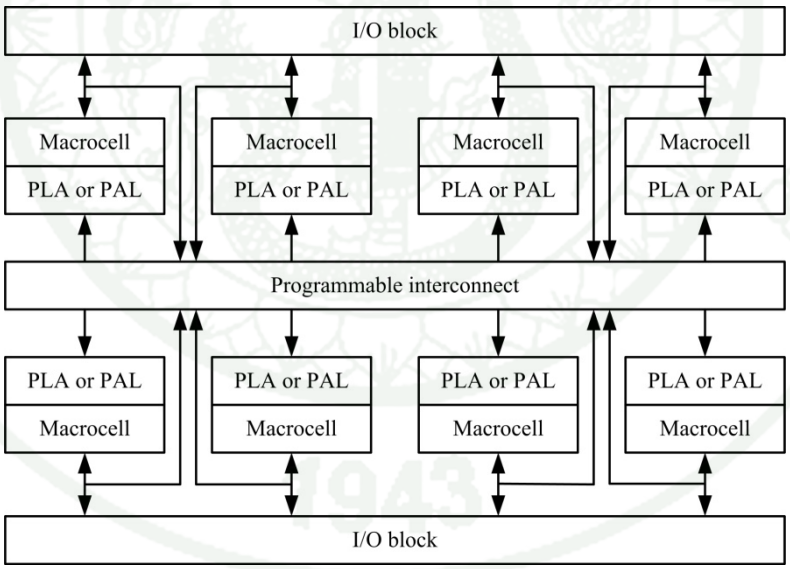

Figure 2 Generic architecture of Programmable logic device (PLD)

7.2 Field-programmable gate array (FPGA) device

The FPGA is a logic device that contains a two-dimensional array of the configurable logic blocks, which are enclosed with the configurable input/output

blocks and linked each other by the interconnection programmable network. The FPGA allows a user to configure and reconfigure the algorithm into the logic gate such as *and*, *or*, *xor*, *not* or more complex combinational functions. The FPGA can use as a stand-alone, real-time application to compute the complex algorithm with very fast speed and low energy consumption. Illustration of generic architecture of FPGA is shown in Figure 3.

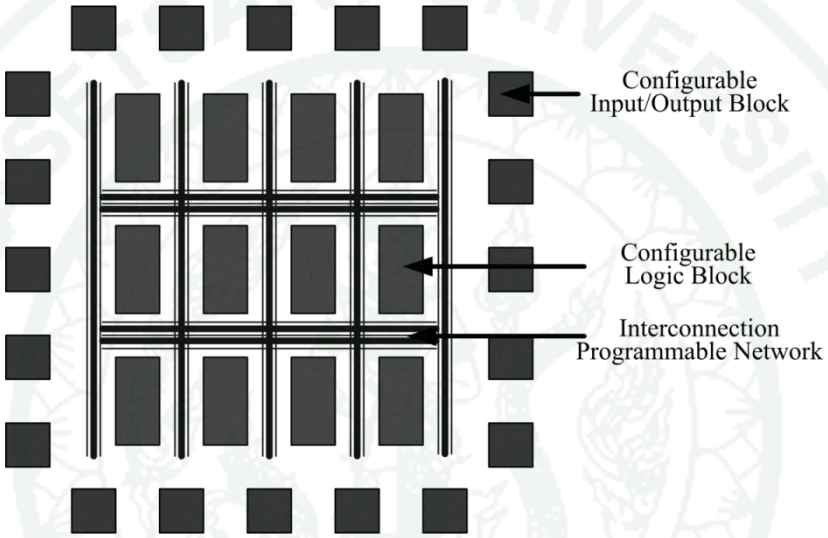

Figure 3 Generic architecture of Field-programmable gate array (FPGA)

7.3 Applications of FPGA

In present, many advances have made in embedded technology to apply into various engineering areas. Especially, application of the field-programmable gate array (FPGA) for real-time control is an attractive solution for a system engineer. The engineer can be a reconfigurable system to perform the different control algorithm into a FPGA based control device. With a fast calculating speed and low energy consumption, the various applications of FPGA were presented in many research fields for the stand-alone controller or the soft sensor in real-time. For example, the movement control of autonomous mobile robots (Pin *et al.*, 1992), the soft sensor for calculating the confidence level of iron-melting cupola furnaces (Mahmoud *et al.*, 2004), and the engine control unit for motorcycle (Dase *et al.*, 2006). Ling *et al.*

(2006) presented the implementation of model predictive control into FPGA. The control performance of the embedded controller was tested through the application of the aircraft system with a linear model. In chemical engineering area, only a work of FPGA application was applied to control a drug delivery system. Bleris *et al.*, (2007) implemented model predictive controller into a prototype board containing the FPGA and microcontroller for performing closed-loop simulation control of the glucose and insulin plasma levels. The coprocessor was used for performing matrix multiplication and the microcontroller is calculated in and the control action. The process model was run in the non-real-time on a computer host, and the microcontroller was communicated to the computer host with the limited speed due to the limitation of the RS232 communication.

MATERIALS AND METHODS

Materials

1. Personal computer with 2.13 GHz of Intel Core 2 Duo processor, 4.00 GB of RAM

2. National Instruments Compact Reconfigurable I/O (National Instruments)

3. National Instruments Compact Data Acquisition (National Instruments)

4. Non-minimum phase pilot process

5. Software

5.1 Mathematica version 7.0 (Wolfram Research, Inc.)

5.2 MATLAB Version R2008b (MathWorks, Inc.)

5.3 LabVIEW version 8.2, LabVIEW Real-time module version 8.2, and LabVIEW FPGA module version 8.2 (National Instruments, Inc.)

Methods

The proposed controller and the embedded model-based controller were developed and the procedures were summarized in a flow diagram as shown in Figure 4. First, the complexity of the feedback controller for nonlinear systems with non-minimum phase behavior was designed by using the combination of the approximated I/O linearization and the series solution method. Second, the compensator and state observer are cooperated with the feedback controller to achieve the closed-loop stability despite the appearance of process-model mismatch or the unmeasured disturbance. Next, the control system is applied to the chemical transport reaction processes by using the process simulation technique in order to analyze the system

response. The feedback controller equation is in the series solution is then embedded into the FPGA device. Finally, the embedded model-based controller is applied to the real-time control of pilot process that is simulated non-minimum phase behavior.

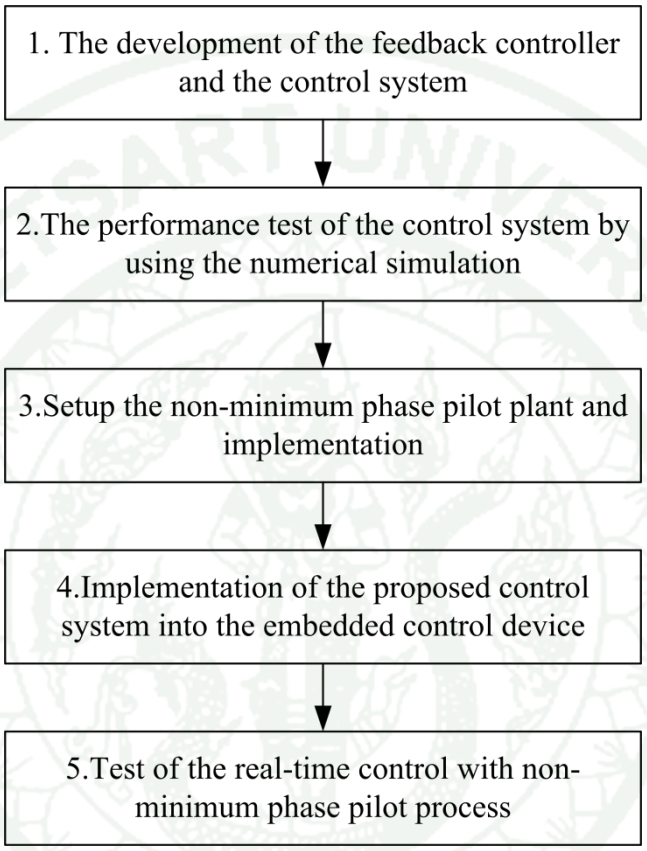

Figure 4 The development of the embedded model-based controller

1. The development of the feedback controller and the control system

1.1 Stability analysis method

Consider the class of multivariable nonlinear processes described by the mathematical model of the form

$$\begin{aligned} \dot{x} &= f(x,u) \\ y &= h(x) \end{aligned} \tag{8}$$

where $x \in R^n$ is the vector of state variables, $u \in R^m$ is the vector of manipulated inputs, $y \in R^m$ is the vector of output variables, $f(x,u)$ is analytic vector functions and $h(x)$ is smooth vector functions.

The stability analysis of an open-loop model is then evaluated by following the stability analysis method. To determine the stability of the process, the equilibrium points of this process are obtained from the dynamic equations at steady state. The defining function is therefore:

$$f\left(x_{ss}, u_{ss}\right) = 0 \tag{9}$$

The nonlinear processes in the form of Equation (8) can be approximately linearized around the desired equilibrium pairs $\left(x_{ss}, u_{ss}\right)$ as shown in equation (10):

$$\dot{x} = \tilde{A}x + \tilde{B}u \tag{10}$$

where x is an $n \times 1$ vector of state deviations from an operating point defined by the state vector, x, and the input vector, u,

u is an $m \times 1$ vector of input deviations from the input vector, u,

$\tilde{A}$ is the $n \times n$ Jacobian matrix, defined as:

$$\tilde{A} = \frac{\partial f}{\partial x} = \begin{bmatrix} \frac{\partial f_1}{\partial x_1} & \frac{\partial f_1}{\partial x_2} & \cdots & \frac{\partial f_1}{\partial x_n} \\ \frac{\partial f_2}{\partial x_1} & \frac{\partial f_2}{\partial x_2} & \cdots & \frac{\partial f_2}{\partial x_n} \\ \vdots & \vdots & \cdots & \vdots \\ \frac{\partial f_n}{\partial x_1} & \frac{\partial f_n}{\partial x_2} & \cdots & \frac{\partial f_n}{\partial x_n} \end{bmatrix}$$

$\tilde{B}$ is the $n \times m$ input-Jacobian matrix, defined as:

$$\tilde{B} = \frac{\partial f}{\partial u} = \begin{bmatrix} \frac{\partial f_1}{\partial u_1} & \frac{\partial f_1}{\partial u_2} & \cdots & \frac{\partial f_1}{\partial u_n} \\ \frac{\partial f_2}{\partial u_1} & \frac{\partial f_2}{\partial u_2} & \cdots & \frac{\partial f_2}{\partial u_n} \\ \vdots & \vdots & \cdots & \vdots \\ \frac{\partial f_{n-r}}{\partial u_1} & \frac{\partial f_{n-r}}{\partial u_2} & \cdots & \frac{\partial f_{n-r}}{\partial u_n} \end{bmatrix}$$

The stability of the process is determined by evaluating the eigenvalues of the Jacobian matrix of equation (11) at a steady state(x_{ss}, u_{ss}). The eigenvalues are found by setting the determinant to zero:

$$|J - \lambda I| = 0 \tag{11}$$

The character of a steady state can be summarized as follows:

i) Stable node, if both eigenvalues are real and negative.

ii) Unstable node, if both eigenvalues are real and positive.

iii) Saddle node, if the eigenvalues are real with opposite signs.

iv) Stable focus, if the eigenvalues are complex conjugate with negative real parts.

v) Unstable focus, if the eigenvalues are complex conjugate with positive real parts.

Following the same concept, to determine the stability of the zero dynamic .The zero dynamics will be:

$$\begin{aligned} \dot{\zeta}_1 &= F_1\ (0,0,\ldots,0,\zeta_1,\ldots,\zeta_{n-r}) \\ &\vdots \\ \dot{\zeta}_{n-r} &= F_{n-r}(0,0,\ldots,0,\zeta_1,\ldots,\zeta_{n-r}) \end{aligned} \tag{12}$$

The equilibrium points of the zero dynamic are the set of solutions obtained from the dynamic equations at steady state. The defining function is therefore:

$$F\left(\zeta_{ss}\right)=0 \tag{13}$$

The approximated linearization of zero dynamics defined by equation (12) is

$$\dot{\zeta}=\tilde{F}\zeta \tag{14}$$

where ζ is an $(n-r)\times 1$ vector of the state variables of the zero dynamics

$\tilde{F}$ is the $(n-r)\times(n-r)$ Jacobian matrix, defined as:

$$\tilde{F}=\frac{\partial\zeta}{\partial x}=\begin{bmatrix} \frac{\partial F_1}{\partial\zeta_1} & \frac{\partial F_1}{\partial\zeta_2} & \cdots & \frac{\partial F_1}{\partial\zeta_{n-r}} \\ \frac{\partial F_2}{\partial\zeta_1} & \frac{\partial F_2}{\partial\zeta_2} & \cdots & \frac{\partial F_2}{\partial\zeta_{n-r}} \\ \vdots & \vdots & \cdots & \vdots \\ \frac{\partial F_{n-r}}{\partial\zeta_1} & \frac{\partial F_{n-r}}{\partial\zeta_2} & \cdots & \frac{\partial F_{n-r}}{\partial\zeta_{n-r}} \end{bmatrix}$$

The stability of the zero dynamics is determined by evaluating the eigenvalues of the Jacobian matrix of equation (12) at a steady state $\left(x_{ss},u_{ss}\right)$. The eigenvalues are found by setting the determinant to zero:

$$\left|J-\lambda I\right|=0 \tag{15}$$

If the eigenvalues of the dynamics in equation (12) lies in the left-half complex plane, the process has stable mode in zero dynamics.

1.2 Relative order

For the nonlinear process in the form of equation (8), the relative order of the output y_i with respect to the manipulated inputs is denoted by r_i, where r_i is the smallest integer for which a change in the manipulated input u_i can affect the output. $\partial[d^{r_i} y_i / dt^{r_i}] / \partial u \neq 0$. The following notation will be used:

$$
\begin{aligned}
& y_i = h_i(x) \\
& \frac{dy_i}{dt} \triangleq \left[\frac{\partial h_i(x)}{\partial x}\right] f(x,u) = h_i^1(x) \\
& \quad \vdots \\
& \frac{d^{r_i-1} y_i}{dt} \triangleq \left[\frac{\partial h_i^{r_i-2}(x)}{\partial x}\right] f(x,u) = h_i^{r_i-1}(x) \\
& \frac{d^{r_i} y_i}{dt} \triangleq \left[\frac{\partial h_i^{r_i-1}(x)}{\partial x}\right] f(x,u) = h_i^{r_i}(x,u) \qquad i = 1,\ldots,m \\
& \frac{d^{r_i+1} y_i}{dt^{r_i+1}} \triangleq \left[\frac{\partial h_i^{r_i}(x,u)}{\partial x}\right] f(x,u) + \left[\frac{\partial h_i^{r_i}(x,u)}{\partial u}\right] u^{(1)} = h_i^{r_i+1}(x,u^{(0)},u^{(1)}) \\
& \quad \vdots \\
& \frac{d^{p_i} y_i}{dt^{p_i}} \triangleq \left[\frac{\partial h_i^{p_i-1}(x,u^{(0)},\ldots,u^{(p_i-r_i-1)})}{\partial x}\right] f(x,u) + \left[\frac{\partial h_i^{p_i-1}(x,u^{(0)},\ldots,u^{(p_i-r_i-1)})}{\partial u}\right] u^{(1)} + \ldots \\
& \quad + \left[\frac{\partial h_i^{p_i-1}(x,u^{(0)},\ldots,u^{(p_i-r_i-1)})}{\partial u}\right] u^{(p_i-r_i)} = h_i^{p_i}(x,u,u^{(1)},\ldots,u^{(p_i-r_i)}), \quad p_i \geq r_i
\end{aligned}
\tag{16}
$$

where p_i is a requesting order of output y_i that $p_1 > r_1, \ldots, p_m > r_m$.

1.3 Nonlinear feedback controller design

To decrease the complexity of the controller synthesis, this work presents a new formulation of approximate I/O linearization in the form of simplifies solution. The proposed method is applicable to the process whether minimum or non-minimum phase. The time derivative of the output in equation (16) is truncated around the nominal equilibrium point by applying the Taylor series expansion. The static feedback controller is obtained by solving the equation of requesting close-loop I/O

response. The state observer is applied for estimating unmeasured state variables. The compensator is used to estimate a disturbance in the process.

1.3.1 Approximate Input-Output linearization

For the processes in the form of equation (8), the closed-loop responses of output dynamics described by equation (17) are requested

$$\begin{bmatrix} (\beta_1 D+1)^{p_1} y_1 \\ \vdots \\ (\beta_m D+1)^{p_m} y_m \end{bmatrix} = y_{sp} \tag{17}$$

where D is the differential operator defined by $D=d/dt$, and $\beta_1,\ldots,\beta_m$ are positive constant that set the speed of output $y_1,\ldots,y_m$ in the closed-loop process responses. The requesting orders of outputs, $p_1,\ldots,p_m$, should be chosen such that the state feedback places the eigenvalues of closed-loop system at the eigenvalues of open-loop process (Kanter *et al*., 2002). By substituting for the derivatives of process outputs defined in equation (16) and setting all the time derivatives of u in equation (16) to zero, the response of equation (18) can be denoted as

$$\begin{bmatrix} h_1(x)+\binom{p_1}{1}\beta_1 h_1^1(x)+\cdots+\binom{p_1}{p_1}\beta_1^{p_1} h_1^{p_1}(x,u,0,\ldots,0) \\ \vdots \\ h_m(x)+\binom{p_m}{1}\beta_m h_m^1(x)+\cdots+\binom{p_m}{p_m}\beta_m^{p_m} h_m^{p_m}(x,u,0,\ldots,0) \end{bmatrix} = y_{sp} \tag{18}$$

where $\binom{a}{b} \triangleq \frac{a!}{b!(a-b)!}$.

1.3.2 Series Solution of state feedback controller

Although the requesting response in equation (18) is possible to solve for the control output analytically, sometime, the controller equation is too complex and not suitable for the control hardware. To reduce the complexity of the controller synthesis, the time derivative of the output in equation (16) is truncated around the nominal equilibrium point by applying the Taylor series expansion. The approximations are as follows:

when $r = 0,...,r_i - 1$,

$$\begin{aligned} h_i^0(x) &\approx \sum_{N_1=0}^{N} \cdots \sum_{N_n=0}^{N} \left(\frac{\partial^{N_1+\cdots+N_n} h_i^0(x)}{\partial x_1^{N_1} \cdots \partial x_n^{N_n}} \right)\Bigg|_{x=x_{ss}} \frac{(x_1 - x_{ss})^{N_1} \cdots (x_n - x_{ss})^{N_n}}{N_1! \cdots N_n!} \\ &\vdots \\ h_i^{r_i-1}(x) &\approx \sum_{N_1=0}^{N} \cdots \sum_{N_n=0}^{N} \left(\frac{\partial^{N_1+\cdots+N_n} h_i^{r_i-1}(x)}{\partial x_1^{N_1} \cdots \partial x_n^{N_n}} \right)\Bigg|_{x=x_{ss}} \frac{(x_1 - x_{ss})^{N_1} \cdots (x_n - x_{ss})^{N_n}}{N_1! \cdots N_n!} \end{aligned} \tag{19.1}$$

and when $r = r_i, \ldots, p_i$

$$\begin{aligned} h_i^{r_i}(x,u) &\approx \sum_{N_1=0}^{N} \cdots \sum_{N_n}^{N} \left(\frac{\partial^{N_1+\cdots+N_n} h_i^{r_i}(x,u)}{\partial x_1^{N_1} \cdots \partial x_n^{N_n}} \right)\Bigg|_{x=x_{ss}} \frac{(x_1 - x_{ss})^{N_1} \cdots (x_n - x_{ss})^{N_n}}{N_1! \cdots N_n!} \\ &\vdots \\ h_i^{p_i}(x,u,0,\ldots) &\approx \sum_{N_1=0}^{N} \cdots \sum_{N_n}^{N} \left(\frac{\partial^{N_1+\cdots+N_n} h_i^{p_i}(x,u)}{\partial x_1^{N_1} \cdots \partial x_n^{N_n}} \right)\Bigg|_{x=x_{ss}} \frac{(x_1 - x_{ss})^{N_1} \cdots (x_n - x_{ss})^{N_n}}{N_1! \cdots N_n!} \end{aligned} \tag{19.2}$$

N is denoted the N^{th} order of Taylor series expansion, and x_{ss} is a equilibrium point corresponding to the desired set-point, y_{sp}, which satisfies:

$$\begin{aligned} 0 &= f(x_{ss}) + g(x_{ss})u_{ss} \\ y_{sp} &= h(x_{ss}) \end{aligned}$$

The dependence of a nominal equilibrium point, x_{ss}, is obtained by solving above relation, which is denoted by:

$$x_{ss} = \zeta(y_{sp}) \tag{20}$$

Substituting for the approximation defined in (19.1), (19.2) into (18), the state feedback can be represented by:

$$u = \psi(x, y_{sp}, \beta) \tag{21}$$

1.3.3 Open-loop State observer

In generally, measurements of all state variables are not available. Therefore, the open-loop state observer is used to estimate unmeasured states of the process. The dynamics of open-loop state observer is described by the following equation

$$\begin{aligned} \dot{\tilde{x}} &= f(\tilde{x}, u) \\ \tilde{y} &= h(\tilde{x}) \end{aligned} \tag{22}$$

where $\tilde{x}$ is the vector of state observer and $\tilde{y}$ is the vector of estimate outputs.

1.3.3 Compensator

In the real application, the disturbance is frequently occurred in the process due to the model mismatch or the measurement noise. To resolve these problems, the compensator is used to estimate a disturbance in the process. The compensator is represented by:

$$\begin{aligned} \hat{d} &= y - \tilde{y} \\ v &= y_{sp} + \hat{d} \end{aligned} \tag{23}$$

where $\hat{d}$ is the disturbance, $\tilde{y}$ is the vector of estimate outputs with disturbance free, y is the vector of controlled output, and v is a new corrected set-point.

1.3.4 Control system

The use of the proposed state feedback method of equation (21) the open-loop state observer of equation (22), and the compensator equation (23) leads to the following control system represented by

$$\begin{aligned} \dot{\tilde{x}} &= f(\tilde{x}, u) \\ \tilde{y} &= h(\tilde{x}) \\ v &= y_{sp} + y - \tilde{y} \\ u &= \psi(v, \tilde{x}, \beta) \end{aligned} \tag{24}$$

The proposed control system structure is implemented as shown in Figure 5.

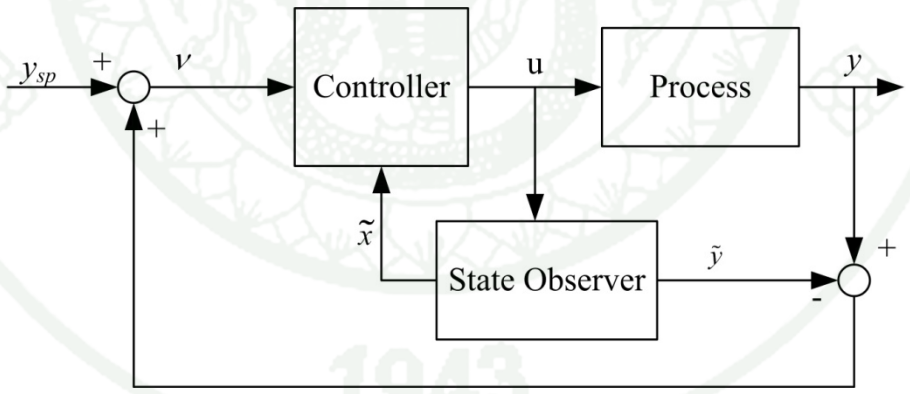

Figure 5 Schematic diagram of the state feedback control structure

2. The performance test of the control system by using the numerical simulation

The applications for the presented control technique are illustrated through various simulations of the chemical reactors, which are a single-input, single-output of the CSTR, and a multi-input, multi-output of the CSTR reactor. The feedback controller equations are obtained by a symbolic software package such as MAPLE or MATHEMATICA while the simulations are carried out by using MATLAB software.

The control performance test is divided into two types, the servo and the regulatory. The servo performance is tested by adjusting the input set-point to the new value after the output responses approach the required set-point while the regulatory performance is tested by introducing the disturbance to the process.

3. Setup the non-minimum phase pilot plant

3.1 The non-minimum phase pilot process

The pilot process consists of the integrated set of the equipments that represent the CSTR with non-minimum phase behavior, in which the CSTR model is described by:

$$\begin{aligned} T(k+1) &= T(k)+\Delta t\left[\gamma k_0 \exp\left(-\frac{E_a}{RT(k)}\right)C_A(k)+\left(T_i-T(k)\right)\frac{F(k)}{V}+q\right] \\ C_A(k+1) &= C_A(k)+\Delta t\left[-k_0 \exp\left(-\frac{E_a}{RT(k)}\right)C_A(k)+\left(C_{Ai}-C_A(k)\right)\frac{F(k)}{V}\right] \end{aligned} \quad (25)$$

where C_A is the concentration of species A, C_{Ai} is the concentration of A in the fresh feed stream, F is the volumetric flow rate of the reactor feed, q is a cooling rate of the reactor, and V is the reactor volume. The process is the exothermic reaction in which the reaction $A \rightarrow B$ takes place in the liquid phase. The reactor parameter values are given in Table 1.

Table 1 Parameters of the chemical reactor model in pilot process

Process Parameter	Values
C_{Ai}	12 kmol/m^3
T_i	302.5 K
V	7.8×10^{-3} m^3
E_a/R	8087 K
k_0	1.76×10^{12} hr^{-1}
γ	4.1 m^3 K kmol^{-1}
q	-120 K/hr

The figure of the pilot process is illustrated in Figure 6. The pilot process comprises of the exchanger unit, the hot-bath, flow controllers and peristaltic pumps. *A* simple diagram of the pilot process is illustrated in Figure 7. The water assumed to be a fresh feed reactant of *A* is fed into the exchanger unit through the 1st pump. The amount of the net heat occurred in the CSTR is calculated by the equation (26) in the host computer.

$$Net\ heat = \gamma k_0 \exp\left[-\frac{E_a}{RT}\right] C_A + q \tag{26}$$

where q is the heat of reaction and $\gamma k_0 \exp\left[-\frac{E_a}{RT}\right] C_A$ is the rate of reaction. The concentration of *A* and the reactor temperature in the net heat calculation is obtained from the simulation of the process model in equation (26).

The 2nd pump feeds the hot water from the hot-bath to the immerging coil of the exchanger unit, in which the flow rate of the hot water is obtained from the equation (27).

$$\dot{m}_{hw} = \frac{Net\ heat}{C_{p,hw}\left(T_{ho} - T_{hi}\right)} \tag{27}$$

where m_{hw} is a flow rate of the hot water, $C_{p,hw}$ is a heat capacity of water, T_{ho} is a temperature of the hot water at the outlet coil, and T_{hi} is a temperature of the hot water at the inlet coil.

Figure 6 The non-minimum phase pilot process

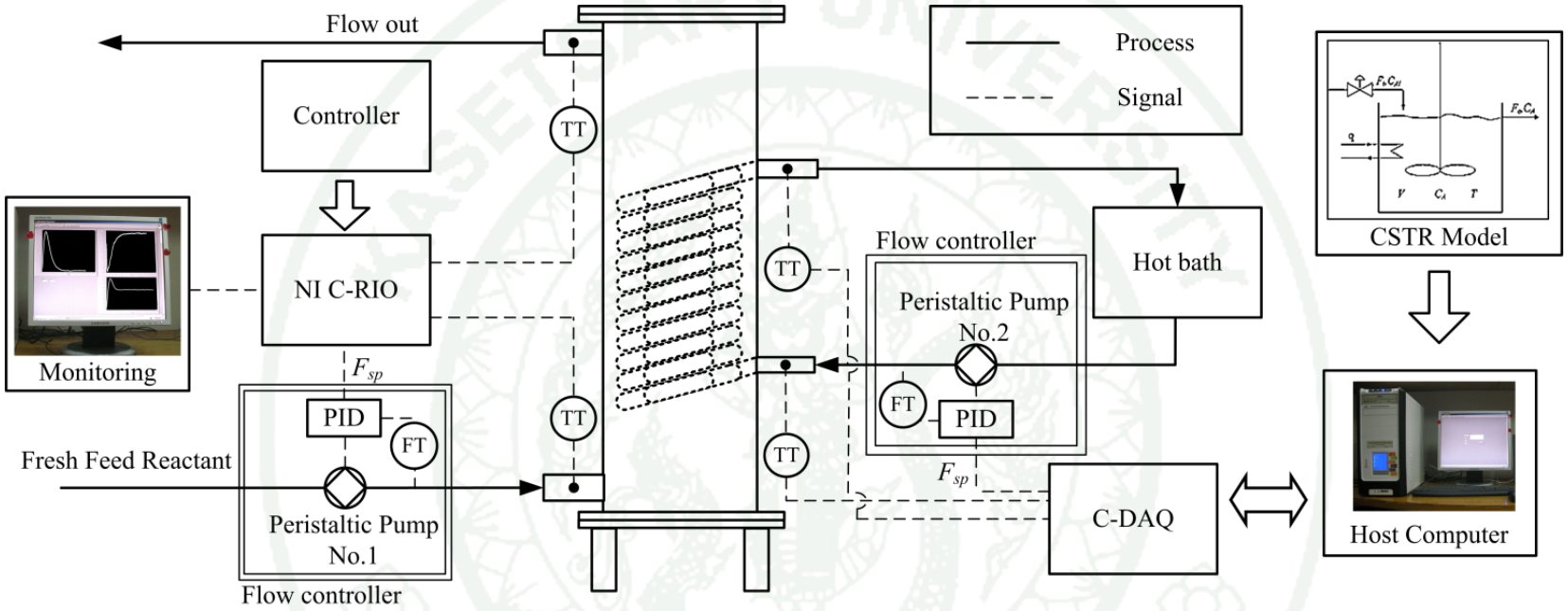

Figure 7 A simple diagram of the non-minimum phase pilot process

Figure 8 The exchanger unit of the non-minimum phase pilot process

Figure 8 shows the exchanger unit that is used to transfer heat from the hot water to the reactor. The hot-bath presented in Figure 9 is used for supplying the hot water to the reactor. The hot bath has the temperature controller to maintain the hot water at given condition.

Figure 9 The hot-bath of the non-minimum phase pilot process

The turbine flow sensor and flow transmitter shown in Figure 10 are devices for sensing and monitoring the rate of fluid flow. The turbine flow sensors are connected to flow transmitter and PID controller in order to monitor the data and adjust the flow rate by using the peristaltic pumps. The turbine flow sensor and flow transmitter were implemented in this work into two parts. In the first part, the turbine flow sensor and flow transmitter send the analog signal to PID controller for controlling the feed flow rate of water. The PID controller is received the signal from NI C-RIO to update the set-point. In the second part, the set-point of PID controller is obtained from NI C-DAQ to manipulate the feed flow rate of hot water.

(a) (b)

Figure 10 The picture of (a) turbine flow sensor, and (b) flow transmitter used in the non-minimum phase pilot process

The peristaltic pump shown in Figure 11 is used to manipulate the feed corresponding to receive the analog signal. This work uses the peristaltic pump into two parts. In the first part, the peristaltic pump receives the analog signal from the 1st flow controller to manipulate the feed flow rate of water. In the second part, it receives the analog signal from the 2nd flow controller to manipulate the feed flow rate of hot water.

Figure 11 The peristaltic pump used in the non-minimum phase pilot process

The National Instruments Compact Reconfigurable I/O (NI C-RIO) from National Instruments, Inc. is used as an embedded device for implementing the developed control algorithm. The NI C-RIO receives the analog signal from the process, proceeds with the calculation of the proposed control method, and sends the control action back to control the flow rate of the fresh feed stream.

3.1.1 Description of the National Instruments Compact Reconfigurable I/O (NI C-RIO)

The NI C-RIO consists of the reconfigurable FPGA, the real-time processor and the I/O module, which the hardware is shown in Figure 12. The reconfigurable FPGA (NI C-RIO-9104, 3M gate reconfigurable embedded chassis containing the XC2V300-4FG676I Xilinx FPGA) comprises of the programmed control logic blocks that are represented the desired algorithm. The real-time processor (NI C-RIO-9004) has a built-in real-time operating system that is used for managing, analyzing and processing the data streams. The I/O module is a device that interconnects the process signal, either the analog or digital, into the data streams. The modules of thermocouple input (NI-9211), analog input (NI- 9201), and analog voltage output (NI-9263) are used in the experiment. The NI C-RIO has many advantages. For example, it has a small size, durable hardware and it can work as the reliable stand-alone controller with low-power consumption. The NI C-RIO has a high speed control because of the algorithm is embedded into the control circuit as a

logic gate in the reconfigurable FPGA. The NI C-RIO using in this work has the limitation in 3 million logic gates and 64 MB of DRAM.

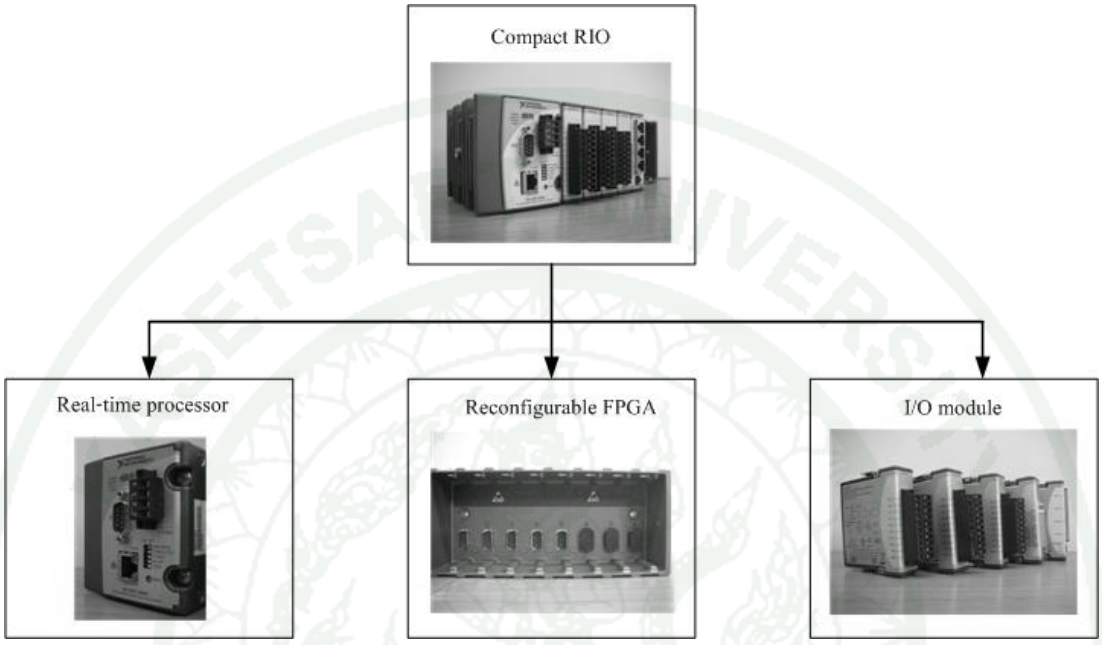

Figure 12 The embedded device NI C-RIO consisting of the real-time controller (NI C-RIO 9004) and the reconfigurable FPGA (C-RIO 9104) from National Instruments

3.1.2 Description of the NI C- DAQ

The National Instruments Compact Data acquisition (NI C- DAQ) is the process of measuring an electrical or physical phenomenon such as voltage, current and temperature. The NI C-DAQ uses a combination of modular hardware, application software, and a computer to take measurements. In this work, the NI C-DAQ consists of NI C- DAQ chassis and the I/O module. The NI C- DAQ chassis (NI C-DAQ 9174) can be used for controlling the synchronization, timing and data transfer between a host computer and the I/O module. The I/O module is a device that interconnects the process signal, either the analog or digital, into the data streams. The modules of thermocouple input (NI-9211), analog input (NI-9201), analog voltage

output (NI-9263) and are used in the experiment. The simplified diagram of the NI C-RIO is shown in Figure 13.

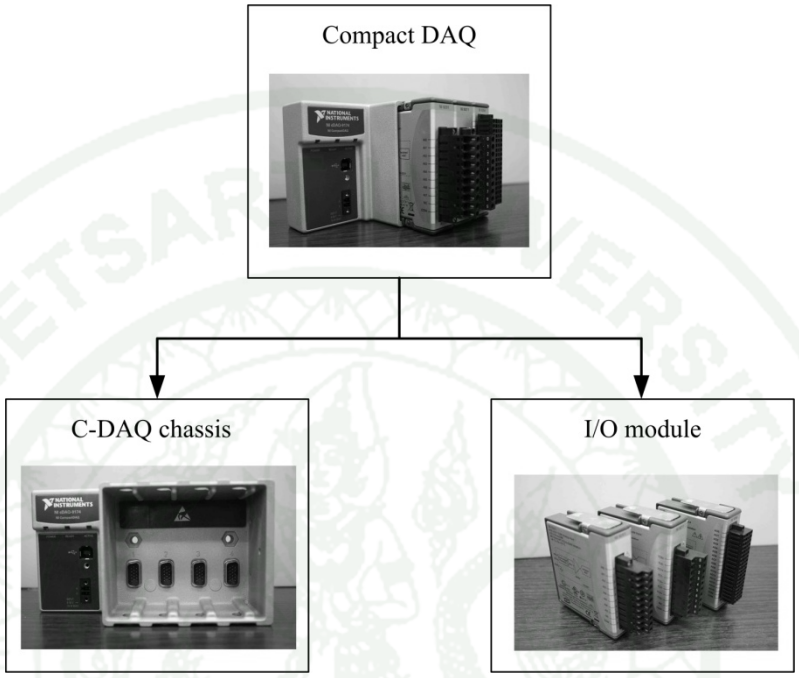

Figure 13 The data acquisition device NI C-DAQ consisting of the NI C- DAQ chassis (NI C-DAQ 9174) and the I/O module from National Instruments

4. Implementation of the proposed control system into the embedded control device

Controller algorithms are implemented in the digital electronics using digital or discrete time form. The discrete time control method is developed based on the approximate I/O feedback controller under series solution. The developed control system is used to implement into the control hardware device to control the non-minimum phase pilot plant.

4.1 Control system design

4.1.1 Relative order

Consider the class of multivariable nonlinear processes described by the discrete-time, mathematical model of the form

$$\begin{aligned} x(k+1) &= f\left(x(k), u(k)\right) \\ y(k) &= h\left(x(k)\right) \end{aligned} \tag{28}$$

where $x(k) \in R^n$ is the vector of state variables, $u(k) \in R^m$ is the vector of manipulated inputs, $y \in R^m$ is the vector of output variables, $f\left(x(k), u(k)\right)$ is the vector of analytic functions and $h\left(x(k)\right)$ is smooth vector functions. For the nonlinear process in the form of equation (28), the relative order of the output y_i with respect to the manipulated inputs is denoted by r_i, where r_i is the smallest integer for which a change in the manipulated input u_i can affect the output. $\partial[d^{r_i} y_i / dt^{r_i}] / \partial u \neq 0$. The following notation of time derivative of the output is used:

$$
\begin{aligned}
y_i(k) &= h_i\left(x(k)\right) \\
y_i(k+1) &\triangleq \left[\frac{\partial h_i\left(x(k)\right)}{\partial x(k)}\right] f\left(x(k),u(k)\right) \\
&\vdots \\
y_i(k+r_i-1) &\triangleq \left[\frac{\partial h_i^{r_i-2}\left(x(k)\right)}{\partial x(k)}\right] f\left(x(k),u(k)\right) = h_i^{r_i-1}\left(x(k)\right) \\
y_i(k+r_i) &\triangleq \left[\frac{\partial h_i^{r_i-1}\left(x(k)\right)}{\partial x(k)}\right] f\left(x(k),u(k)\right) = h_i^{r_i}\left(x(k),u(k)\right) \qquad i=1,...,m \\
y_i(k+r_i+1) &\triangleq \left[\frac{\partial h_i^{r_i}\left(x(k),u(k)\right)}{\partial x(k)}\right] f\left(x(k),u(k)\right) + \left[\frac{\partial h_i^{r_i}\left(x(k),u(k)\right)}{\partial u(k)}\right] \cdot u(k)^{(1)} \\
&= h_i^{r_i+1}(x(k),u(k)^{(0)},u(k)^{(1)}) \\
&\vdots \\
y_i(k+p_i) &\triangleq \left[\frac{\partial h_i^{p_i-1}(x(k),u(k)^{(0)},...,u(k)^{(p_i-r_i-1)})}{\partial x(k)}\right] f\left(x(k),u(k)\right) \\
&\quad + \left[\frac{\partial h_i^{p_i-1}(x(k),u(k)^{(0)},...,u(k)^{(p_i-r_i-1)})}{\partial u(k)}\right] u(k)^{(1)} + ... \\
&\quad + \left[\frac{\partial h_i^{p_i-1}(x(k),u(k)^{(0)},...,u(k)^{(p_i-r_i-1)})}{\partial u(k)^{(p_i-r_i-1)}}\right] u(k)^{(p_i-r_i)} \\
&= h_i^{p_i}(x(k),u(k),u(k)^{(1)},...,u(k)^{(p_i-r_i)}) \qquad p_i \geq r_i
\end{aligned}
\tag{29}
$$

where p_i is a requesting order of output y_i that $p_1 > r_1$,…, $p_m > r_m$.

4.1.2 Approximate Input-Output linearization

Motivated by the previous work of the approximate I/O linearization controller in the continuous-time developed by (Kanter *et al*., 2002), this work focuses on the development of the approximate I/O control technique in discrete-time to apply with the digital implementation. For the processes in the form of equation (28), the closed-loop responses of the output dynamics described by equation (30) are requested

$$\begin{bmatrix} (\beta_1 D+1)^{p_1}\, y_1(k) \\ \vdots \\ (\beta_m D+1)^{p_m}\, y_m(k) \end{bmatrix} = y_{sp} \tag{30}$$

where the differential operator in discrete-time defined by $D^l y_i(k) \triangleq \left[y_i(k+l) - y_i(k+l-1) \right] / \Delta t$ for $l = 1,..., p_i$, and $\beta_1,...,\beta_m$ are positive constants that set the speed of in the closed-loop process responses. The requesting orders of the outputs, which are p_1 ,…, p_m , should be chosen such that the state feedback places the eigenvalues of closed-loop system at the eigenvalues of open-loop process. By substituting for the derivatives of process outputs defined in equation (29) and setting all the time derivatives of u in equation (29) to zero, the response of equation (30) can be denoted as

$$\begin{bmatrix} h_1(x(k)) + \binom{p_1}{1}\beta_1 h_1^1(x(k)) + \cdots + \binom{p_1}{p_1}\beta_1^{p_1} h_1^{p_1}(x(k),u(k),0,\ldots,0) \\ \vdots \\ h_m(x(k)) + \binom{p_m}{1}\beta_m h_m^1(x(k)) + \cdots + \binom{p_m}{p_m}\beta_m^{p_m} h_m^{p_m}(x(k),u(k),0,\ldots,0) \end{bmatrix} = y_{sp} \tag{31}$$

where $\binom{a}{b} \triangleq \dfrac{a!}{b!(a-b)!}$.

4.1.3 Series Solution of state feedback

Although the requesting response in equation (31) is possibly solved for the control output analytically, sometime, the complexity of the controller equation may become from many differentiations or relation between state variables in the process model. To reduce the complexity of the controller synthesis, the time derivative of the output in equation (29) is truncated around the nominal equilibrium point by applying the Taylor series expansion. The approximations are as follows:

when $r = 0,...,r_i - 1$,

$$h_i^0\left(x(k)\right) \approx \sum_{N_1=0}^{N} \cdots \sum_{N_n=0}^{N} \left(\frac{\partial^{N_1+\cdots+N_n} h_i^0\left(x(k)\right)}{\partial x_1^{N_1} \cdots \partial x_n^{N_n}} \right)\Bigg|_{x=x_{ss}} \frac{(x_1 - x_{ss})^{N_1} \cdots (x_n - x_{ss})^{N_n}}{N_1! \cdots N_n!}$$

$$\vdots \qquad (32.1)$$

$$h_i^{r_i-1}\left(x(k)\right) \approx \sum_{N_1=0}^{N} \cdots \sum_{N_n=0}^{N} \left(\frac{\partial^{N_1+\cdots+N_n} h_i^{r_i-1}\left(x(k)\right)}{\partial x_1^{N_1} \cdots \partial x_n^{N_n}} \right)\Bigg|_{x=x_{ss}} \frac{(x_1 - x_{ss})^{N_1} \cdots (x_n - x_{ss})^{N_n}}{N_1! \cdots N_n!}$$

and when $r = r_i, \ldots, p_i$

$$h_i^{r_i}\left(x(k),u(k)\right) \approx \sum_{N_1=0}^{N} \cdots \sum_{N_n}^{N} \left(\frac{\partial^{N_1+\cdots+N_n} h_i^{r_i}\left(x(k),u(k)\right)}{\partial x_1^{N_1} \cdots \partial x_n^{N_n}} \right)\Bigg|_{x=x_{ss}} \frac{(x_1 - x_{ss})^{N_1} \cdots (x_n - x_{ss})^{N_n}}{N_1! \cdots N_n!}$$

$$\vdots \qquad (32.2)$$

$$h_i^{p_i}\left(x(k),u(k),0,\ldots\right) \approx \sum_{N_1=0}^{N} \cdots \sum_{N_n}^{N} \left(\frac{\partial^{N_1+\cdots+N_n} h_i^{p_i}\left(x(k),u(k)\right)}{\partial x_1^{N_1} \cdots \partial x_n^{N_n}} \right)\Bigg|_{x=x_{ss}} \frac{(x_1 - x_{ss})^{N_1} \cdots (x_n - x_{ss})^{N_n}}{N_1! \cdots N_n!}$$

N is denoted the N^{th} order of Taylor series expansion, and x_{ss} is a equilibrium point corresponding to the desired set-point, y_{sp}, which satisfy

$$0 = f(x_{ss}, u_{ss})$$
$$y_{sp} = h(x_{ss})$$

The dependence of a nominal equilibrium point, x_{ss}, is obtained by solving above relation, which is denoted by:

$$x_{ss} = \zeta(y_{sp}) \qquad (33)$$

Substituting for the approximation defined in equation (32.1), (32.2) into equation (31), the state feedback can be represented by

$$u = \psi(x(k), y_{sp}, \beta) \tag{34}$$

Note that the Taylor series expansion and the feedback controller equation have been evaluated with the algebraic manipulation language such as MAPLE or MATHEMATICA.

4.1.4 The control system

In the real application, the disturbance is frequently occurred in the process due to the model mismatch or the measurement noise. Then, the performance of the controller is degraded to regulate the process. To resolve these problems, the state feedback of equation (34) is implemented with a disturbance estimator. An estimate of the disturbance is $y(k) - \tilde{y}(k)$, where $\tilde{y}(k)$ is the vector of a disturbance free, and $y(k)$ is the vector of controlled output. To estimate that information, the open-loop observer is applied. Open-loop state observer is applicable to the process which operates only within the domain of attraction of an asymptotically stable, steady state (Kanter *et al*., 2002). The dynamics of open-loop state observer is described by the following equation

$$\begin{aligned} \tilde{x}(k+1) &= f\left(\tilde{x}(k), u(k)\right) \\ \tilde{y}(k) &= h\left(\tilde{x}(k)\right) \end{aligned} \tag{35}$$

where $\tilde{y}(k)$ denote the vectors of estimated states.

Using the proposed state feedback method of equation (34), and the open-loop state observer of equation (35) leads to the following control system represented by

$$\begin{aligned} \tilde{x}(k+1) &= f\left(\tilde{x}(k), u(k)\right) \\ \tilde{y}(k) &= h\left(\tilde{x}(k)\right) \\ \nu &= y_{sp} + y(k) - \tilde{y}(k) \\ u &= \psi(\nu, \tilde{x}(k), \beta) \end{aligned} \tag{36}$$

The proposed control system structure is implemented as shown in Figure 14.

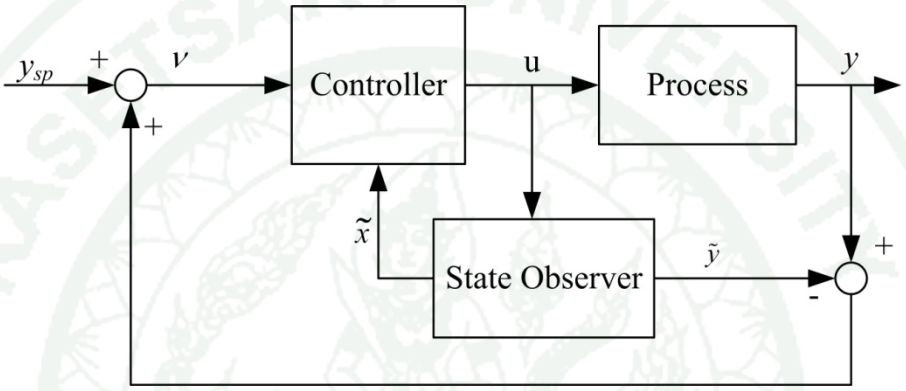

Figure 14 Schematic diagram of the proposed control structure

4.2 Implementation of control algorithm

The recently developed control system was created using NI's (National Instruments) LabVIEW, Version 8.2 with the LabVIEW module. The algorithm of the proposed control system is implemented into the NI C-RIO by following the sequence in Figure 15.

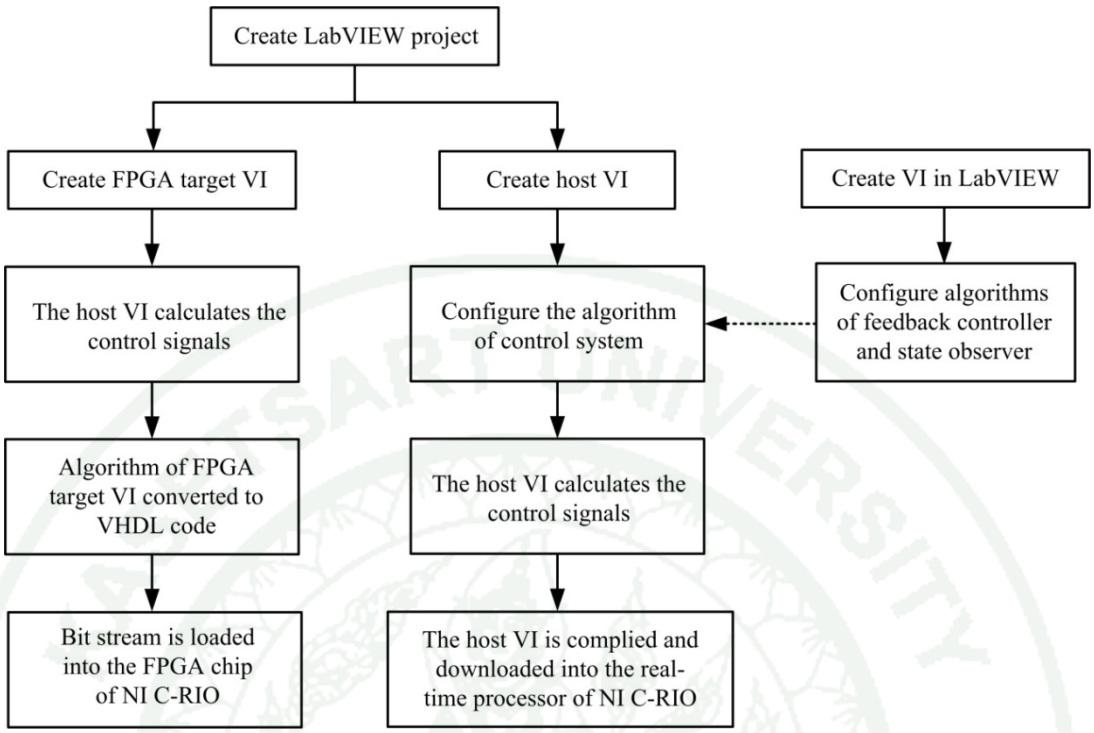

Figure 15 Flow diagram of the algorithm implementation into NI C-RIO

First, a FPGA target VI (Virtual Instrument) and a host VI are created in the project of the LabVIEW environment. The FPGA target VI is used in the data communication level to read/write data to the existing I/O modules on the NI C-RIO. Then, the FPGA target VI is compiled and downloaded into the NI C-RIO FPGA. The host VI is used for calculating the control action based on the control system algorithm, and sending control action value back to FPGA target. The host VI runs on a real-time processor. The dataflow of the LabVIEW control software is depicted in Figure 16.

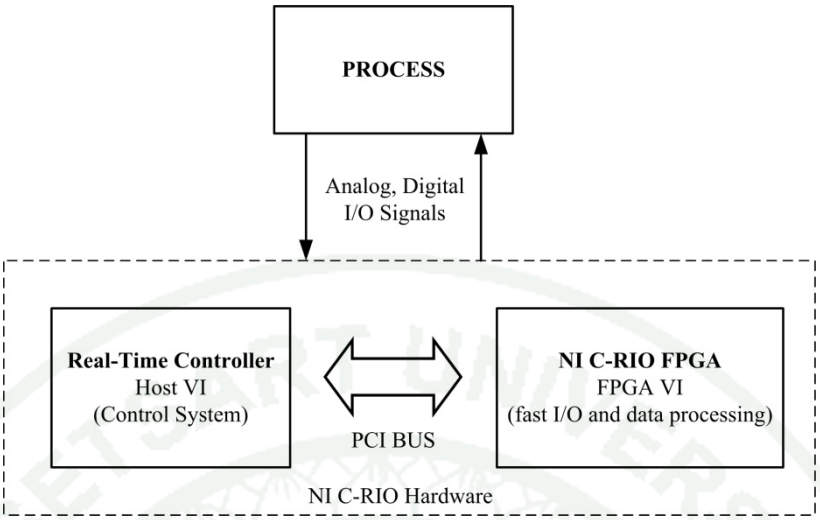

Figure 16 Dataflow of the NI C-RIO hardware

5. Test the of real-time control with non-minimum pilot process

To setup the real-time control, embedded model-based control device is connected with non-minimum pilot process. Before starting the experiment, the non-minimum pilot process needs to warm up until it is reached the given initial condition. Both servo and regulatory test are applied to evaluate the performance of embedded model-based control device. The responses of the input and output can be plotted by using the recorded data. To collate the efficient of the proposed control method with another technique, the performance of embedded approximate I/O controller is compared with the digital PI controller with the same set-points. The percentage of memory usage is used to check capacity of the NI C-RIO of each control method that consists of PI controller, approximate I/O linearization, and the proposed control system. The more memory allocate by the controller implementation, the more likely it will adversely affect application performance. The computer and NI C-RIO for check the percentage of memory usage are used in the same condition.

RESULTS AND DISCUSSION

Part I: The Performance Test of the Control System by Using the Numerical Simulation

1. Illustrative example for control of chemical processes with non-minimum phase behavior

1.1 Single-Input, Single-Output Chemical Reactor

Consider in continuous-stirred tank reactor in the constant-volume, non-isothermal operation as shown in Figure 17, in which the following exothermic irreversible reaction $A \rightarrow B$ takes place in the liquid phase. The reactor model has the form:

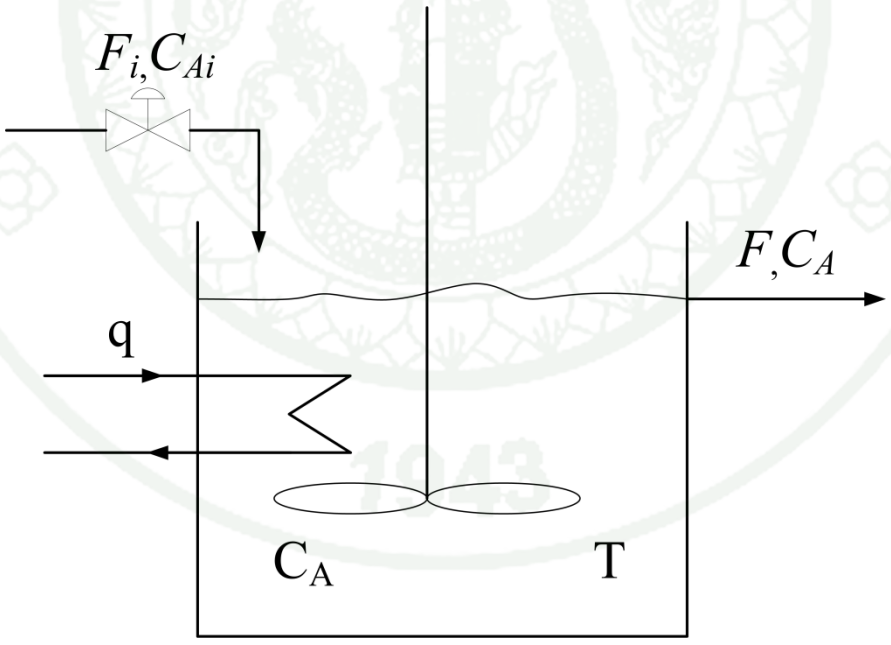

Figure 17 Schematic of the non-isothermal reactor.

$$\frac{dC_A}{dt} = -k_0 \exp\left(-\frac{E_a}{RT}\right) C_A + (C_{Ai} - C_A)\frac{F}{V}$$
$$\frac{dT}{dt} = \gamma k_0 \exp\left(-\frac{E_a}{RT}\right) C_A + (T_i - T)\frac{F}{V} + q$$

where C_A is the concentration of species A, C_{Ai} is the concentration of A in the fresh feed streams, F is the volumetric flow rate of the reactor feed, q is a cooling rate of the reactor, and V is the reactor volume. The reactor parameter values are given in Table 2.

Table 2 Parameters of non-isothermal reactor

Process Parameter	Values
C_{Ai}	12 kmol/m^3
T_i	302.5 K
V	7×10^{-3} m^3
E_a/R	8080 K
k_0	1.76×10^{12} hr^{-1}
γ	4.1 m^3 K kmol^{-1}
q	-120 K/h

The objective of this example is to maintain the reactor temperature, T , at the given set-point by manipulating the feed flow rate, u . Let $x = [C_A, T]^T$, $u = [F]$, and $y = [T]$. The desired set-point corresponding to y_{sp} = 317.5 K is (C_{Ass} = 3.206 kmol/m^3, T_{ss} =317.5 K, F_{ss} = 0.04 m^3/hr) is stable (the eigenvalues of process evaluated at the steady state pair are {-5.714, -4.876}, lie in the left half-plane). The zero dynamics of the process is governed by

$$\dot{\xi} = -\frac{q(C_{Ai} - \xi)}{T_i - y_{sp}} + k_0 \exp\left(-\frac{E_a}{R \cdot y_{sp}}\right)\left(-1 - \frac{\gamma(C_{Ai} - \xi)}{T_i - y_{sp}}\right)\xi \qquad (37)$$

whose Jacobian evaluated at $\xi_{ss} = [C_{Ass}]$ has eigenvalues in the right half-plane (RHF) at 16.146. Thus, the process has a non-minimum phase. The feedback controller in equation (24) with p=2 and the tuning parameter with $\beta = 0.3$ is applied to this example. In order to evaluate the optimal number of truncation term, the control output obtained from nonlinear process model is treated as validation data. The comparison result is shown in Figure 18 and Table 3. The 5th order truncation is considered in this work due to because the numerical convergence $\left|M^{i+1} - M^{i}\right|$ is less than the design criteria $(\leq 1.5\times10^{-4})$.

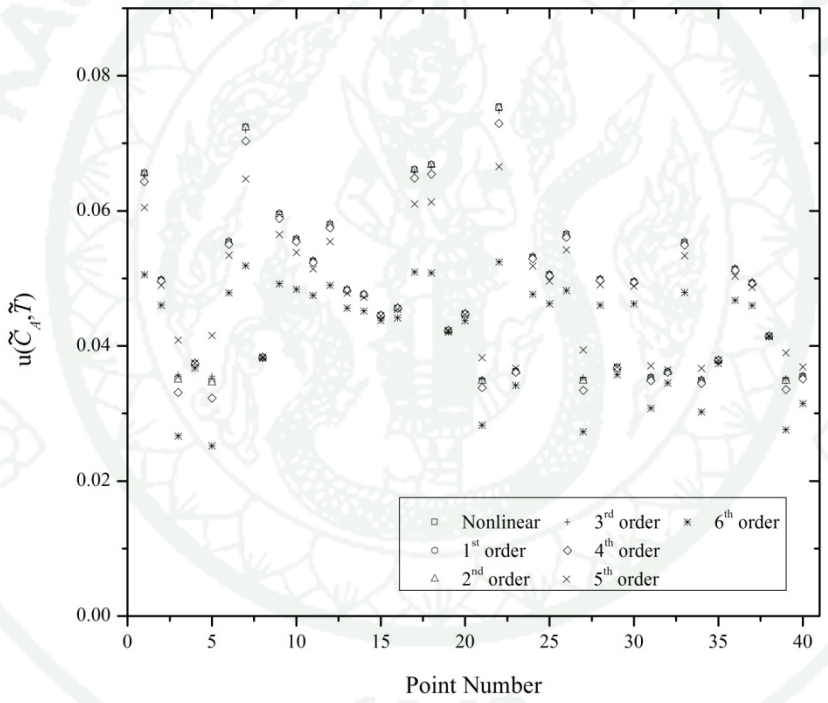

Figure 18 Validation data of the manipulated input under various truncated orders of the nonlinear model

Table 3 Mean Absolute Error for various truncation orders

Order of truncation (i)	Mean Absolute Error (MAE)	$\left\|M^{i+1}-M^{i}\right\|$
1	5.43×10^{-3}	8.90×10^{-4}
2	4.54×10^{-3}	2.63×10^{-3}
3	1.91×10^{-3}	9.90×10^{-4}
4	9.19×10^{-4}	3.06×10^{-4}
5	6.13×10^{-4}	1.02×10^{-4}
6	5.11×10^{-4}	-

The 5th order Taylor series of relative order equation is substituted into the proposed control method. Then, the feedback controller takes the form:

$$
\begin{aligned}
u = {} & (\beta(\text{-4.32E4} + 142.85T) + \beta^2(\text{-5.83E-4}(\text{-279.87} + T)\cdot(\text{9.97E4}+(\text{-624.09} + T)T)\cdot(\text{8.75E4}+(\text{-589.39} + T)T) + \text{3.73E4}C_A(\text{-292.97} + T)\cdot(\text{9.85E4} + (\text{-621.93} + T)T)\cdot(\text{8.71E4} + (\text{-589.25}+ T)T)) + 0.5(\beta^2((\text{8.64E4} - \text{2.85E9}\beta - \text{7.46E4}\beta C_A(\text{-292.97} + T)\cdot(\text{9.85E4} + (\text{-621.93} + T)T\cdot(\text{8.71E4} + (\text{-589.25} + T)T) + T(\text{-285.71} + \text{4.72E7}\beta + \text{1.16E-3}\beta(\text{-792.2} + T)T(\text{3.39E5} + (\text{-701.15} + T)T)))^2 - 4(\text{-6.17E6} + \text{2.04E4}T)\cdot(\text{-2.14E-6}\beta(\text{1.12E8} + \beta) - y_{sp} + T + \beta(\text{1.5E-4}\beta C_A^2(\text{-302.44} + T)\cdot(\text{1.01E5} + (\text{-635} + T)T)(\text{9.34E4} + (\text{-611.03}+ T)T) + T(\text{-1.15E-11} + \text{3.36E-8}\beta + T(\text{5.85E-14} - \text{2.11E-10}\beta + T(\text{-1.3E-16} + \text{6.63E-13}\beta + T(\text{1.08E-19} - \text{1.04E-15}\beta + \text{6.50E-19}\beta T)))) + C_A(\text{-3.33E6} + \text{1.67E9}\beta + T(\text{5.51E4} - \text{2.69E7}\beta + T(\text{-366.02} + \text{1.73E5}\beta + T(\text{1.21} - \text{559.06}\beta + T(\text{-2.03E-3} + 0.9\beta + (\text{1.36E-6} - \text{5.81E4}\beta)T)))))))^{0.5})/(\beta^2(\text{-6.17E6} + \text{2.04E4}T))
\end{aligned}
\tag{38}
$$

1.1.1 Controller Performance

The 5th order of state feedback controller has been applied to the process. The process is initially at the steady state ($C_A(0)$ = 3.72 kmol/m^3, $T(0)$ = 314.35 K). The set-point y_{sp} = 317.53 K and C_{Ai} = 12 kmol/m^3. The closed-loop

process responses are shown in Figure 19. The results show that the state feedback controller successfully forces the output to desired set-point. Initially, the reactor temperature is decrease due to the effect of low reaction rate. The controller is trying to decrease the fresh feed flow rate for increasing the reactor temperature to the desired set-point.

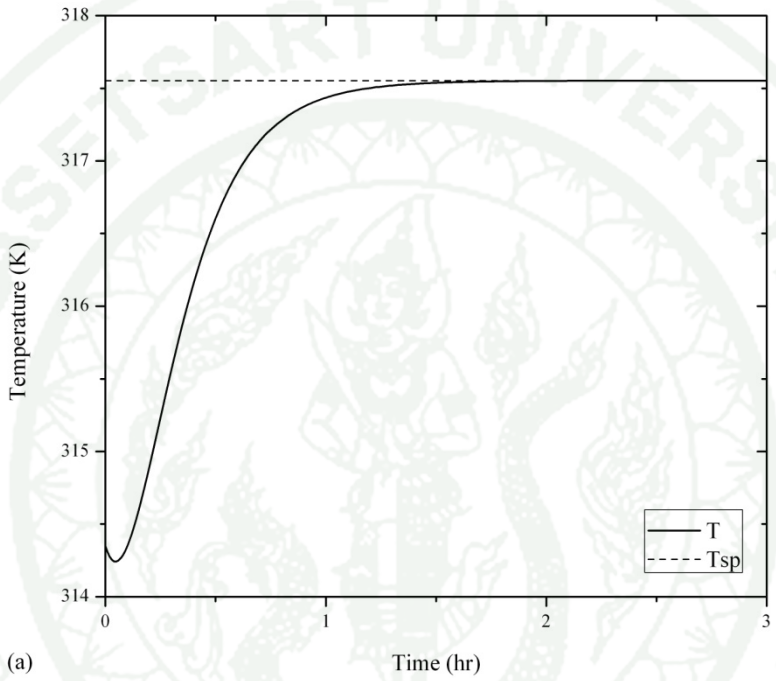

Figure 19 Closed-loop response of (a) the reactor temperature, (b) the concentration of *A*, and (c) the feed flow rate

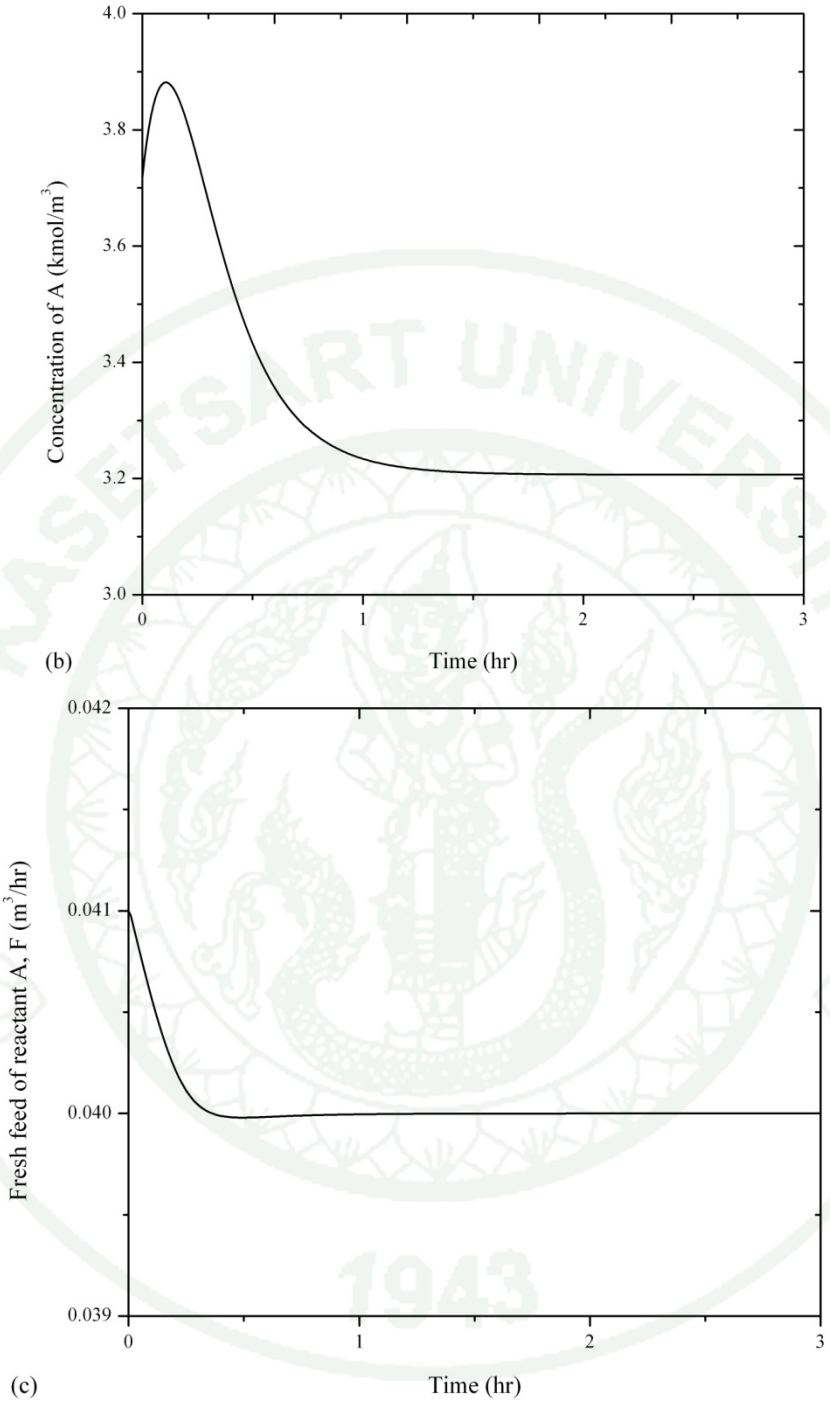

Figure 19 (Continuted)

The performance is tested by having step change in the set-points from 317.53 K to 320 K at time equal to 3 hours when the initially condition is at the steady state ($C_A(0)$ = 3.72 kmol/m^3, $T(0)$ = 314.35 K). The close-loop response of the

process with servo test is illustrated in Figure 20. The results show that the proposed controller successfully regulates the process close to their nominal equilibrium values.

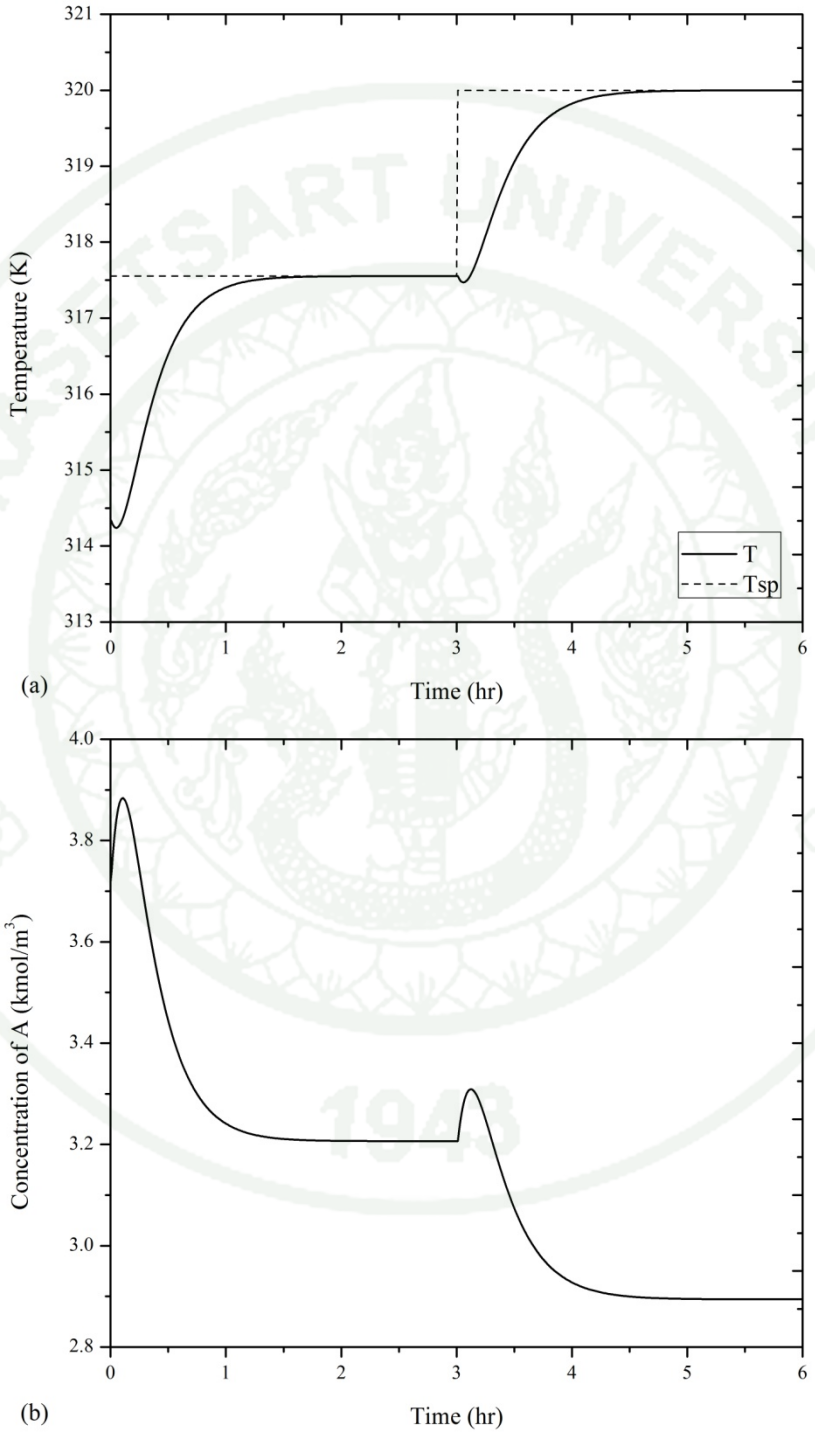

Figure 20 The responses of (a) the reactor temperature, (b) the concentration of *A*, and (c) the feed flow rate under servo test

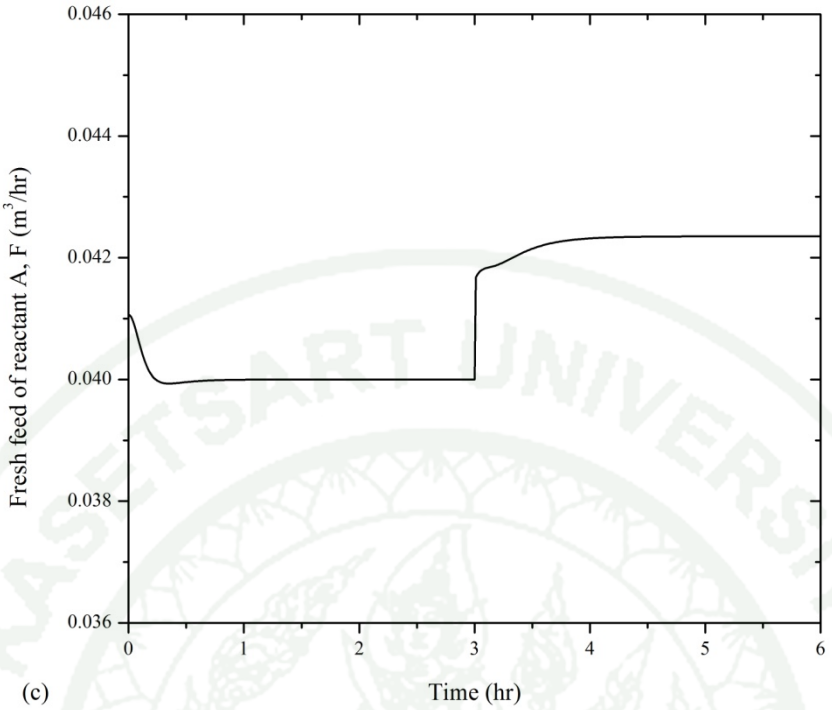

Figure 20 (Continuted)

The robustness of the proposed control system is tested by having step change in the unmeasured disturbance in reactor temperature, T ,+2 K at time equal to 1 hours. The control objective is to maintain the reactor temperature at 317.53 K when the process is initially at the steady state ($C_A(0)$ = 3.72 kmol/m^3, $T(0)$ = 314.35 K). The close-loop response of the process with regulatory test is illustrated in Figure 21. The results show that the proposed controller successfully maintains the output at the desired set-point although the disturbance is occurred in the process. The controller attempt to decrease the fresh feed flow rate for reject the disturbance in the process.

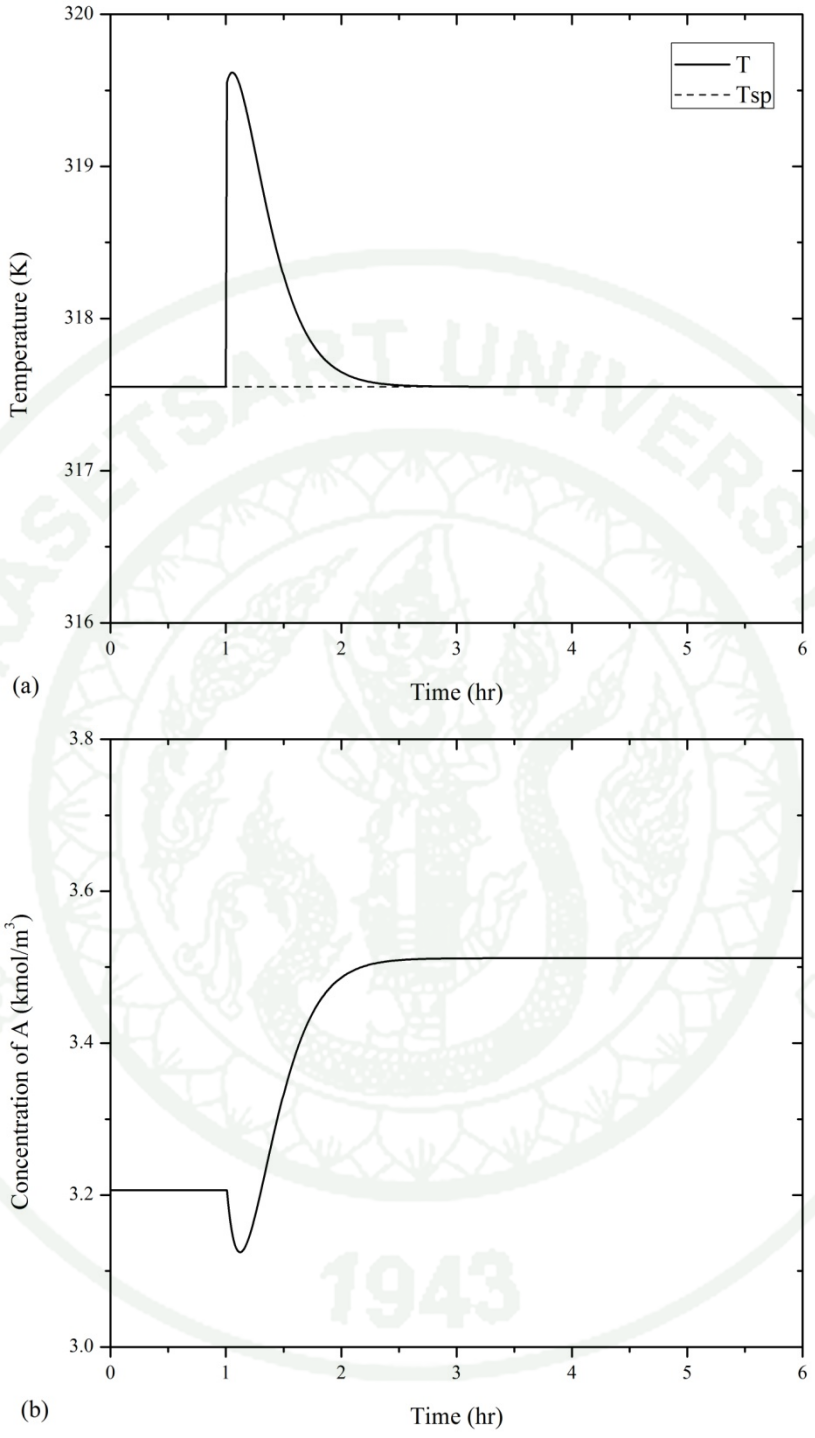

Figure 21 The responses of (a) the reactor temperature, (b) the concentration of *A*, and (c) the feed flow rate under regulatory test

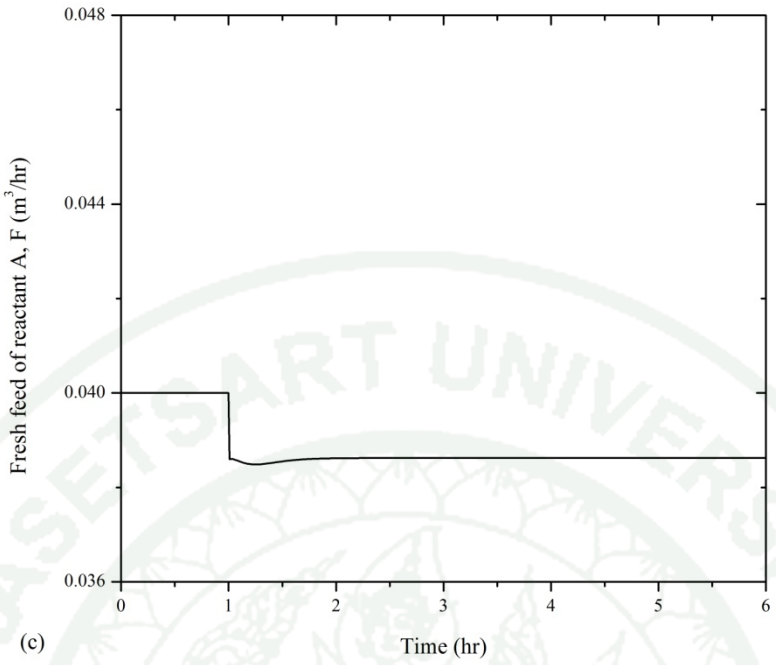

Figure 21 (Continuted)

1.2 Multi-Input, Multi-Output Chemical Reactor

Consider in two constant-volume, non-isothermal, continuous-stirred tank reactor as shown in Figure 22, in which the following irreversible series reactions, $A \rightarrow B \rightarrow C$, take place in the liquid phase. The reactor has a fresh feed stream consisting of pure A. The process dynamics are represented by the following model:

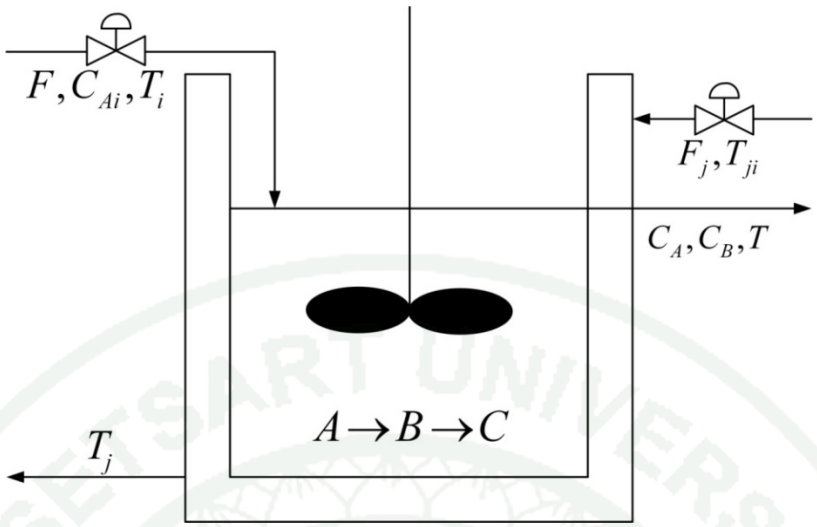

Figure 22 Schematic of multivariable, non-isothermal chemical reactor

$$\frac{dC_A}{dt} = \frac{F}{V}\left(C_{A_i} - C_A\right) - k_{A0}\exp\left(-\frac{E_1}{RT}\right)C_A^2$$

$$\frac{dC_B}{dt} = -\frac{F}{V}C_B + k_{A0}\exp\left(-\frac{E_1}{RT}\right)C_A^2 - k_{B0}\exp\left(-\frac{E_2}{RT}\right)C_B$$

$$\frac{dT}{dt} = \frac{F}{V_2}\left(T_i - T\right) + \frac{\left(-\Delta H_1\right)}{\rho c_p}k_{A0}\exp\left(-\frac{E_1}{RT}\right)C_A^2 + \frac{\left(-\Delta H_2\right)}{\rho c_p}k_{B0}\exp\left(-\frac{E_2}{RT}\right)C_B + \frac{US}{\rho c_p V}\left(T_j - T\right)$$

$$\frac{dT_j}{dt} = \frac{F_j}{V}\left(T_{ji} - T_j\right) - \frac{US}{\rho_j c_{pj} V_j}\left(T_j - T\right)$$

where C_A and C_B are the concentrations of A and B in reactors, C_{A_i} is the concentration of A in the fresh feed streams, F is the volumetric flow rate of the reactor feed, T is the reactor temperature, T_j is the jacket temperature, V is the reactor volumes, and V_j is the jacket volumes. The reactor parameter values are given in Table 4.

Table 4 The parameters of multivariable, non-isothermal chemical reactor

Process Parameter	Values
C_{Ai}	5 mol/L
T_i	400 K
T_{ji}	298.15 K
V	10 L
V_j	5 L
E_1/R	8023 K
E_2/R	9758 K
k_{A0}	9×10^{9} L mol^{-1} hr^{-1}
k_{B0}	1.287×10^{12} hr^{-1}
ρ	1 kg L^{-1}
ρ_j	1.1 kg L^{-1}
c_p	2.25 kJ kg^{-1} K^{-1}
c_{pj}	3 kJ kg^{-1} K^{-1}
S	0.225 m^2
U	3825 kJ m^{-2} K^{-1} s^{-1}
$-\Delta H_1$	39 kJ/mol
$-\Delta H_2$	10 kJ/mol

The objective of this example is to maintain the concentration of B in reactors, C_B and reactor temperature, T at the given set-point by manipulating the feed flow rate, F and cooling water, F_j. Let $x=[C_A\ C_B\ T\ T_j]^T$, $u=[F\ F_j]^T$, and $y=[C_B\ T]$. The desired set-point corresponding to set-point, y_{sp_1} = 1 mol/L and y_{sp_2} = 398 K, is (C_A = 0.4849 mol/L C_B = 1 mol/L T = 398 K T_j = 396 K) is stable (the eigenvalues of process evaluated at the steady state pair, {-83.179, -12.915, -7.755, -4.317 }, lie in the stable region). The zero dynamics of the process are governed by

$$\dot{\xi} = -k_{A0}\exp\left(-\frac{E}{Ry_{sp2}}\right)\xi^2 + (Cai - \xi) \times \left(\frac{\left(\exp\left(-\frac{E_1}{Ry_{sp2}}\right)k_{A0}\xi^2 - \exp\left(-\frac{E_2}{Ry_{sp2}}\right)k_{B0}y_{sp1}\right)}{y_{sp1}}\right) \quad (39)$$

whose Jacobian evaluated at $\xi_{ss} = [C_{A_{ss}}]^T$ has eigenvalues in the right half-plane (RHF) at 53.127. Thus, the process has a non-minimum phase. The feedback controller in equation(5) with p = [2 2] and the tuning parameter with $\beta_1 = 0.13$, and $\beta_2 = 0.15$ are applied to this example. In order to evaluate the optimal number of truncation term, the relative order of the control output equation obtained from nonlinear process model is treated as validation data. The comparison result is shown in Figure 23 and Tables 5 and 6. The 4th order truncation is considered in this work due to because the numerical convergences $\left|M^{i+1} - M^{i}\right|$ are less than the design criteria $(\leq 1.5\times10^{-4})$.

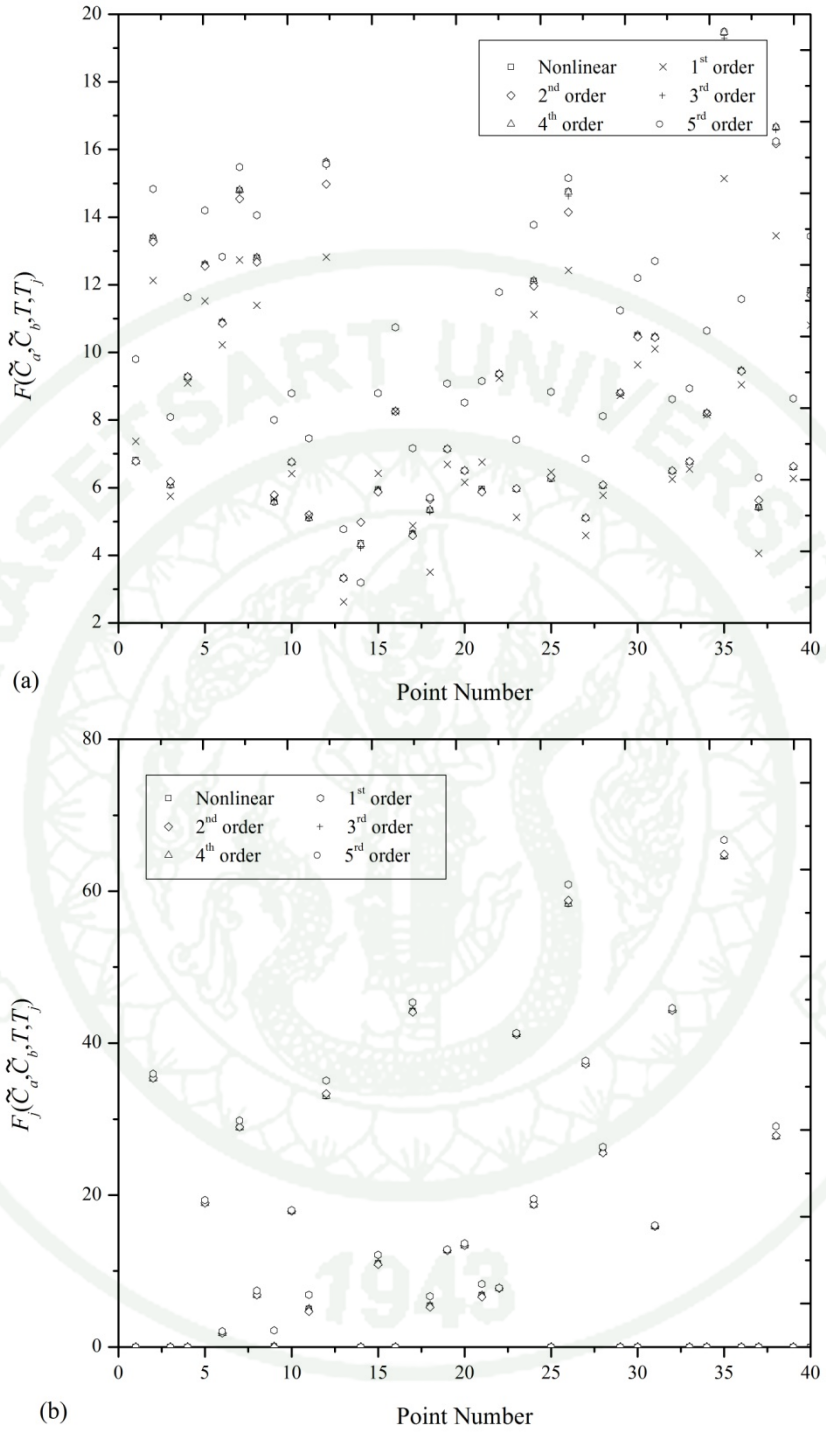

Figure 23 Validation data of the (a) the reactor feed flow rate (b) the jacket coolant flow rate under various truncation orders of the nonlinear model

Table 5 Mean Absolute Error for various truncation orders of reactor feed flow rate

Order of truncation (i)	Mean Absolute Error (MAE)	$\left\|M^{i+1}-M^{i}\right\|$
1	0.9098	0.777
2	0.1328	0.1092
3	0.0236	1.11×10^{-2}
4	0.0125	2×10^{-5}
5	0.01248	-

Table 6 Mean Absolute Error for various truncation orders of jacket coolant flow rate

Order of truncation (i)	Mean Absolute Error (MAE)	$\left\|M^{i+1}-M^{i}\right\|$
1	0.5905	0.5227
2	0.0678	0.0611
3	0.0067	3.90×10^{-3}
4	0.0028	5×10^{-5}
5	0.00275	-

The 4th order Taylor series of relative order equation is substituted into the proposed control method. The full equation of the feedback controller is given in Appendix A. Then, the feedback controller takes the form:

$$u=\psi_{[2\ \ 2]}(\hat{C}_A,C_B,T,\hat{T}_j,\beta_1,\beta_2,y_{sp1},y_{sp2}) \tag{40}$$

1.2.1 Controller Performance

The 4th order of state feedback controller has been applied to the process. The initially condition at the steady state ($C_A(0) = 0.9615$ mol/L $C_B(0) = 0.5$ mol/L $T(0) = 390$ K $T_j(0) = 383$ K). The set-point $y_{sp_1} = 1$ mol/L and $y_{sp_2} = 398$ K, and $C_{Ai} = 5$ mol/L. The closed-loop process responses are shown in Figures 24-26. The results show that the state feedback controller successfully forces the output to desired set-point. Initially, the reactor temperature is decreasing due to the effect of the low reaction rate. The controllers try to regulate the cooling water flow rate and fresh feed reactant for increasing the reactor temperature.

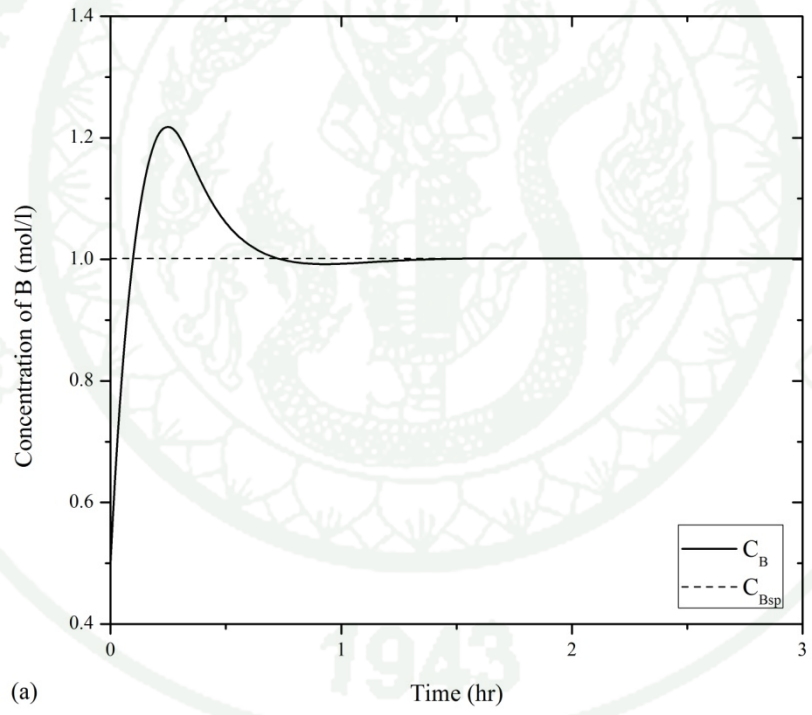

Figure 24 Closed-loop responses of (a) the concentration of *B* and (b) the reactor temperature of the chemical stirred tank reactor

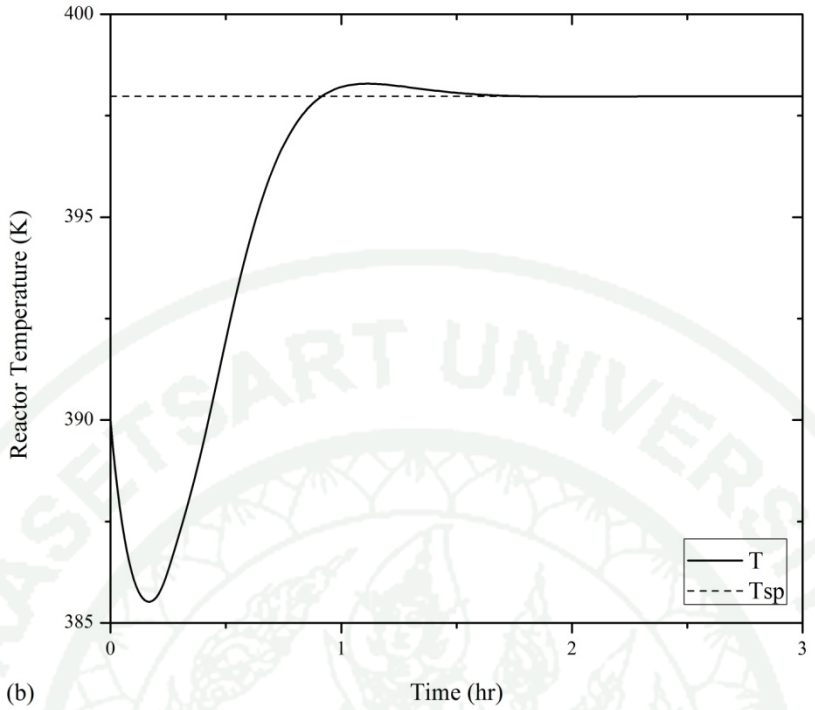

Figure 24 (Continuted)

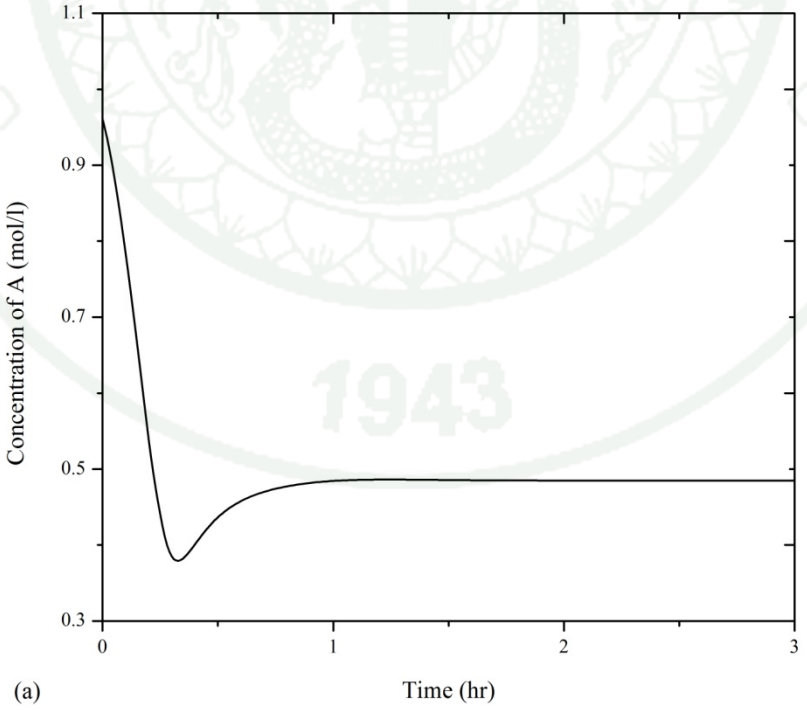

Figure 25 Closed-loop responses of (a) the concentration of *A* and (b) cooling jacket temperature of the chemical stirred tank reactor

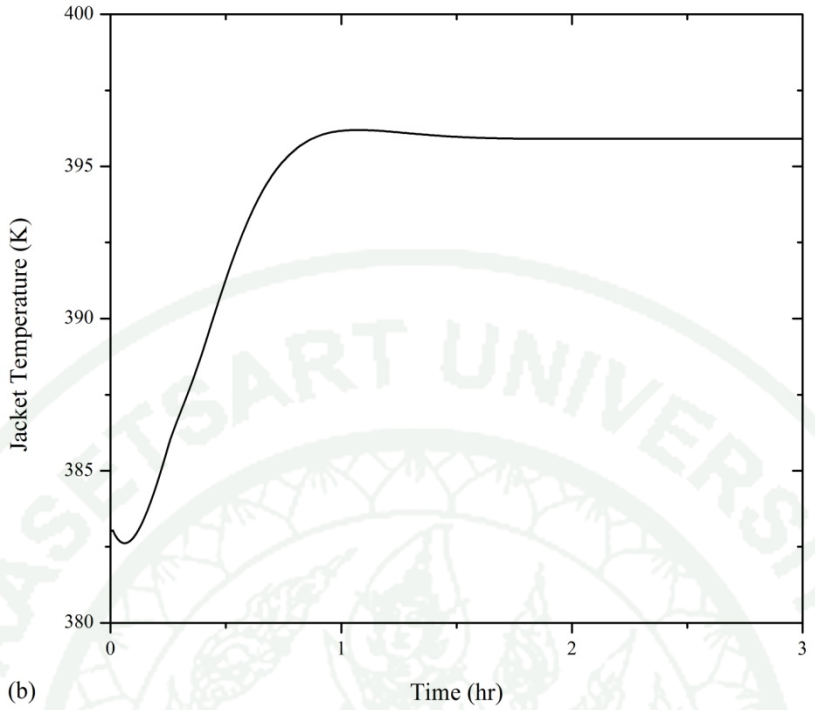

Figure 25 (Continued)

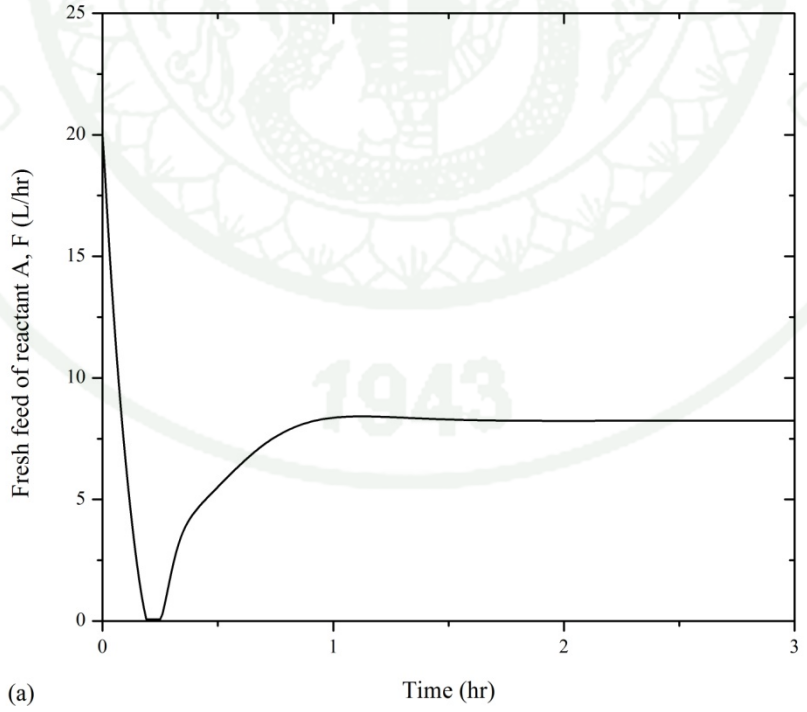

Figure 26 Closed-loop responses of (a) the reactant feed flow rate and (b) the cooling water flow rate of the chemical stirred tank reactor

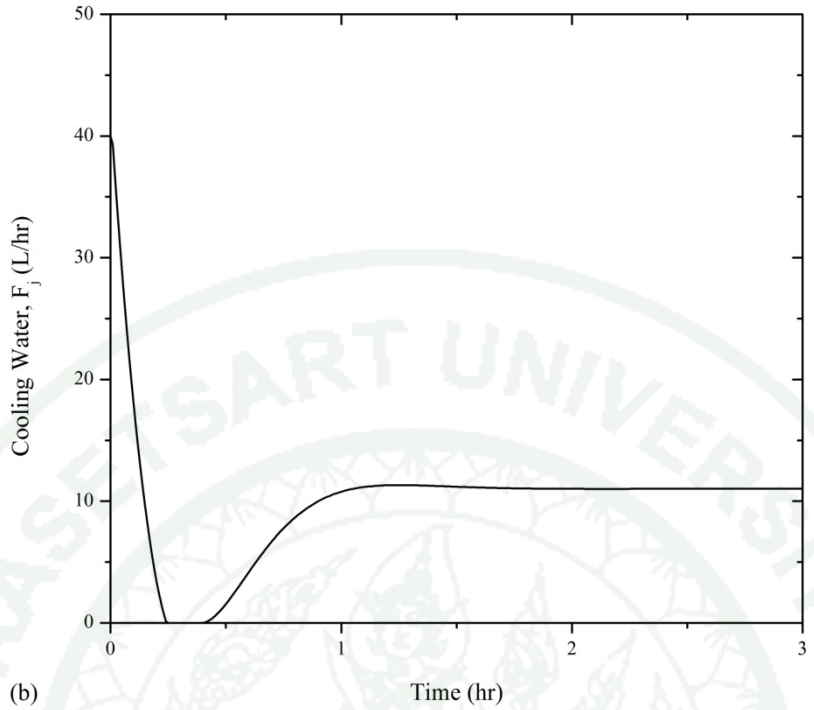

Figure 26 (Continuted)

The performance were tested by having step change in the set-points, y_{sp_1}, from 1 mol/L to 0.6 mol/L and y_{sp_2}, from 398 K to 392 K at time equal to 4 hours. The initially at the steady state is ($C_A(0) = 0.9615$ mol/L $C_B(0) = 0.5$ mol/L $T(0) = 390$ K $T_j(0) = 383$ K). The close-loop response of the process with servo test is illustrated in Figure 27-29. The results show that the proposed controller successfully regulates the process close to their nominal equilibrium values.

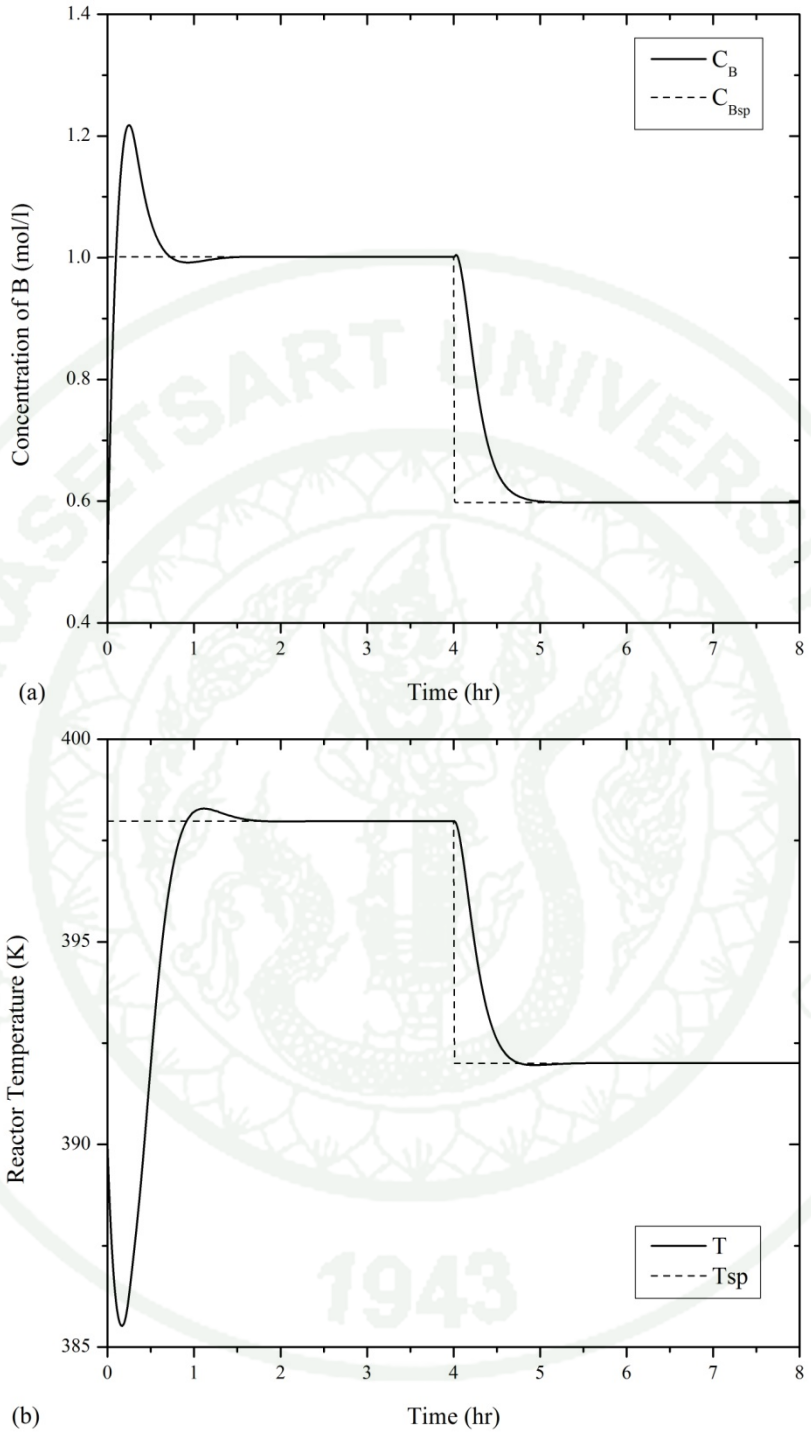

Figure 27 The responses of (a) the concentration of *B* and (b) the reactor temperature of the chemical stirred tank reactor under servo test

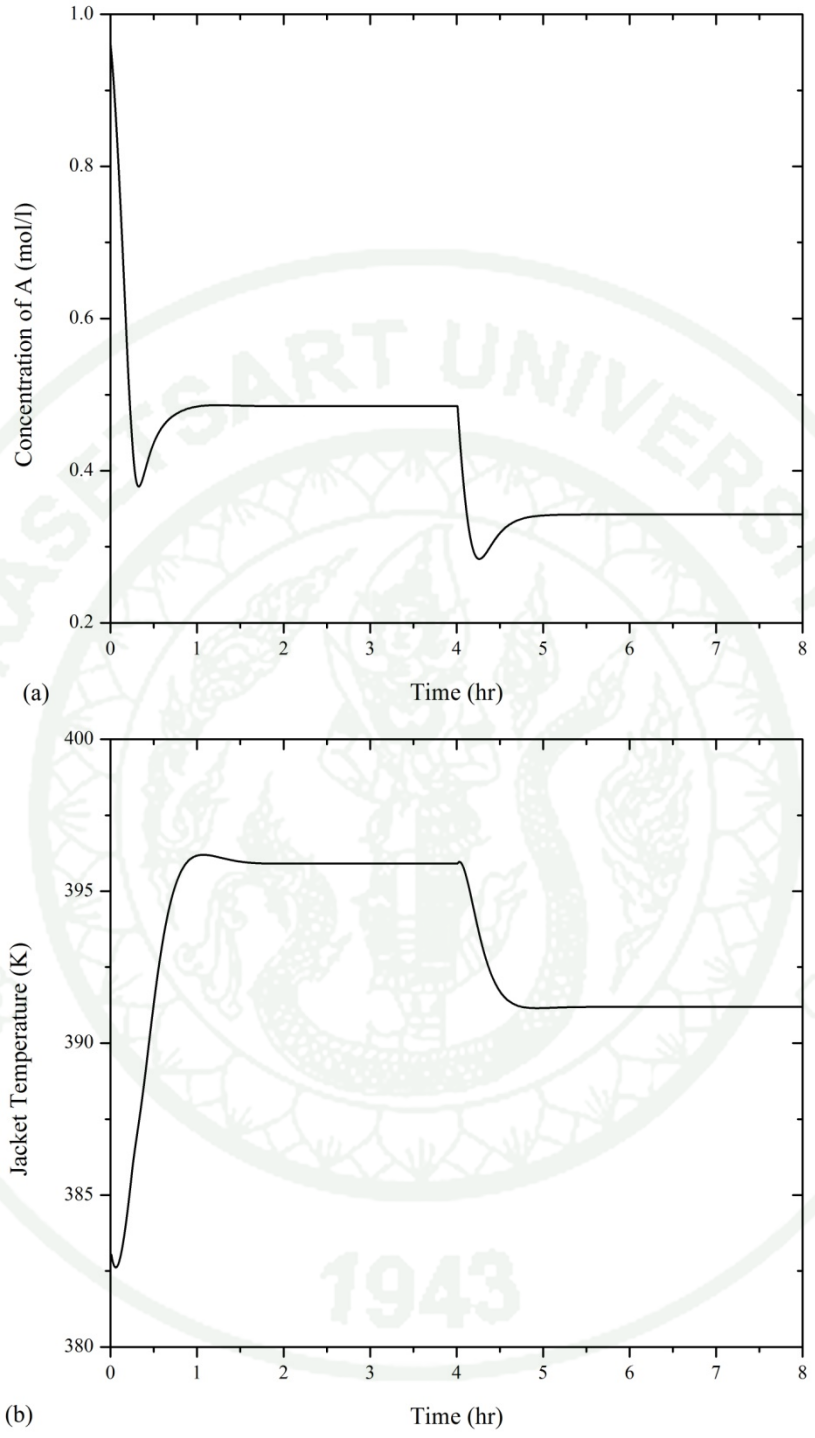

Figure 28 The responses of (a) the concentration of *A* and (b) the cooling jacket temperature of the chemical stirred tank reactor under servo test

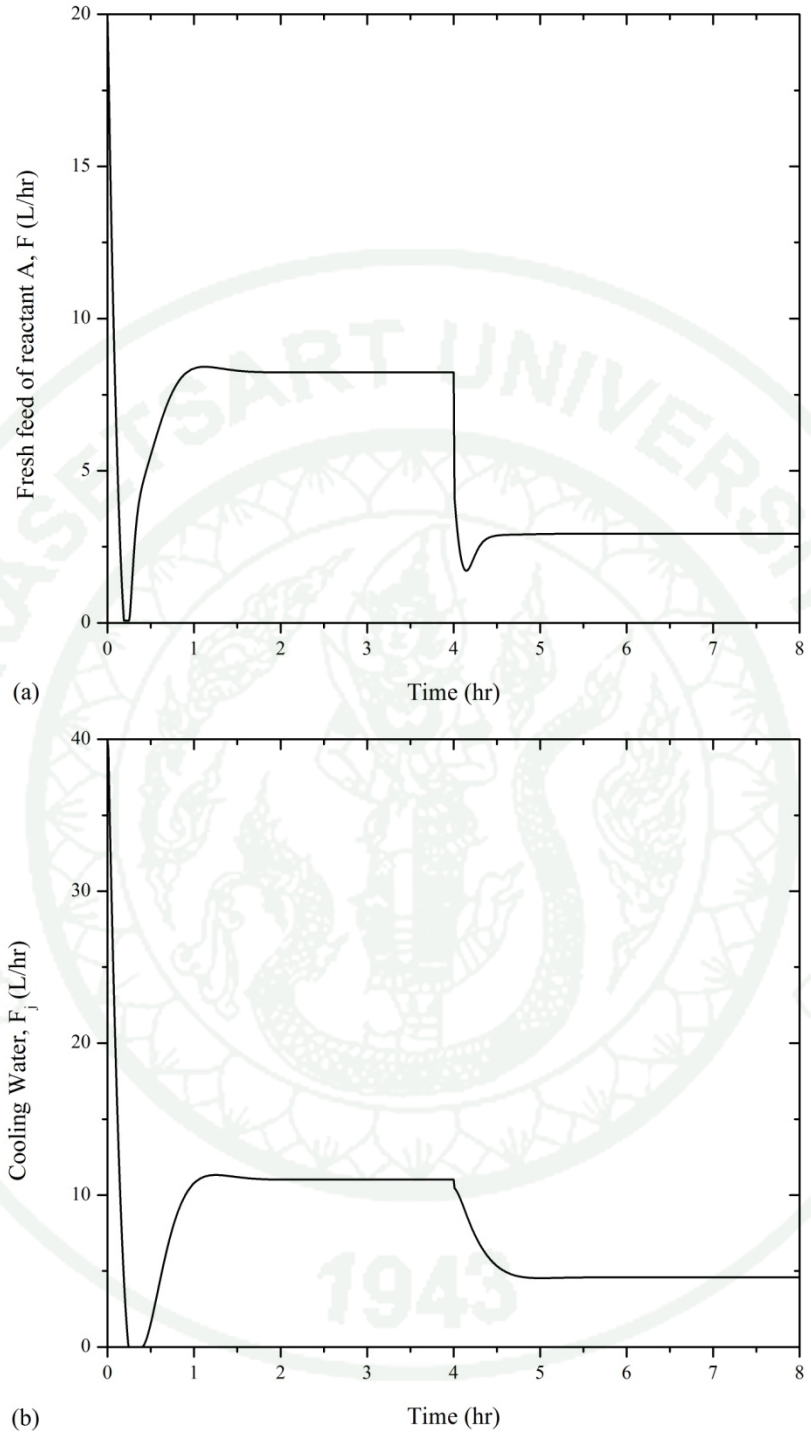

Figure 29 The responses of (a) the reactant feed flow rate and (b) the cooling water flow rate of the chemical stirred tank reactor under servo test

The robustness of proposed control system were tested by having step change in the unmeasured disturbance in concentration of B, C_B, +0.2 mol/l, and reactor temperature, T ,+2 K at time equal to 1 hours. The control objective is to maintain the reactor temperature at 398K when the initially condition is at ($C_A(0) =$ 0.9615 mol/L $C_B(0) =$ 0.5 mol/L $T(0) =$ 390 K $T_j(0) =$ 383 K). The closed-loop response of the process with regulatory test is illustrated in Figures 30-32. The results show that the proposed controller successfully maintains the output at desired set-point although the disturbance is occurred in the process.

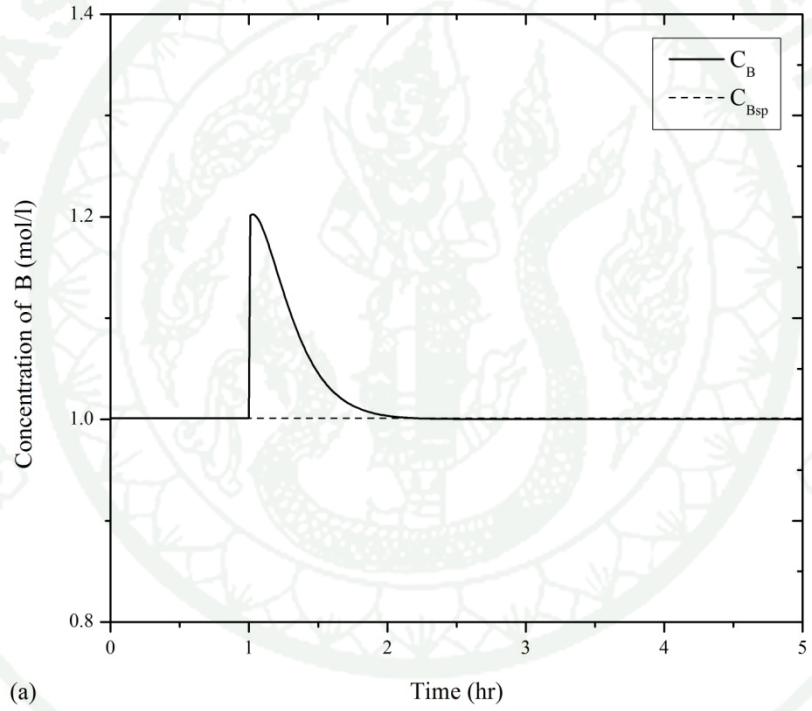

Figure 30 The responses of (a) the concentration of B and (b) reactor temperature of the chemical stirred tank reactor under regulatory test

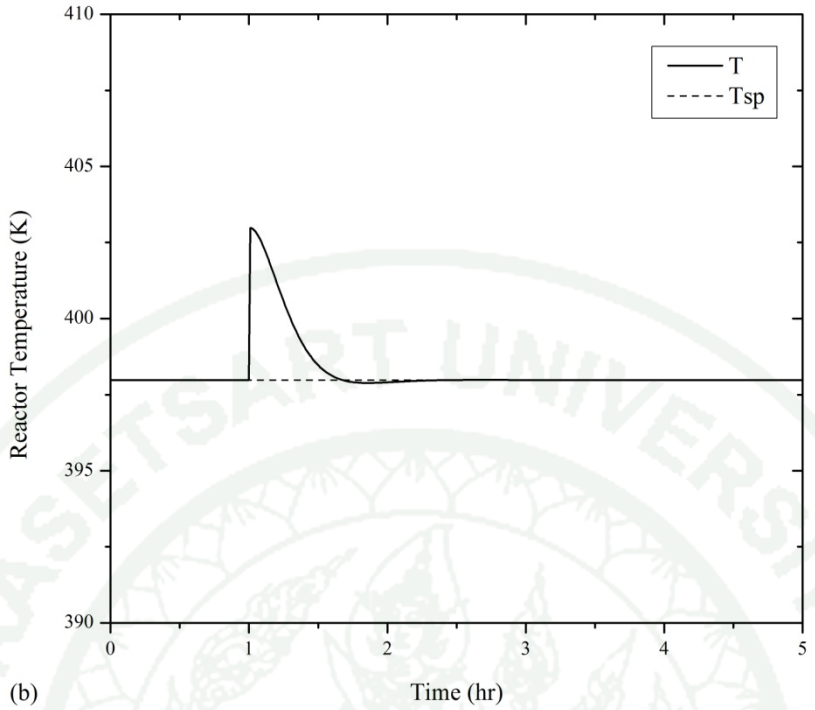

Figure 30 (Continuted)

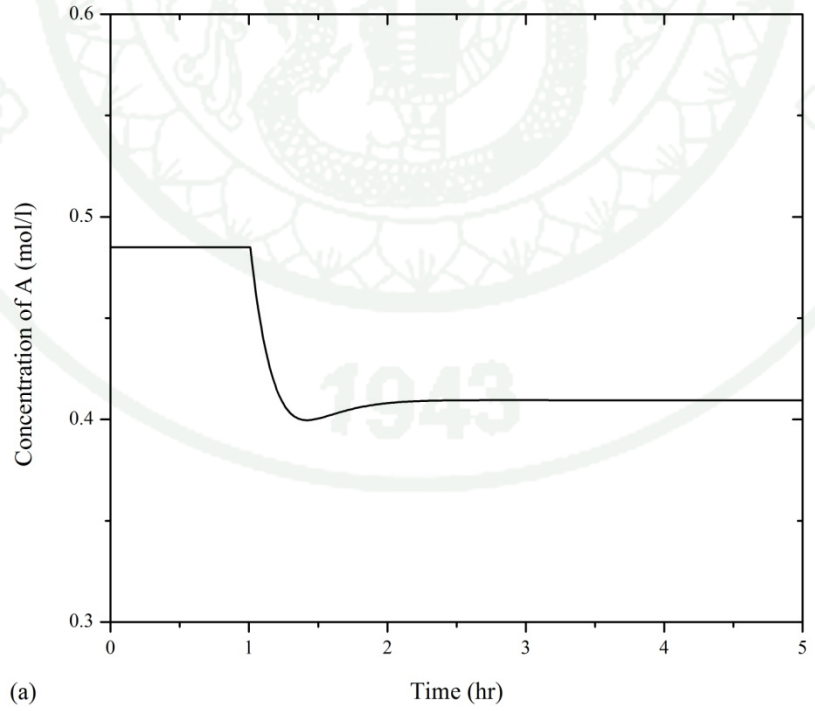

Figure 31 The responses of (a) the concentration of reactant A and (b) cooling jacket temperature of the chemical stirred tank reactor under regulatory test

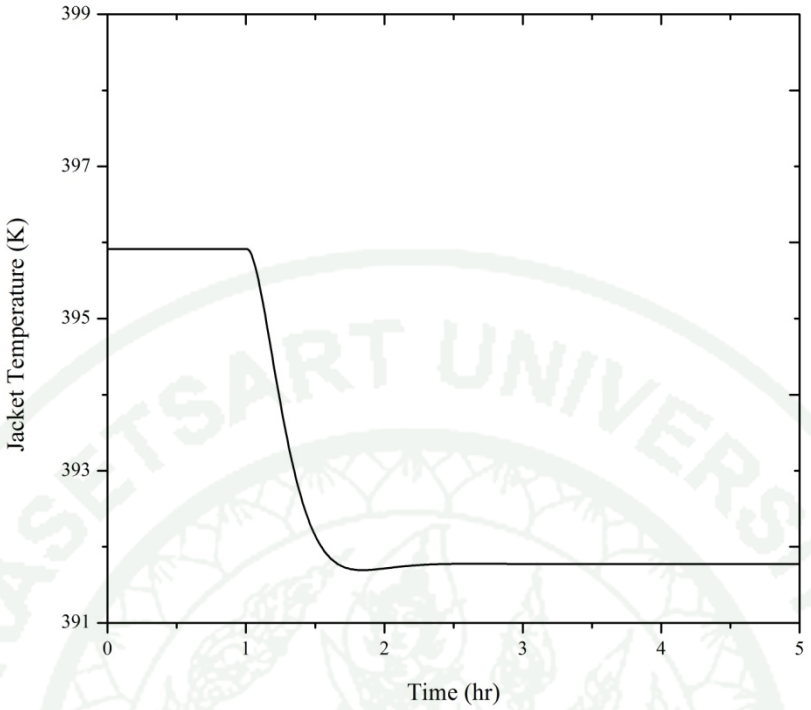

Figure 31 (Continuted)

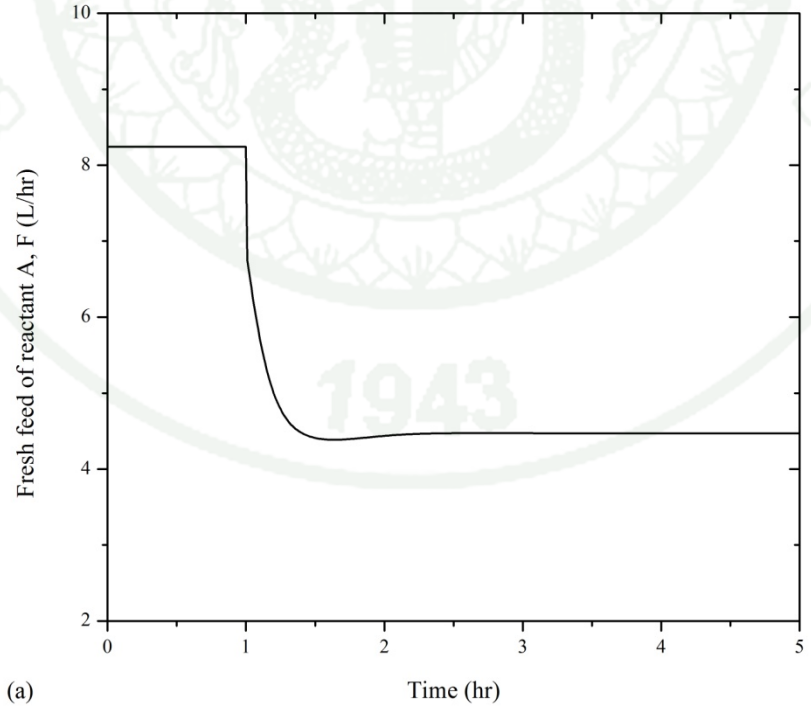

Figure 32 The responses of (a) the reactant feed flow rate and (b) cooling water flow rate of the chemical stirred tank reactor under regulatory test

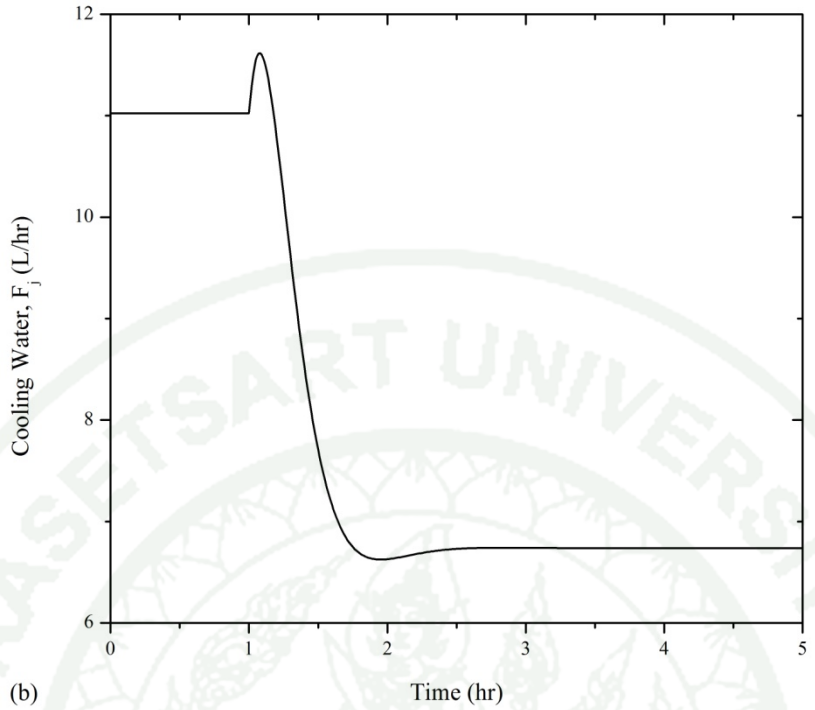

Figure 32 (Continuted)

<u>Part II:</u> Test of the Real-Time Control with Non-Minimum Phase Pilot Process

1. Real-time implementation of embedded model-based controller in the embedded device

1.1 The series solution of feedback controller for the non-minimum phase pilot process

The objective of the pilot process is to control the reactor temperature, T , at the given set-point by manipulating the feed flow rate, F . Let $x = [C_A, T]^T$, $u = [F]$, and $y = [T]$. The nominal equilibrium point corresponding to desired set-point y_{sp} = 317.4 K is {C_{Ass} = 3.335 kmol/m^3, T_{ss} = 317.4 K, u_{ss} = 0.045 m^3/h}, which is the stable and non-minimum phase region. The eigenvalues of process and zero dynamics evaluated at the given equlibrium point are {-5.802,-4.325} and 15.231, respectively. The requesting order with p=2 is applied in the controller formulation in equation (34). In order to evaluate the optimal number of truncation term, the values of the manipulated input obtained from given equilibrium states of the process in equation (25) are treated as validation data. The comparison result is shown in Figure 33 and Table 7.

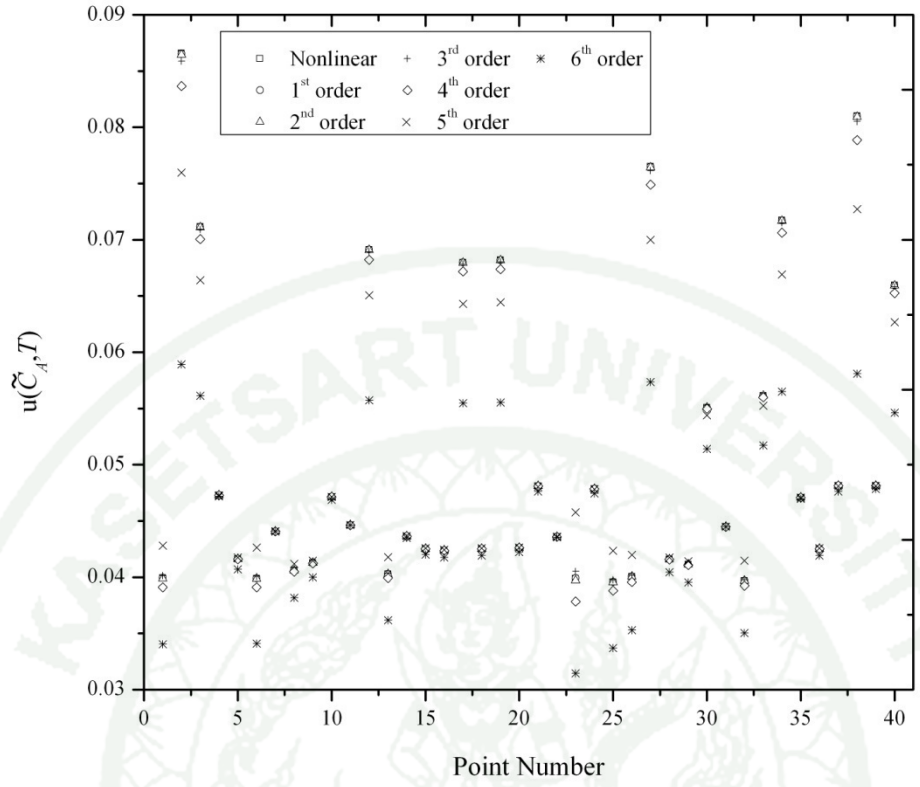

Figure 33 Validation data of the manipulated input under various truncation orders of the nonlinear model

Table 7 Mean Absolute Error for various truncation orders

Order of truncation (i)	Mean Absolute Error (MAE)	$\left\|M^{i+1}-M^{i}\right\|$
1	5.24×10^{-3}	3.43×10^{-3}
2	1.82×10^{-3}	1.36×10^{-3}
3	4.54×10^{-3}	3.35×10^{-4}
4	1.03×10^{-4}	8.26×10^{-5}
5	2.12×10^{-5}	1.33×10^{-5}
6	7.94×10^{-6}	-

The 5th order truncation is considered in this work because the numerical convergences $\left|M^{i+1}-M^{i}\right|$ is less than the design criteria ($\leq 1.5\times10^{-4}$). Then, the feedback controller takes the form:

$$
\begin{aligned}
u = {} & (-3.9E5\beta + 1.25E9\beta^2 - 8.23E8\beta^2 C_a + 128.94\beta T - 2.07\,\beta^2 T + 1.357E7\,\beta^2 C_A T + \\
& 13.7E5\,\beta^2 T^2 - 8.97E5\,\beta^2 C_a T^2 - 458.8\,\beta^2 T^3 + 297.23\,\beta^2 C_A T^3 + 0.76\,\beta^2 T^4 - \\
& 0.49\,\beta^2 C_A T^4 - 5.1E\text{-}3\,\beta^2 T^5 + 3E\text{-}3\,\beta^2 C_A T^5 + 0.5(\beta^2 2((7.8E\text{-}5 - 2.50E9\beta + (- \\
& 257.898 + 4.15E7\beta)T - 2.75E5\beta T^2 + 917.61\beta T^3 - 1.53\beta T^4 + 1.02E4\beta T^5 - \\
& 6.563E4\beta C_A(T\text{-}292.857)(98467.427\text{-}621.5781T+T^2)\times(8.7E3 - 5.8E2T + \\
& T^2))^2 - (-5.03E6 + 1.66E5T) \times (-2.39E2\beta - 2.91E\text{-}6\beta^2 - y_{sp} + (1 - 1.42E\text{-} \\
& 10\beta + 4.56E\text{-}8\beta^2)T + (8.77E\text{-}13 - 2.86E\text{-}10\beta)\beta T^2 + (-2.69E\text{-}15 + 8.90E\text{-} \\
& 13\beta)\beta T^3 + (4.14E\text{-}18 - 1.39E\text{-}15\beta)\beta T^4 + (-2.54E\text{-}21 + 8.67E\text{-}19\beta)\beta T^5 + 1.41E\text{-} \\
& 3\beta^2 C_A^2 + (T\text{-}302.270)(1.01E5 - 634.6T + T^2)(9.33E5 - 610.67T + T^2) + \beta C_A(- \\
& 3.23E6 + 1.56E9\beta + (53593.90 - 2.51E7\beta)T + (-356.097 + 1.62E5\beta)T^2 + (1.18 \\
& - 523.04\beta)T^3 + (-0.00198 + 0.84\beta)T^4 + (1.32E\text{-}6 - 0.000544\beta)T^5))^{0.5})))/(\beta^2(- \\
& 5.03E6 + 1.6627E\text{-}4T))
\end{aligned}
\tag{41}
$$

It is clear that the controller equation is in a simple form and requires only standard operator such as multiplication, subtraction, division, and addition operation.

1.2 Control algorithm implementation

The control system, including the feedback controller in equation (42), is configured in the host VI as shown in Figure 34. The state observer can configure into the LabVIEW by using Formula Node. Finally, host VI and FPGA target VI is compiled and embedded into NI C-RIO via the use of LabVIEW FPGA. The LabVIEW FPGA translates the host VI to text-based VHSIC Hardware Description Language (VHDL) code. The bit stream file of VHDL code is loaded into the FPGA chip and reconfigures the gate array logic for obtaining the stand-alone embedded controller.

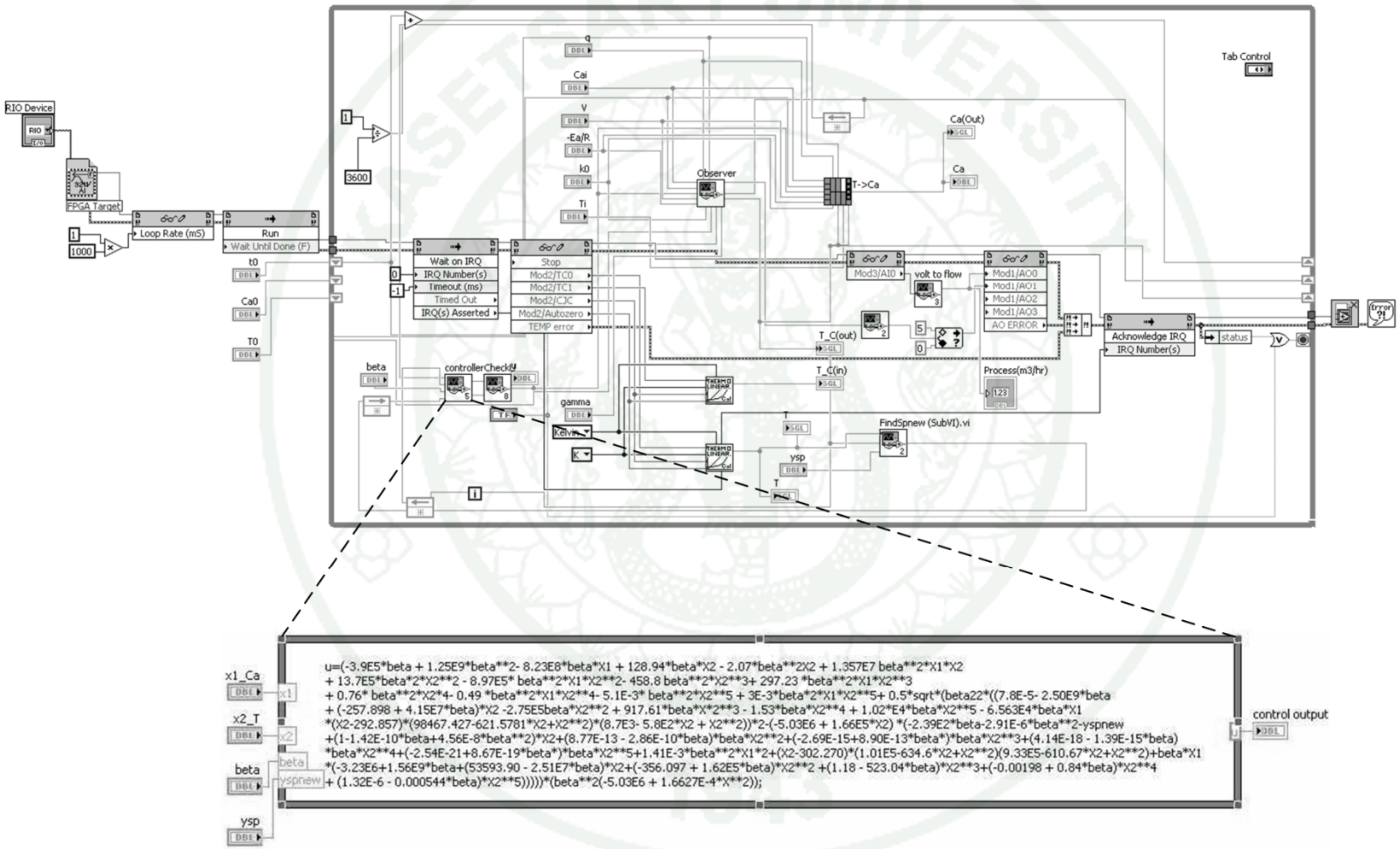

Figure 34 LabVIEW block diagram of the developed control system in NI C-RIO device

1.3 Real-time implementation

In the experimental results, first, the effect of turning parameter β on the output response is discussed. Next, the real-time embedded controller with the selected tuning parameter is evaluated the control performance both servo and regulatory tests. Then, the comparison of the control performances between the embedded model-based control device and PI controller is discussed. Finally, the percentage of memory usage of the proposed method is compared with other types of the controller equations that implement into the NI C-RIO device.

1.3.1 Effect of tuning parameter on the process response.

The control system in equation (42) is applied to the pilot process for studying the effect of tuning parameter (β) on process response by varying tuning parameters to be 0.2, 0.3 and 0.4 respectively. The initially at the steady state ($C_A(0)$ = 4.29 kmol/m^3, $T(0)$ = 310 K). The set-point y_{sp} = 317.4 K and C_{Ai} = 12 kmol/m^3. The experimental results are shown in Figure 35.

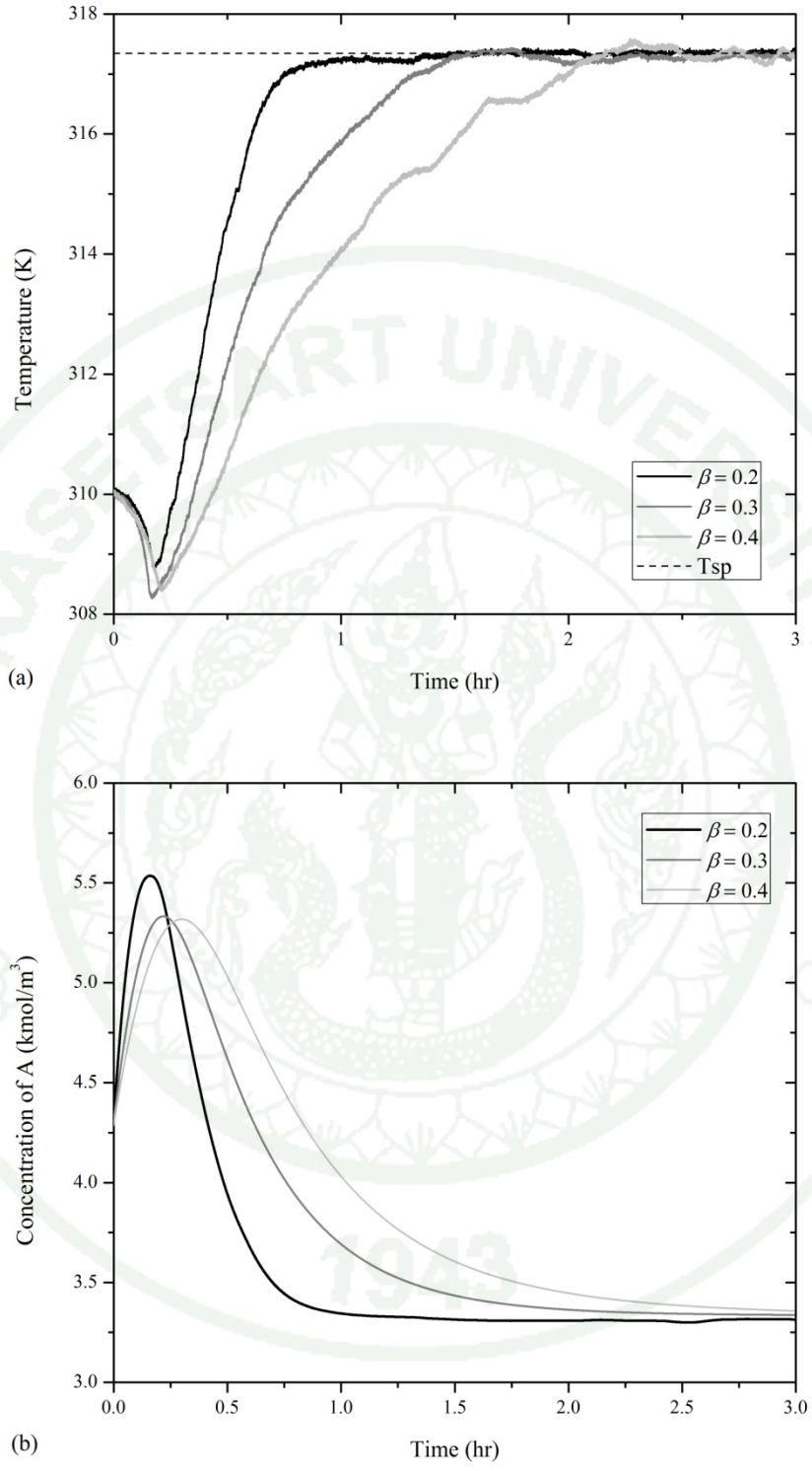

Figure 35 The effect of tuning parameter on the responses of (a) the reactor temperature, (b) the concentration of *A*, and (c) the feed flow rate in the real-time implementation of the non-minimum phase pilot process

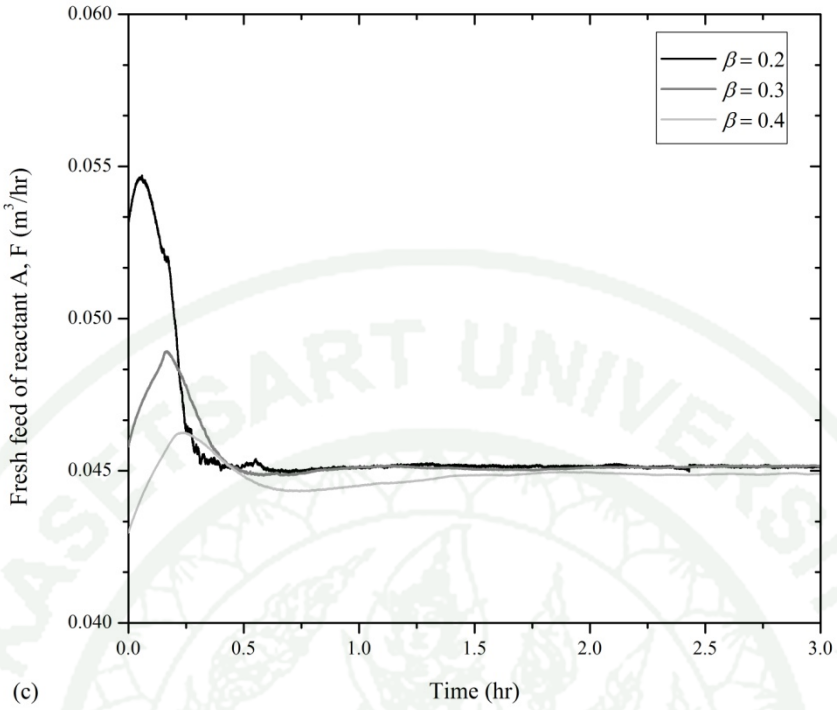

Figure 35 (Continuted)

When the value of tuning parameter β decreases, the output response trends reach the given set-point quickly. However, when the value of tuning parameter cannot decrease lower than 0.2 because the instability of the closed-loop system. The performance of the following tuning parameter that can be quantified by the integral square error (ISE) performance index:

$$\text{ISE}=\int_0^\infty (y_{sp}-h(x))^2 dt\,.$$

The ISE values corresponding to the tuning parameter are shown in Table 8. The result can be observed that the tuning parameter equal to 0.2 shows the lower ISE values. The embedded model-based control device with the tuning parameter, $\beta = 0.2$, show the best performance to control the non-minimum phase pilot plant. Thus, the tuning parameter $\beta = 0.2$ is chosen for the tests of servo and regulatory control performance in the following subsections.

Table 8 Quantitative analysis for the tuning parameter

The values of tuning parameter	ISE values for control output
$\beta = 0.2$	7.79
$\beta = 0.3$	11.40
$\beta = 0.4$	15.46

1.3.2 Servo performance

In this test, two initially at the steady state [$C_A(0)$, $T(0)$] = [4.297 kmol/m^3, 310 K] and [$C_A(0)$, $T(0)$] = [3.098 kmol/m^3, 319 K] which lie in the non-minimum phase region. The pilot process is desired to control at two different set-points that are initially at y_{sp1} = 317.4 K and then are changed to y_{sp2} = 314 K after 3 hours. The results in Figure 36 are shown that the proposed control system can force the output to both desired set-points with offset-free, regardless of the initial conditions of the process

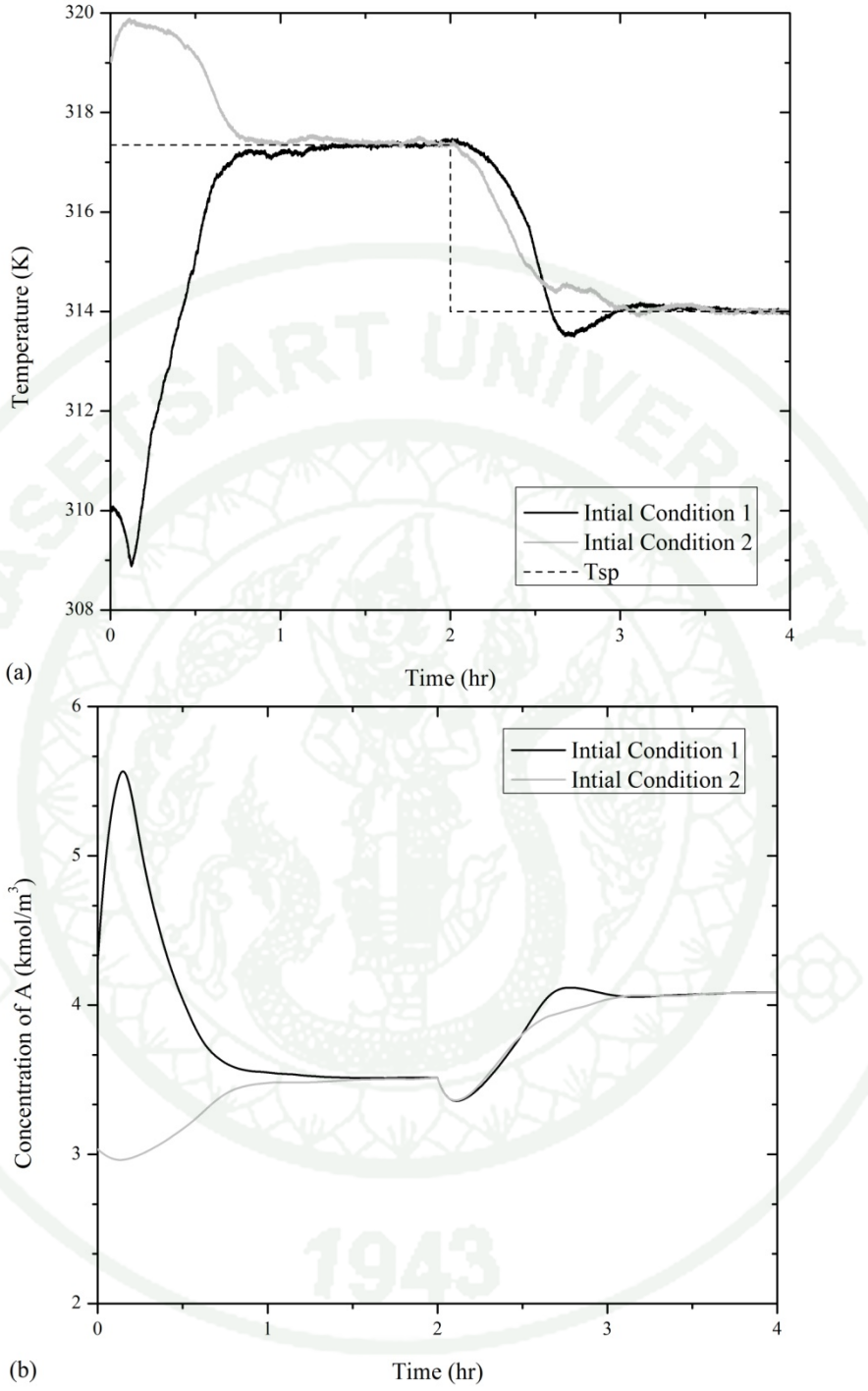

Figure 36 The responses of (a) the reactor temperature, (b) the concentration of *A*, and (c) the feed flow rate under servo test in the real-time implementation of the non-minimum phase pilot process

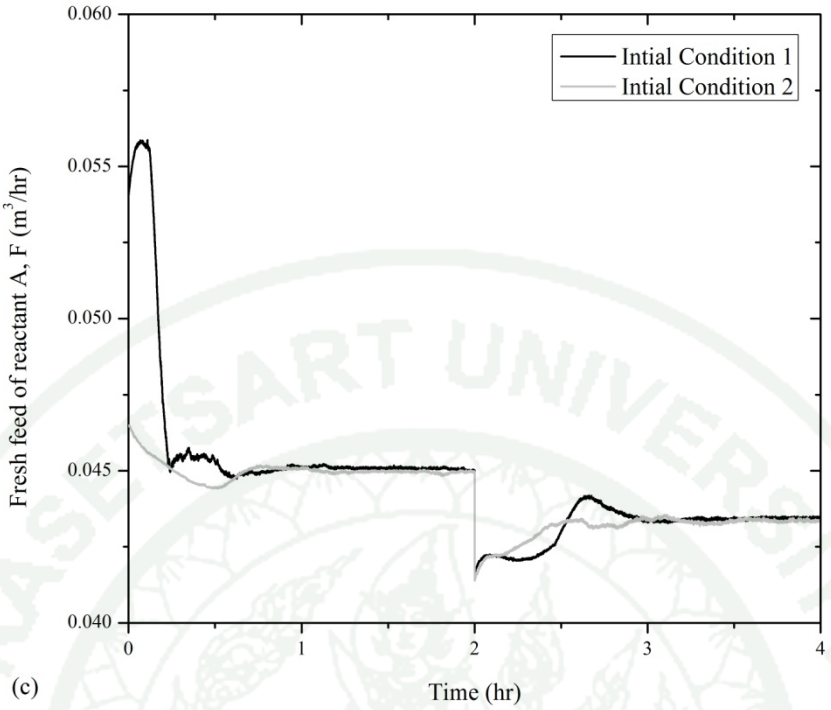

Figure 36 (Continuted)

1.3.3 Regulatory performance

In the experiment, the disturbance is occurred in the reactor outlet temperature, *T*. The unmeasured disturbance was assigned to +2 K of the reactor outlet temperature at time equal to 2 hours. The initially at the steady state ($C_A(0)$ = 4.2975 kmol/m^3, $T(0)$ = 310 K) is used and it is desired to provide the temperature at 317.4 K. The output responses of process are illustrated in Figure 37 and the result shows the responses of the state variables under the proposed control system lead to offset-free response in the presence of the unmeasured disturbance.

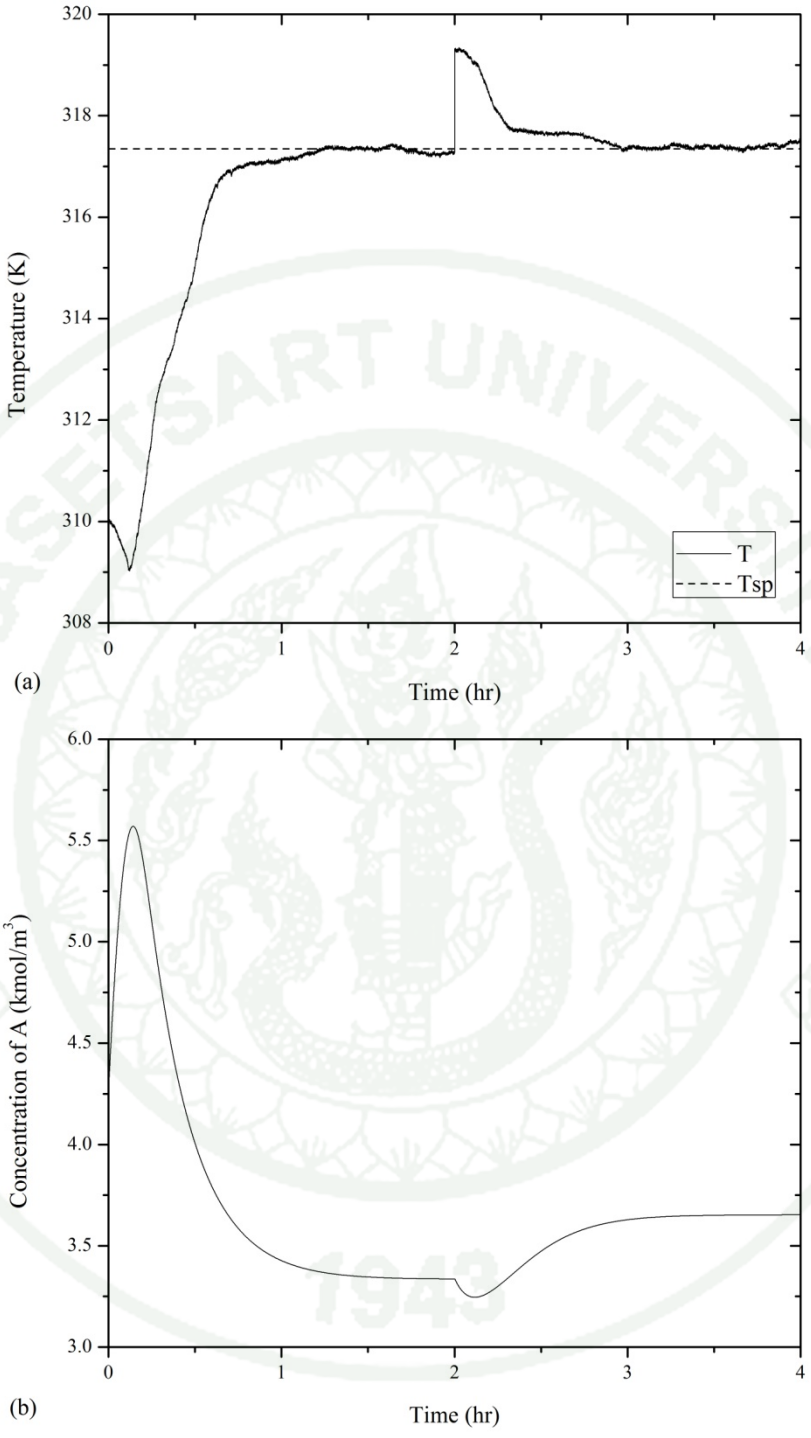

Figure 37 The responses of (a) the reactor temperature, (b) the concentration of *A*, and (c) the feed flow rate under regulatory test in the real-time implementation of the non-minimum phase pilot process

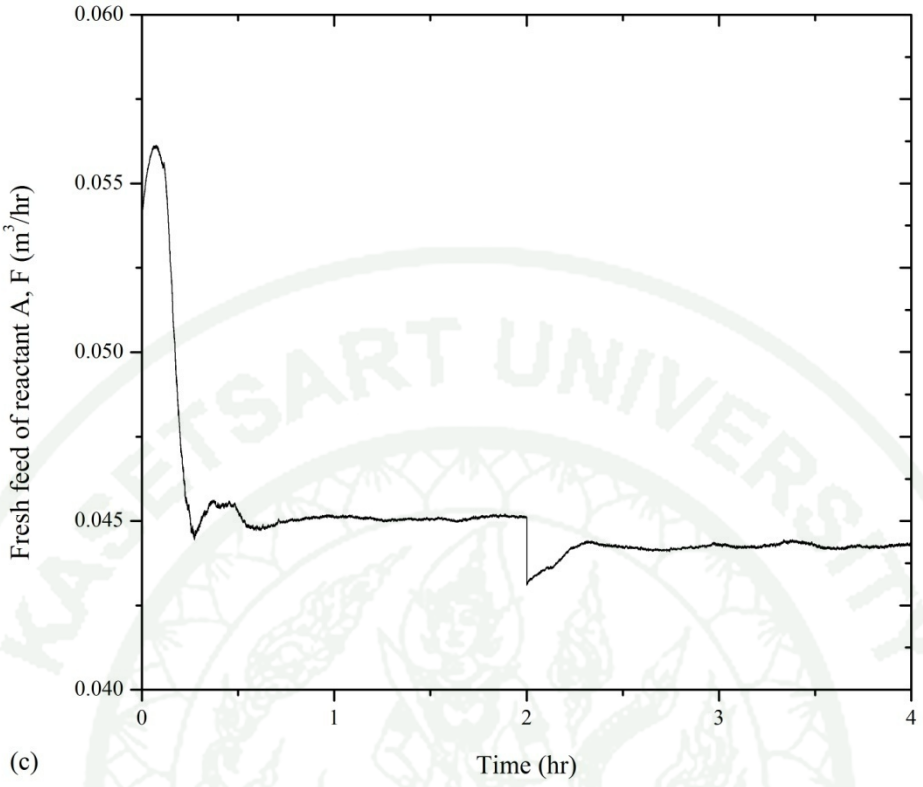

Figure 37 (Continuted)

1.3.4 Compare with PI control performance

The performance of embedded approximate I/O controller is compared with the digital PI controller described in equation (42) that is also embedded in NI-CRIO.

$$u_k = u_{k-1} + K_c\left[\left(y_{sp} - y_k\right) - \left(y_{sp-1} - y_{k-1}\right) + \frac{\Delta t\left(y_{sp} - y_k\right)}{\tau_i}\right] \qquad (42)$$
$$u_{lb} \le u_k \le u_{ub}$$

where u_{lb} and u_{ub} denote lower bound and upper bound of feed flow rate.

The values of tuning parameter of the PI controller, K_c = 6.41 and τ_i = 1 hr, are selected based on Ziegler–Nichols tuning method. In the test, the process

is initially at the steady state ($C_A(0)$ = 4.2975 kmol/m^3, $T(0)$ = 310 K). The experimental results are shown in Figure 38. The results show that the state feedback controller successfully forces the output to desired set-point while the PI controller cannot do it because the effect of non-minimum phase occurs.

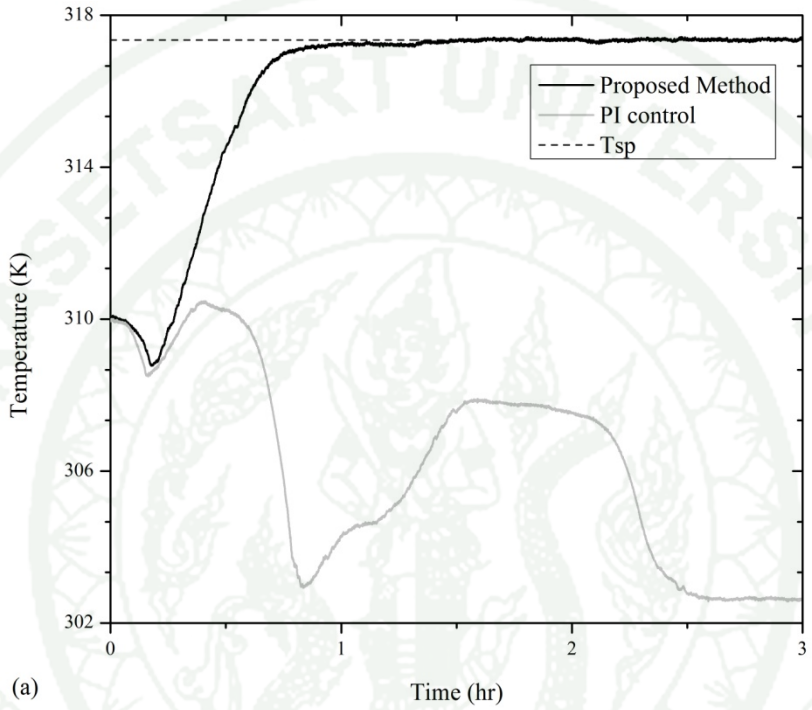

Figure 38 Comparison of the responses of (a) the reactor temperature, (b) the concentration of A, and (c) the feed flow rate under PI controller and the embedded controller

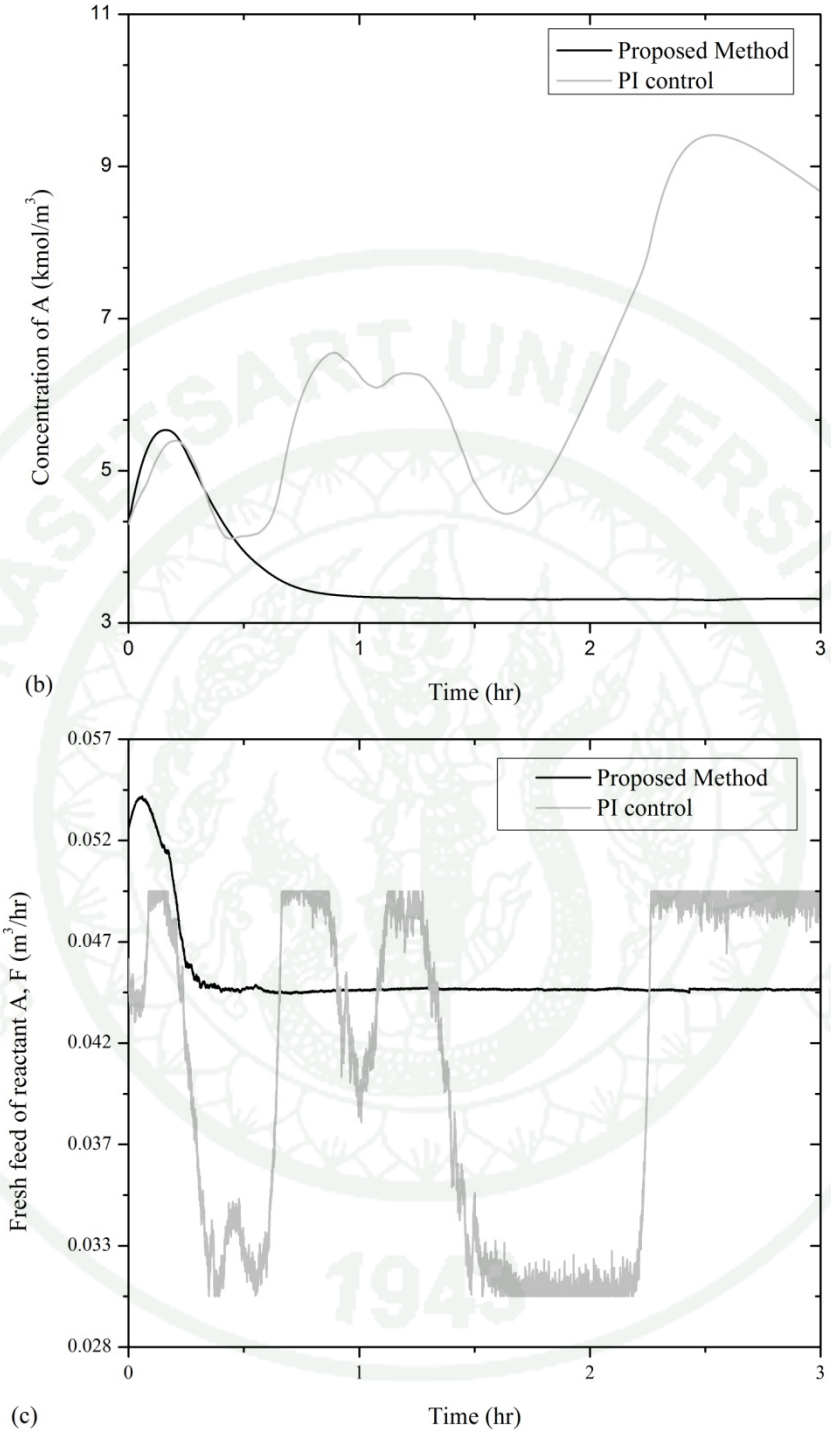

Figure 38 (Continuted)

The performance of the following two control techniques can be quantified by ISE value. The ISE values corresponding to the control techniques are shown in Table 9. The result can be observed that the embedded model-based control

device shows the best performance to control the pilot plant with the lowest ISE values.

Table 9 Quantitative analysis for the control system

The control techniques	ISE values for control output
Proposed method	7.79
PI controller	130.35

1.3.5 Comparison of Memory Usage

The Percentage of memory usage is measured from the individual implementation of the controller system into the NI C-RIO. The more memory allocates by the controller implementation, the more it adversely affects application performance. The comparison result is depicted in Figure 39. The proposed method consumes small amount of memory usage percentage compared with the PI controller and Approximate I/O linearization. Therefore, the proposed method is more applicable to implement into the digital control hardware that has limitations on the memory and instruction capability.

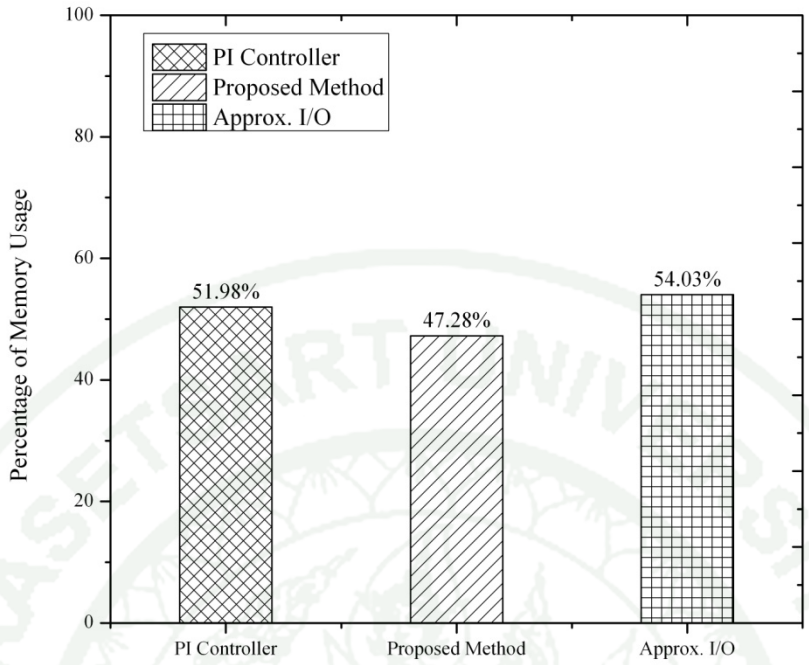

Figure 39 Comparison of the memory usage in PI controller, Approximate I/O controller, and proposed controller

1.3.6 Comparison of computation time in each control technique

The computation time is the time interval from the state variables are measured to the control output is updated. The order of truncation has been affect to the computation time of the hardware device. The effect of more computation time is to decrease the stability of the application. The comparison result is depicted in Table 10. The proposed method over PI controller and Approximate I/O linearization consume relative small amount of computation time. Therefore, the proposed method is more applicable to implement into the digital control hardware. In the case of the proposed method, the analysis of order of truncation becomes a balance between the computation time and the value of MAE. Although the 5^{th} order of truncation takes the most number of computation times, the value MAE is smaller than the other order of truncation.

Table 10 Computation time in each controller

The control techniques	Duration time (μs)
Approximate I/O linearization	324
PI controller	153
Proposed method	
- 1^{st} order	78
- 2^{nd} order	81
- 3^{rd} order	85
- 4^{th} order	87
- 5^{th} order	91

CONCLUSION AND RECOMMENDATION

Conclusion

The new control method for non-minimum phase processes was presented. It was obtained by truncating the relative order equation around the nominal equilibrium point and substituting it into the approximate I/O equation. The feedback controller is now in the simple form that is suitable to embed into the FPGA control hardware. The simulation results of both SISO and MIMO cases showed that the proposed feedback controller successfully forces the outputs of the non-minimum phase process. With the simple form of the controller equation, the proposed method is very attractive for applying to the embedded control device.

The algorithms of the control system in discrete-time including the series solution of the feedback controller, the observer and compensator were embedded into NI C-RIO to be a stand-alone controller device. The experimental results with pilot plant showed that the embedded controller successfully forced the reactor temperature to desired set-point although the control condition was in the non-minimum phase region. Compared with the PI controller, the embedded controller can achieve the control objective while the PI control was lost the control performance. Moreover, the memory consumption and the computation time of the proposed method are less than the other type of the controller formulation. Then, the proposed controller is more applicable to implement into the digital control hardware that has limitations on the memory and instruction capability.

Recommendation

Although the proposed control technique is in the simple form, and it is convenient to embed the controller equation into the control hardware, the performance of the developed control system has been tested only with the CSTR reactor. The extension of the proposed method needs to be considered for a more complex system. In the case of real-time application, the embedded controller successfully controls the pilot process; the test has been studied for only single-input, single-output system. The development of the embedded controller needs to test with the application of multi-input, multi-output system. Furthermore, in the real-time control experiment, the uncertainty occurred in the pilot process is only a step disturbance. The other types of the uncertainties, i.e., ramp and random types are also needed to be concerned. This uncertain may cause performance deterioration and even closed-loop instability. The embedded application of the fault detection, isolation, and fault-tolerant control is also an interesting topic to study when asynchronous signal occurs in the system. The problem of failures such as sensor errors, loss of signal, or controller faults during the operation is also the other interesting topic in real-time control. The developed embedded controller is currently implemented into a NI C-RIO that contains the FPGA chip and microcontroller. The study to implement the control algorithm into the FPGA chip only should be under consideration.

LITERATURE CITED

Agachi, P.S., Z.K. Nagy, M.V. Cristea and A. Imre-lucaci. 2007. **Model based control: case studies in process engineering.** Vch Verlagsgesellschaft Mbh, Weinheim.

Agrawal, P., C. Lee, H. C. Lim and D. Ramkrishna. 1982. Theoretical investigations of dynamic behavior of isothermal continuous stirred tank biological reactors. **Chem. Eng. Sci.** 37: 453–462.

Allgower, F. and F. J. Doyle 1998. Approximate I/O-linearization of nonlinear systems, pp.235-272 *In* R. Berber and C. Kravaris, eds. **Nonlinear Model-based Control**. Kluwer Academic, Dordrecht.

Ball, R. and B.F.Gray. 1995. Transient thermal behavior of the hydration of 2,3-epoxy-1-propanol in a continuously stirred tank reactor. **Ind. Eng. Chem. Res.** 34: 3726-3736.

Balasubramhanya, L.S. and F.J. Doyle III. 2000. Nonlinear model-based control of a batch reactive distillation column. **J. Proc. Contr.** 10: 209-218.

Bauer, M. and I.K. Craig. 2008. Economic assessment of advanced process control-A survey and framework. **J. Proc. Contr.** 18: 2–18.

Biswas, P. P., S. Ray and A. N. Samanta. 2007. Multi-objective constraint optimizing IOL control of distillation column with nonlinear observer. **J. Proc. Contr.** 17: 73-81.

Bleris, L.G., P.D. Vouzis, J.G. Garcia, M.G. Arnold and M.V. Kothare. 2007. Pathways for optimization-based drug delivery. **Contr. Eng. Pract.** 15: 1280–1291.

Cvetanovic, A., A. Deutschinger, I. Giouroudi and W. Brenner, 2010. Design of a novel visual and control system for the prevention of the collision during the micro handling in a SEM chamber. **Microelectron. Eng**. 87: 139-143.

Dase, C., J.S. Falcon and B. Maccleery. 2006. Motorcycle control prototyping using an FPGA-based embedded control system. **IEEE Contr. Syst. Mag.** 26: 17–21.

Dochain, D. 1992. Adaptive control algorithms for nonminimum phase nonlinear bioreactors. **Comp. Chem. Eng.** 16: 449–462.

Dubljevic, S., N. Kazantzis. 2003. A new Lyapunov design approach for nonlinear systems based on Zubov's method. **Automatica**, 38: 1999-2007.

_____. 2003. Application of non-linear discretetime feedback regulators with assignable closed-loop dynamics. **Chem. Ind.** 57: 120–125.

Edwards,C. H. 1995. **Advanced Calculus of Several Variables.** Dover Publications, USA.

Fuente, J.L., P.F. Canamero and M. Fernández-García. 2006. Synthesis and characterization of glycidyl methacrylate/butyl acrylate copolymers obtained at a low temperature by atom transfer radical polymerization. **J. Polym. Sci. Part A**. 44: 1807–1816.

Garcıa-Gabın, W. and E. F. Camacho. 2003. Sliding mode model based predictive control for non minimum phase systems. *In* **Proceedings of the 2003 European Control Conference III.**

Guardabassi, G.O. and S.M. Savaresi. 2001 . Approximate linearization via feedback–an overview* 1. **Automatica**. 37: 1–15.

Grout, I. 2008. **Digital Systems Design with FPGAs and CPLDs.** Newnes, USA.

Hubbard, J.H. 2009. **Vector Calculus, Linear Algebra, and Differential Forms: A Unified Approach.** Matrix Editions, USA.

Henson, M.A. and D.E. Seborg. 1992. Nonlinear control strategies for continuous fermenters. **Chem. Eng. Sci.** 47: 821–835.

Jacobsen, E.W. 1999. On the dynamics of integrated plants–non-minimum phase behavior. **J. Proc. Contr**. 9: 439–451.

Jo, N.H., J. Byun, H. Shim and J.H. Sao. 1998. Robust stabilization of nonminimum phase nonlinear systems, pp. 3359-3363. *In* **Proceedings of the American Control Conference**, Philadelphia, USA.

Kam, K.M. and M.O. Tade. 1999. Nonlinear control of a simulated industrial evaporation system using a feedback linearization technique with a state observer. **Ind. Eng. Chem. Res.** 38: 2995–3006.

Kanter, M., M. Soroush and W.D. Seider. 2002. Nonlinear feedback control of multivariable non-minimum-phase processes. **J. Proc. Contr.** 12: 667-686.

_____ , _____ and _____ . . 2002. Nonlinear controller design for input-constrained, multivariable processes. **Ind. Eng. Chem. Res.**, 41, 3735–3744.

Kajornrungsilp, I. and C. Panjapornpon. 2009. Embedded approximate I/O linearization controller for non-minimum phase process, pp. 552-526. *In* **Proceedings of the 19th Thailand Chemical Engineering and Applied Chemistry Conference,** Kanjanaburi. Thailand.

Kazantzis, N. and C. Kravaris. 2000. Synthesis of state feedback regulators for nonlinear processes. **Chem. Eng. Sci.** 55: 3437–3449.

Kendi, T.A. and F.J. Doyle III. 1996. Nonlinear control of a fluidized bed reactor using approximate feedback linearization. **Ind. Eng. Chem. Res**. 35: 746–757.

Kravaris, C., M. Niemiec, R. Berber and C.B. Brosilow. 1998. Nonlinear model-based control of nonminimum-phase processes, pp. 155-200. *In* **Proceedings of the NATO Advanced Study Institute,** Antalya, Turkey.

_____ and P. Daoutidis. 1990. Nonlinear state feedback control of second-order nonminimum-phase nonlinear systems. **Comput. Chem. Eng.** 14: 439–449.

Kumar, A. and P. Daoutidis. 1999. Modeling, analysis and control of ethylene glycol reactive distillation column. **AIChE J.** 45: 51–68.

Kurtz, M.J. and M.A. Henson. 1997. Input-output linearizing control of constrained nonlinear processes. **J. Proc. Contr.** 7: 3-17.

Kwok, K.E., M.C. Ping and P. Li. 2000. A model-based augmented PID algorithm. **J. Proc. Contr.** 10: 9–18.

Lee, J., D.G. Koo and T.F. Edgar. 2000. Robust controller design method for systems with parametric uncertainties. **Trans. Cont., Auto. &System. Engr.** 2: 140-148

Ling, K.V., S.P. Yue and J.M. Maciejowski 2006. A FPGA implementation of Model Predictive Control, pp. 528-532. *In* **proceedings of the American Control Conference 2006.**

Lukes, D.L. 1969. Optimal regulation of nonlinear dynamical systems. **SIAM J. Control.** 7: 75-100.

Mahmoud, W.H., M. Abdelrahman and R.L. Haggard. 2004. Field programmable gate arrays implementation of automated sensor self-validation system for cupola furnaces. **Comput. Ind. Eng.** 46: 553–569.

Niemiec, M. P. and C. Kravaris. 2003. Nonlinear model-state feedback control for nonminimum-phase processes. **Automatica.** 39: 1295–1302.

Ogunnaike, B.A. and W.H. Ray. 1994. **Process dynamics, modeling, and control.** Oxford University Press, USA.

Palanki, S. and C. Kravaris. 1997. Controller synthesis for time-varying systems by input/output linearization. **Comput. Chem. Eng.** 21: 891–903.

Panjapornpon, C., M. Soroush and W.D. Seider. 2006. Model-based controller design for unstable, non-minimum-phase, nonlinear processes. **Ind. Eng. Chem. Res.** 45: 2758–2768.

_____ and M. Soroush. 2007. Shortest-prediction-horizon non-linear model-predictive control with guaranteed asymptotic stability. **J. Proc. Contr.** 80: 1533-1543.

_____ , _____ and W.D. Seider. 2006. Model-based controller design for unstable, non-minimum-phase, nonlinear processes. **Ind. Eng. Chem. Res.** 45 : 2758–2768.

Pin, F.G., R.S. Pattay, H. Watanabe and J. Symon. 1992. Using custom-designed VLSI fuzzy inferencing chips for the autonomous navigation of a mobile robot, pp. 1-14. *In* **Proceedings of the IEEE International Conference on Intelligent Robots and Systems,** Raleigh, North Carolina.

Rohani, S., M. Haeri and H.C. Wood. 1999. Modeling and control of a continuous crystallization process Part 2. Model predictive control. **Comput. Chem. Eng.** 23: 279–286.

Shamsuzzoha, M. and M. Lee. 2008. PID controller design for integrating processes with time delay. **Korean J. Chem. Eng.** 25: 637–645

Shkolnikov, I.A. and Y.B. Shtessel. 2000. Nonminimum phase tracking in MIMO systems with square input–output dynamics via dynamic sliding manifolds. **J. Frankl. Inst.** 337: 43–56.

Siri-arayaphan, P. and C. Panjapornpon. 2008. Model-based Controller Design in FPGA for Applying in Chemical Engineering Process, pp. 50-55. *In* **Proceedings of the 18th Thailand Chemical Engineering and Applied Chemistry Conference,** Pattaya Thailand.

Soroush,.M. 1997. Nonlinear state-observer design with application to reactors. **Chem. Eng. Sci.** 52: 387–404.

Van de Vusse, J.G. 1964. Plug-flow type reactor versus tank reactor. **Chem. Eng. Sci.** 19: 994–996.

Wu, W. 1999. Adaptive nonlinear control of nonminimum-phase processes. **Chem. Eng. Sci.** 54: 3815–3829.

Wolfram, S. 1999. **The Mathematica Book, Fourth Edition**. Cambridge University Press, UK.

APPENDICES

Appendix A

The formulation of control system for multi-input, multi-output chemical reactor

The formulation of the control system for the multi-input, multi-output chemical reactor process is as follows:

The open-loop state observer

$$
\begin{aligned}
\frac{d\tilde{C}_A}{dt} &= \frac{F}{V}\left(C_{A_i} - \tilde{C}_A\right) - k_{A0}\exp\left(-\frac{E_1}{RT}\right)\tilde{C}_A^2 \\
\frac{d\tilde{C}_B}{dt} &= -\frac{F}{V}\tilde{C}_B + k_{A0}\exp\left(-\frac{E_1}{RT}\right)\tilde{C}_A^2 - k_{B0}\exp\left(-\frac{E_2}{RT}\right)\tilde{C}_B \\
\frac{d\tilde{T}}{dt} &= \frac{F}{V_2}\left(T_i - \tilde{T}\right) + \frac{\left(-\Delta H_1\right)}{\rho c_p}k_{A0}\exp\left(-\frac{E_1}{R\tilde{T}}\right)\tilde{C}_A^2 + \frac{\left(-\Delta H_2\right)}{\rho c_p}k_{B0}\exp\left(-\frac{E_2}{R\tilde{T}}\right)\tilde{C}_B \\
&\quad + \frac{US}{\rho c_p V}\left(T_j - \tilde{T}\right) \\
\frac{d\tilde{T}_j}{dt} &= \frac{F_j}{V}\left(T_{ji} - \tilde{T}_j\right) - \frac{US}{\rho_j c_{pj} V_j}\left(T_j - \tilde{T}\right) \\
\tilde{y}_1 &= \tilde{C}_B \\
\tilde{y}_2 &= \tilde{T}
\end{aligned}
\tag{A.1}
$$

The feedback compensator

$$
\begin{aligned}
\nu_1 &= y_{1,sp} - (y_1 - \tilde{y}_1) \\
\nu_2 &= y_{2,sp} - (y_2 - \tilde{y}_2)
\end{aligned}
\tag{A.2}
$$

The feedback controller with 4th order Taylor series of relative order equation and the compensator takes the form:

$$
\begin{aligned}
F = {} & (10\beta_1 \tilde{C}_B + \beta_1^2 (1.43\text{E-}7 \cdot (-398.06 + \tilde{T}) \cdot (-397.89 + \tilde{T}) \cdot (1.58\text{E}5 + (-795.96 + \\
& \tilde{T})\tilde{T}) - 2.96\text{E-}5\,\tilde{C}_B\,(1.49\text{E}5 + (-770.62 + \tilde{T})\tilde{T}) \cdot (1.4\text{E}5 + (-749.85 + \tilde{T})\tilde{T}) \\
& + 7.38\text{E-}5\,C_A^2 (1.47\text{E}5 + (-760.73 + \tilde{T})\tilde{T}) \cdot (1.34\text{E}5 + (-732.55 + \tilde{T})\tilde{T}) - 1.06\text{E-}4\,\tilde{C}_A \\
& (1.48\text{E}5 + (-760.95 + \tilde{T})\tilde{T}) \cdot (1.28\text{E}5 + (-715.48 + \tilde{T})\tilde{T})) + 50(\beta_1^2((-2.8\text{E-}9\beta_1(- \\
& 398.01 + \tilde{T}) \cdot (-397.94 + \tilde{T}) \cdot (1.58\text{E}5 + (-795.96 + \tilde{T})\tilde{T}) - 1.47\text{E-}6\beta_1 C_A^2 (1.47\text{E}5
\end{aligned}
$$

$+ (\text{-}760.73 + \tilde{T})\tilde{T}) \cdot (134E5 + (\text{-}732.55 + \tilde{T})\tilde{T}) + 2.12E\text{-}6\beta_1 \tilde{C}_A\ (1.48E5 + (\text{-}760.95 + \tilde{T})\tilde{T}) \cdot (1.28E5 + (\text{-}715.48 + \tilde{T})\tilde{T}) + \tilde{C}_B\ (\text{-}0.2 + 1.24E5\beta_1 + 5.92E\text{-}7\beta_1(\text{-}760.19 + \tilde{T})\tilde{T}\ (2.9E5 + (\text{-}760.28 + \tilde{T})\tilde{T})))^2 - 0.04\tilde{C}_B\ (5.37E6\beta_1(2.62E\text{-}19 + \beta_1) - \nu_1 + \tilde{C}_B + \beta_1(\text{-}1.4E\text{-}5\beta_1 C_B^2\ (1.55E5 + (\text{-}788.09 + \tilde{T})\ \tilde{T}) \cdot (1.46E5 + (\text{-}764.77 + \tilde{T})\tilde{T}) - 1.59E3\beta 1\, C_A^3 (1.55E5 + (\text{-}786.09 + \tilde{T})\tilde{T}) \cdot (1.44E5 + (\text{-}759.21 + \tilde{T})\tilde{T}) + 5.53E\text{-}4\beta_1 C_A^4 (1.54E5 + (\text{-}785.08 + \tilde{T})\tilde{T}) \cdot (143E5 + (\text{-}757.03 + \tilde{T})\tilde{T}) + \tilde{T}\ (\text{-}1.14E\text{-}14 - 5.4E4\beta_1 + \tilde{T}\ (3.06E\text{-}17 + 203.78\beta_1 + \tilde{T}\ (\text{-}2.71E\text{-}20 - 0.34\beta_1 + 2.1E\text{-}4\beta_1\tilde{T}))) - 2.71E\text{-}20\beta_1 (\text{-}510.34 + \tilde{T}) \cdot (1.65E5 + (\text{-}811.59 + \tilde{T})\tilde{T})\tilde{T}_j + \tilde{C}_A\ (\text{-}2.46E\text{-}11 - 2.15E\text{-}8\beta_1 - 5.42E\text{-}20\beta_1\tilde{C}_B\ (\text{-}420.60 + \tilde{T}) \cdot (\text{-}375.35 + \tilde{T})(1.58E5 + (\text{-}795.96 + \tilde{T})\tilde{T}) + \tilde{T}\ (2.39E\text{-}13 + 2.22E\text{-}10\beta_1 + \tilde{T}\ (\text{-}8.69E\text{-}16 - 8.64E\text{-}13\beta_1 + \tilde{T}\ (1.4E\text{-}18 + 1.49E\text{-}15\beta_1 + (\text{-}8.47E\text{-}22 - 9.75E\text{-}19\beta_1)\ \tilde{T}))) + 3.47E\text{-}18\beta_1(\text{-}485.40 + \tilde{T}) \cdot (\text{-}374.55 + \tilde{T})\tilde{T}_j) + \tilde{C}_B\ (\text{-}4E4 + 1.5E6\beta_1 + \tilde{T}\ (423.65 - 2.35E4\beta_1 + \tilde{T}\ (\text{-}1.68 + 123.77\beta_1 + \tilde{T}\ (0.003 - 0.27\beta_1 + (\text{-}1.97E\text{-}6 + 2E4\beta_1)\ \tilde{T}))) - 1.5E4\beta 1(\text{-}367.60 + \tilde{T}) \cdot (1.45E5 + (\text{-}760.82 + \tilde{T})\tilde{T})\tilde{T}_j) + C_A^2 (8.09E4 - 2.81E7\beta_1 - 1.55E4\beta_1\tilde{C}_B\ (1.55E4 + (\text{-}786.81 + \tilde{T})\tilde{T}) \cdot (1.45E4 + (\text{-}761.33 + \tilde{T})\tilde{T}) + \tilde{T}\ (\text{-}867.06 + 3.01E5\beta_1 + \tilde{T}\ (3.49 - 1.2E4\beta_1 + \tilde{T}\ (\text{-}6.28E\text{-}3 + 2.17\beta_1 + (4.25E\text{-}6 - 1.47E3\beta_1)\ \tilde{T}))) + 3.25E4\beta_1(\text{-}359.44 + \tilde{T})(1.41E5 + (\text{-}747.88 + \tilde{T})\tilde{T})\tilde{T}_j)))))^{0.5})/(\beta_1^2\ \tilde{C}_B)$

$F_j = (9.26^7(\text{-}1.17^{\text{-}18} + \beta_2)\beta_2 + \nu_2 + \beta_2^2 F^2(4 - 0.01\tilde{T}) - \tilde{T} + 0.027\beta_2^2\ C_A^3(1.55E5 + (\text{-}786.09 + \tilde{T})\tilde{T}) \cdot (1.44E5 + (\text{-}759.21 + \tilde{T})\tilde{T}) - 9.6E\text{-}3\beta_2^2\ C_A^4\ (1.55E5 + (\text{-}785.08 + \tilde{T})\tilde{T}) \cdot (1.43E5 + (\text{-}757.03 + \tilde{T})\tilde{T}) + \beta_2 C_A^2\ (\text{-}1.40E6 + 4.03E8\beta_2 - 1.59E\text{-}3\beta_2\tilde{C}_B\ (1.55E5 + (\text{-}786.81 + \tilde{T})\tilde{T}) \cdot (1.44E5 + (\text{-}761.33 + \tilde{T})\tilde{T}) + \tilde{T}\ (1.5E4 - 4.35E6\beta_2 + \tilde{T}\ (\text{-}60.56 + 1.77E4\beta_2 + \tilde{T}\ (0.11 - 32.12\beta_2 + (\text{-}7.37E\text{-}5 + 2.19E\text{-}2\beta_2)\ \tilde{T}))) - 5.64E\text{-}3\beta_2(\text{-}359.44 + \tilde{T}) \cdot (1.42E5 + (\text{-}747.88 + \tilde{T})\tilde{T})\tilde{T}_j) + \beta_2 F(\text{-}80 + 283.44\beta_2 + 0.2\tilde{T} + \beta_2\ (\text{-}4.96E\text{-}8(\text{-}128.89 + \tilde{T})\tilde{T}\ (7.61E5 + (\text{-}1.46E3 + \tilde{T})\tilde{T}) +$

2.63E-6$\tilde{C}_B$ (1.49E5 + (-770.62 + $\tilde{T}$)$\tilde{T}$) · (1.40E5 + (-749.85 + $\tilde{T}$)$\tilde{T}$) + 2E-3C_A^2(1.47E5 + (-760.73 + $\tilde{T}$)$\tilde{T}$) · (1.34E5 + (-732.55 + $\tilde{T}$)$\tilde{T}$) - 3.66E5$\tilde{C}_A$ (1.48E5 + (-760.62 + $\tilde{T}$)$\tilde{T}$) · (1.28E5 + (-715.17+ $\tilde{T}$)$\tilde{T}$) + 3.82$\tilde{T}_j$)) + $\tilde{C}_A$ ((-0.015β_2^2)$\tilde{T}^4$ + $\tilde{C}_B$ (5.68E-14β_2^2) + β_2(-1.09E-10 - 3.83E8β_2 - 5.33E-11$\beta_2\tilde{T}$ $\tilde{T}_j$) + $\beta_2\tilde{T}^2$(-2.07E-15 – 1.45E4β_2 - 1.03E-15$\beta_2\tilde{T}_j$) + $\beta_2\tilde{T}^3$(1.73E-18 + 24.35β_2 + 8.67E-19$\beta_2\tilde{T}_j$) +$\beta_2\tilde{T}$ (8.24E-13 + 3.85E6β_2 + 4.08E-13$\beta_2\tilde{T}_j$)) + β_2(-6.25E-5$\beta_2 C_B^2$(1.55E5 + (-788.09 +$\tilde{T}$)$\tilde{T}$) · (1.46E5 +(-764.77 + $\tilde{T}$)$\tilde{T}$) + $\tilde{T}$ (76.5 – 9.34E5β_2 + $\tilde{T}$ (-6.19E-15 + 3.5E3β_2 + $\tilde{T}$ (1.192E-17 - 5.87β_2 + (-8.47E-21 + 0.0036β_2) $\tilde{T}$))) - 76.5$\tilde{T}_j$ - 2.16E-19β_2(-2.51E7 + $\tilde{T}$) · (6.33E14 + $\tilde{T}$ (2.51E7 + $\tilde{T}$)) · $\tilde{T}_j$ + $\tilde{C}_B$ (-1.78E5 + 1.01E7β_2 + $\tilde{T}$ (1.88E3 - 1.40E5β_2 + $\tilde{T}$ (-7.47 + 692.98β_2 + $\tilde{T}$ (0.013 - 1.46β_2 + (-8.77E-6 + 1.1E-3β_2) $\tilde{T}$))) – 6.71E-4β_2(-367.60 + $\tilde{T}$) · (1.45E5 + (-760.82 + $\tilde{T}$)$\tilde{T}$)$\tilde{T}_j$)))/(β_2^2(1.14E3 - 3.825$\tilde{T}_j$))

Appendix B

Effect of the truncation order term

The closed loop responses of each truncation order for the SISO system are shown in Appendix Figure B1. The results show that the response of the 5th order truncation is most accurate to the response of nonlinear model. For the lower of truncation order, the response of fresh feed flow rate has an oscillation due to the effect of the error in the low order of approximation. The higher order of truncation is directly effect to the computation time of hardware device. The truncation order should be chosen large enough that can fully captures the output dynamics with appropriate computation time.

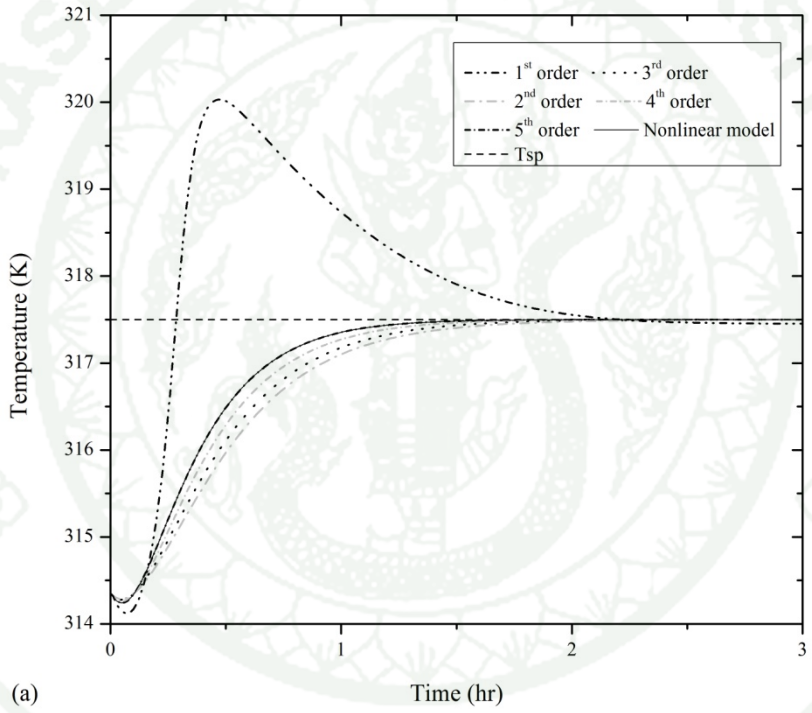

Appendix Figure B1 Closed-loop response of (a) the reactor temperature, (b) the concentration of *A*, and (c) the feed flow rate under various truncation order

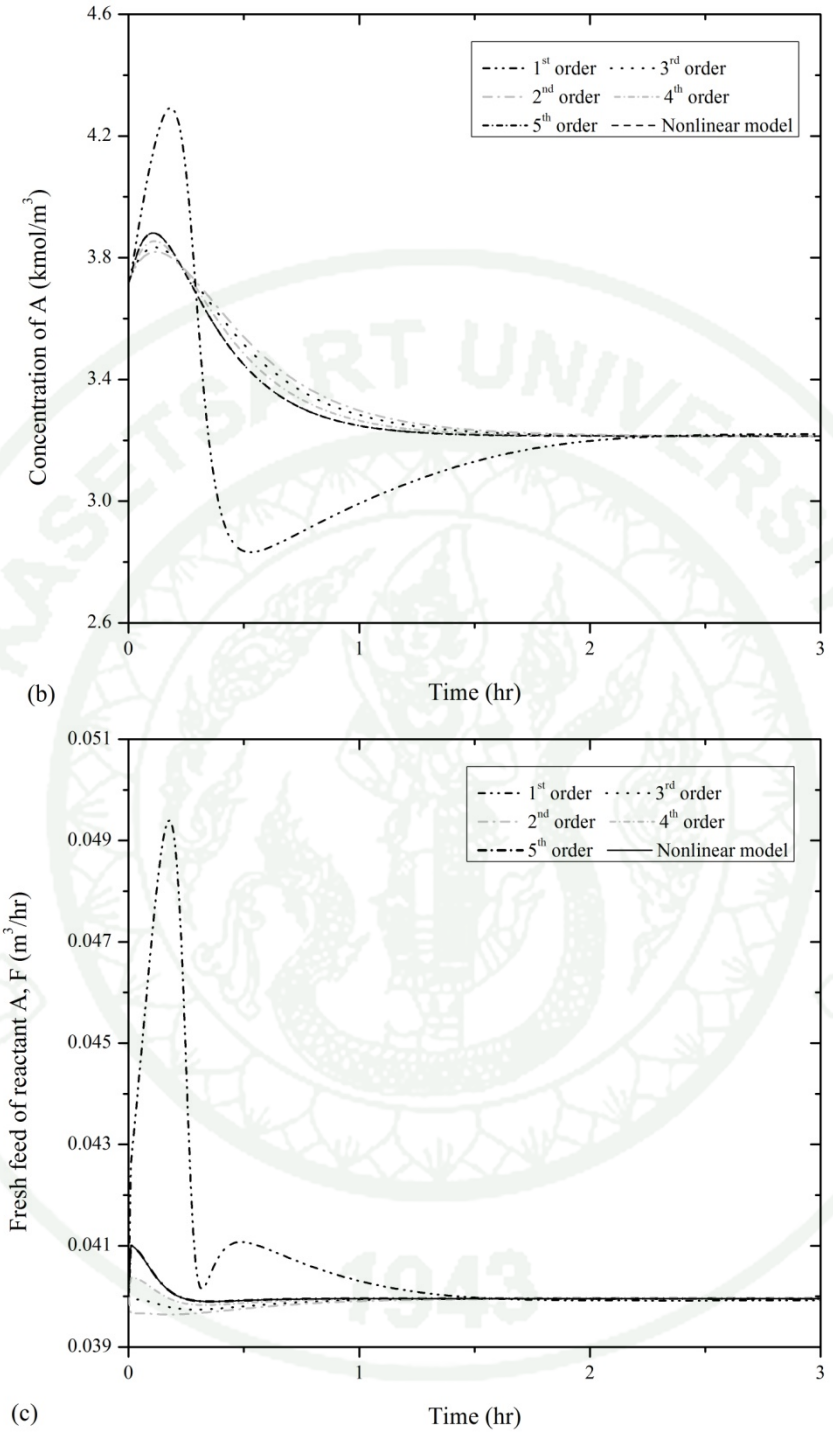

Appendix Figure B1 (Continued)

The closed loop responses of each truncation order for the MIMO system are shown in Appendix Figure B2 - B4. The results show that the response of the 4th order truncation is most close to the response of nonlinear model. For the 1st order of truncation, the controller equation has the highly effect of the approximation error.

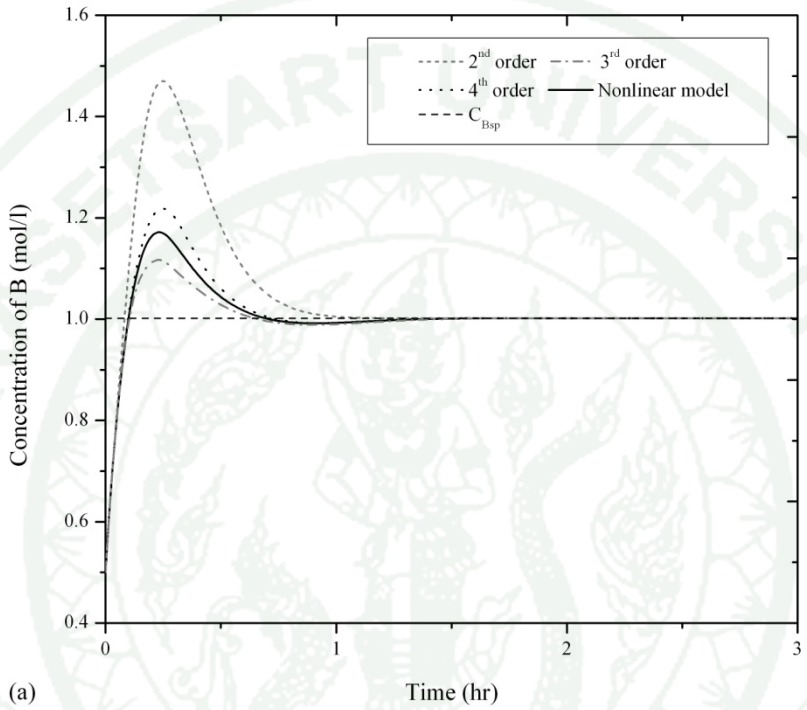

Appendix Figure B2 Closed-loop response of (a) the concentration of *B* and (b) the reactor temperature under various truncation order

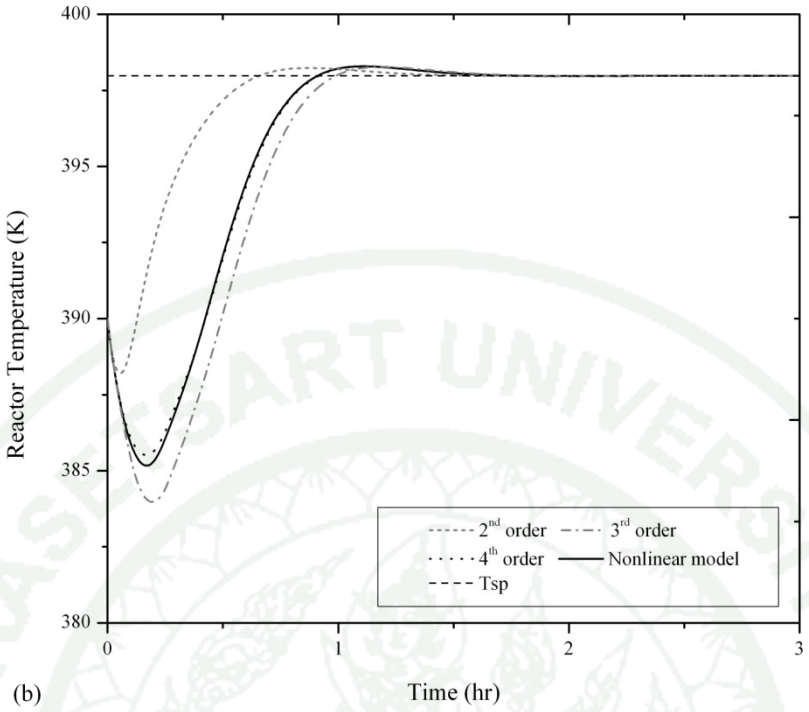

Appendix Figure B2 (Continuted)

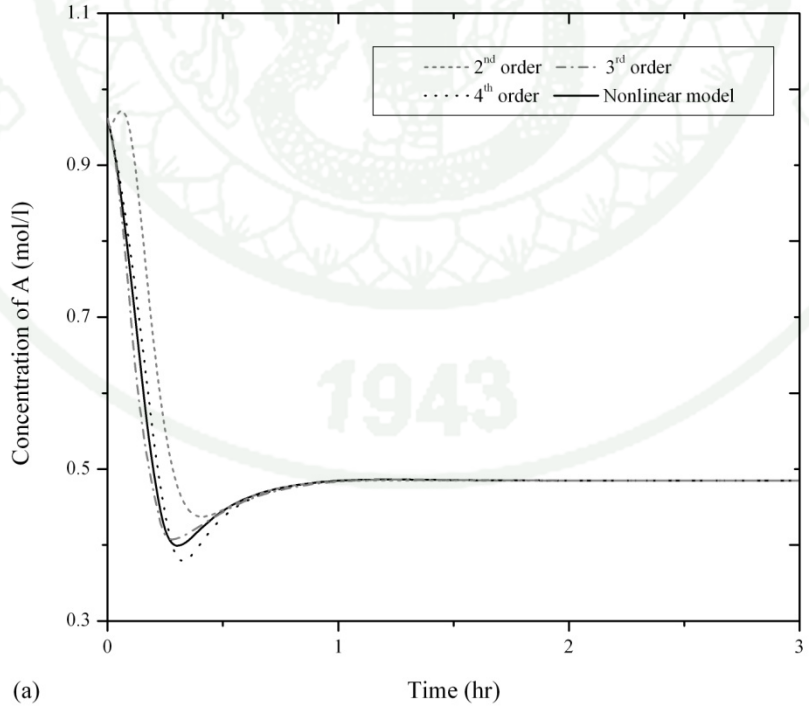

Appendix Figure B3 The responses of (a) the reactant feed flow rate and (b) the cooling water flow rate under various truncation order

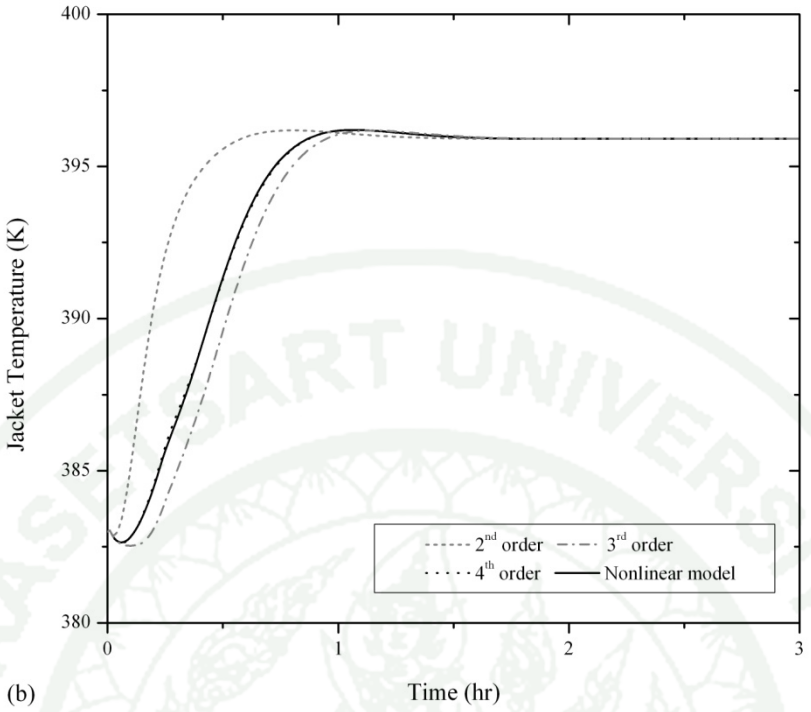

Appendix Figure B3 (Continuted)

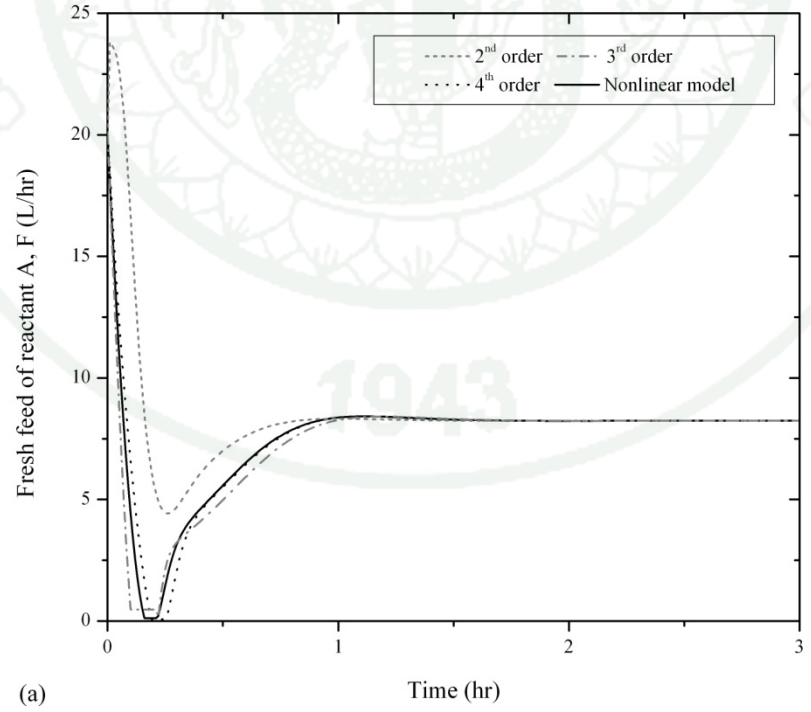

Appendix Figure B4 Closed-loop responses of (a) the concentration of *A* and (b) cooling jacket temperature under various truncation order

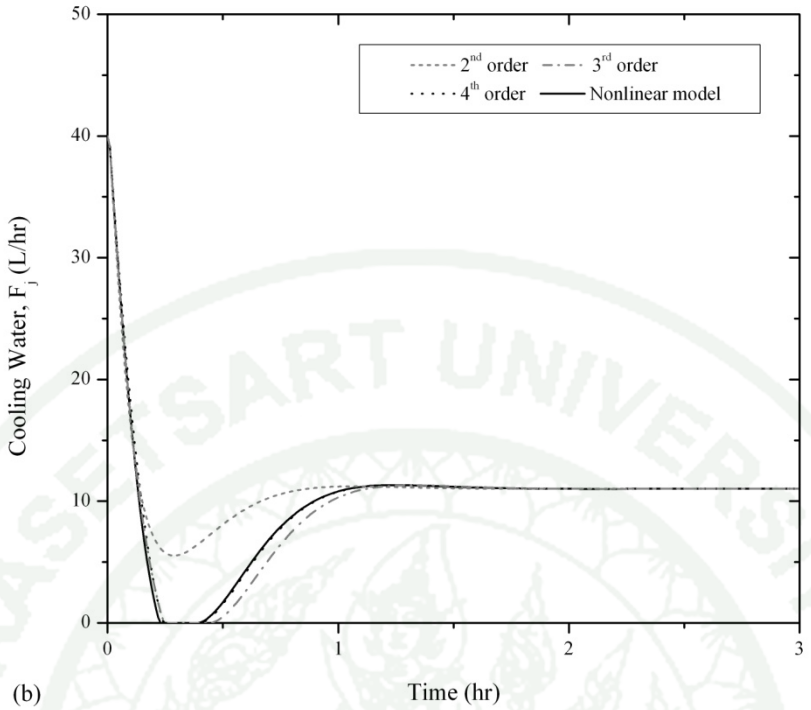

(b)

Appendix Figure B4 (Continuted)

Appendix C

Equipment design in pilot process

Appendix Figure C1 shows the drawing of the pilot process that exhibits non-minimum phase behavior. The non-minimum phase pilot process comprises of the exchanger unit, hot-bath, flow meter, flow transmitter and peristaltic pump. They are illustrated in Appendix Figure 2, Appendix Figure 3, Appendix Figure 4 and Appendix Figure 5 respectively.

Appendix Figure C2 showed the exchanger unit in non-minimum phase pilot process that made of stainless steel (9.124L) with 6 inch diameter and 19.658 inch in height. It was coated polyurethane foam insulation 0.5 inch in thick. The inside of the exchanger unit has the emerging coil made of a copper with 0.635 inch diameter and 51.772 inch in length.

Appendix Figure C3 presented the hot-bath in non-minimum phase pilot process, which made of a stainless steel (24.74L) with 11.811 inch diameter and 13.788 inch in height. A heater (2000W, 220V) and an agitator with the motor speed of 200 rpm are installed inside the tank.

Appendix Figure C4 presented the turbine flow sensor and flow transmitters, which are device for sensing and monitoring the rate of fluid flow. The turbine flow sensors are connected to flow transmitter and PID controller in order to monitor the data and adjust the speed of peristaltic pumps.

The peristaltic pump shown in Appendix Figure C5 is used to manipulate the feed corresponding to receive the analog signal.

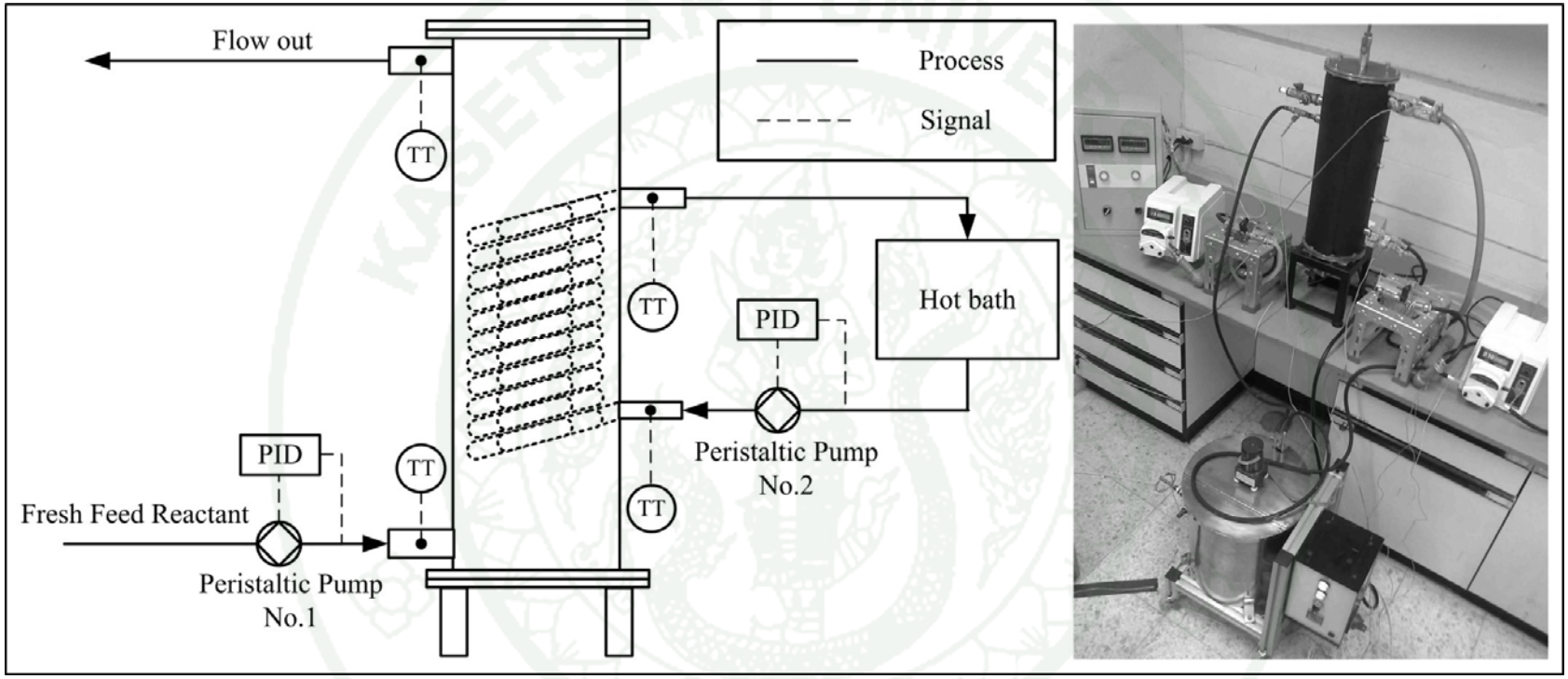

Appendix Figure C1 The exchanger unit of non-minimum phase pilot process

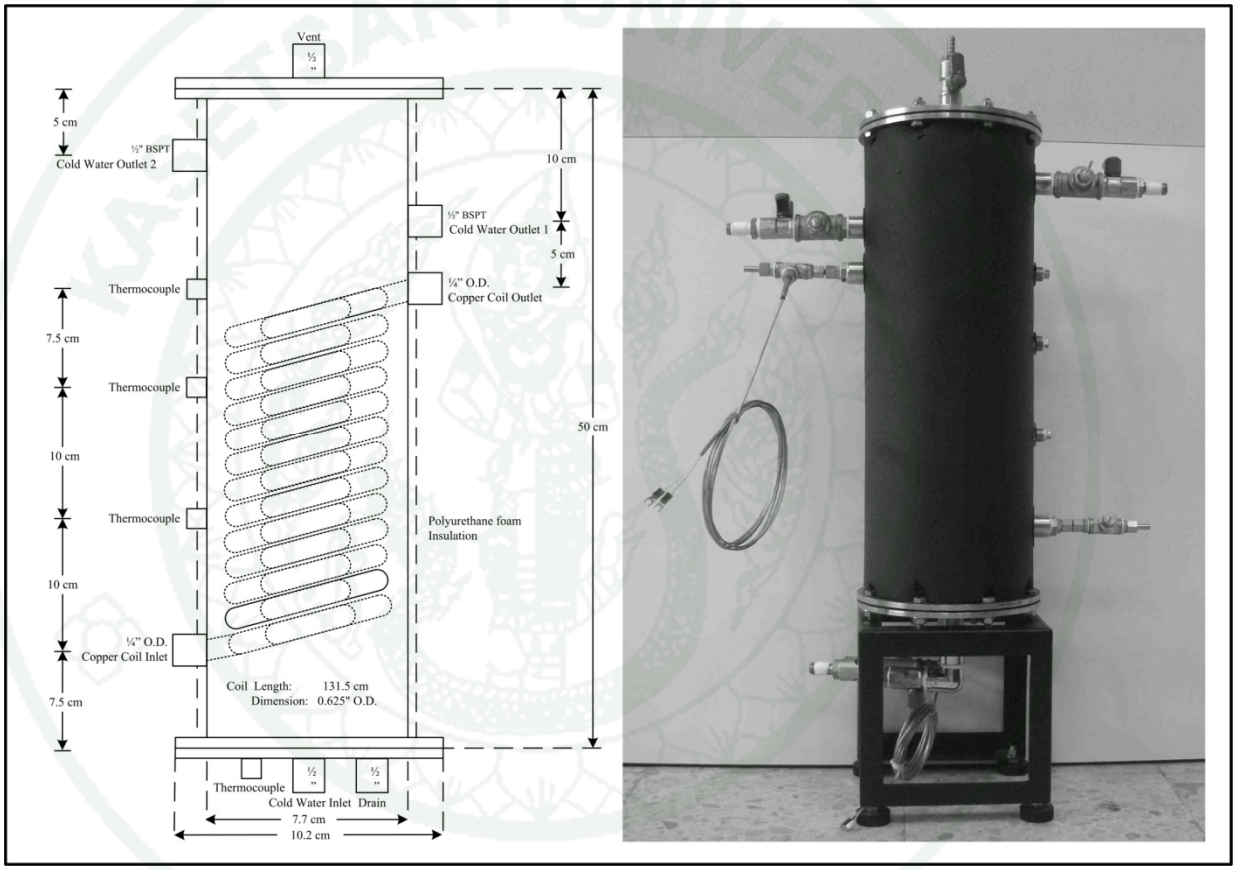

Appendix Figure C2 The exchanger unit of non-minimum phase pilot process

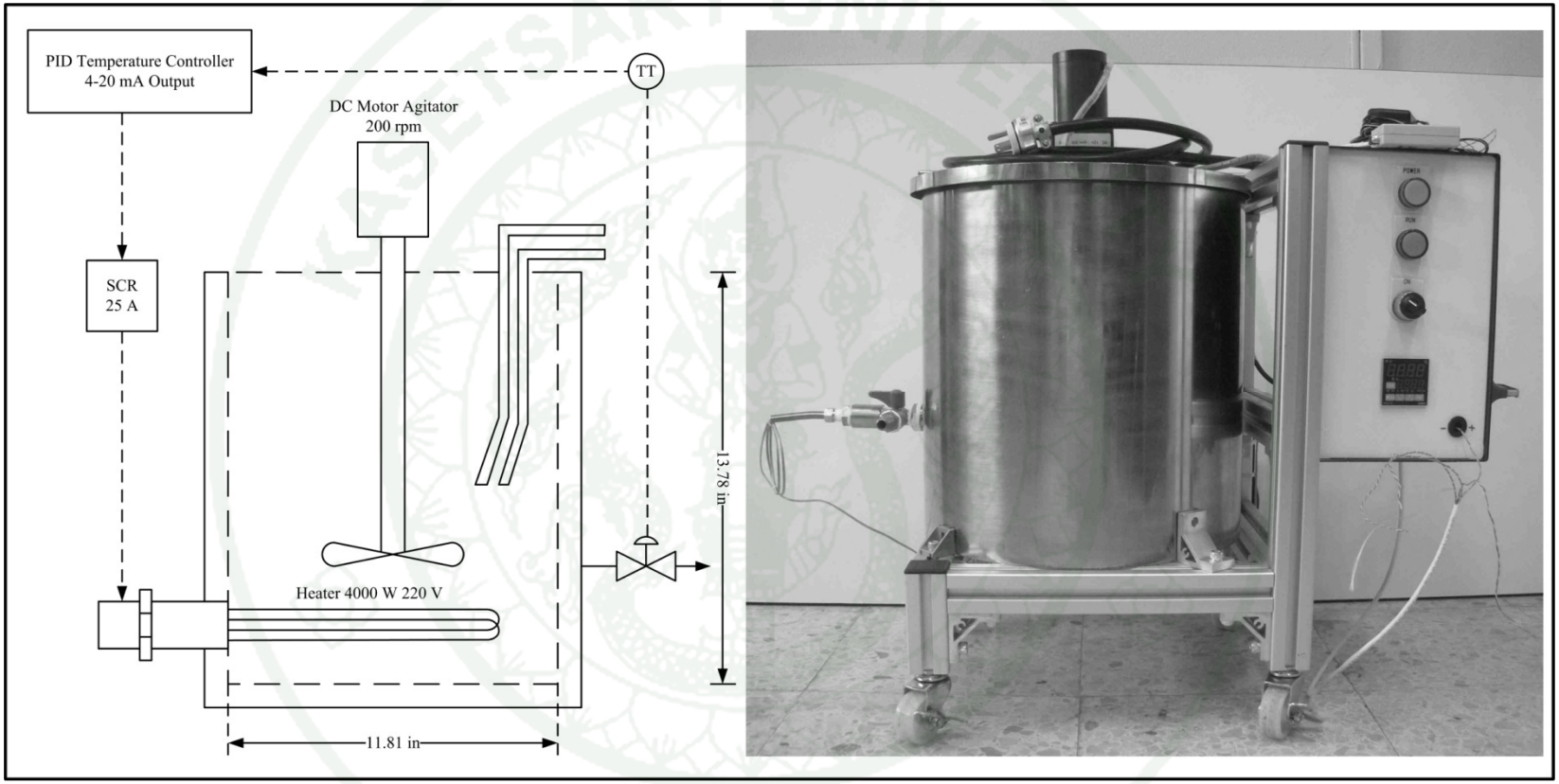

Appendix Figure C3 The hot-bath in non-minimum phase pilot process

(a) (b)

Appendix Figure C4 The picture of (a) turbine flow sensor, and (b) flow transmitter in the non-minimum phase pilot process

Appendix Figure C5 The peristaltic pump in non-minimum phase pilot process

CURRICULUM VITAE

NAME : Mr. Issarush Kajornrungsilp

BIRTH DATE : September 26, 1987

BIRTH PLACE : Bangkok, Thailand

EDUCATION :

YEAR	INSTITUTION	DEGREE/DIPLOMA
2008	Kasetsart University	B. Eng. (Chemical Engineering)
2004	Debsirin School	High School

AWARDS : The runner up of Innovation Award of Kasetsart University, 2009
The Industrial Award of Faculty of engineering, Kasetsart University, 2009